

Titre: Absorption heat pump : simulation and model validation
Title:

Auteur: Keyvan Aghabararpourtabakhi
Author:

Date: 2008

Type: Mémoire ou thèse / Dissertation or Thesis

Référence: Aghabararpourtabakhi, K. (2008). Absorption heat pump : simulation and model validation [Mémoire de maîtrise, École Polytechnique de Montréal]. PolyPublie.
Citation: <https://publications.polymtl.ca/8313/>

 **Document en libre accès dans PolyPublie**
Open Access document in PolyPublie

URL de PolyPublie: <https://publications.polymtl.ca/8313/>
PolyPublie URL:

**Directeurs de
recherche:**
Advisors:

Programme: Non spécifié
Program:

UNIVERSITÉ DE MONTRÉAL

ABSORPTION HEAT PUMP:
SIMULATION AND MODEL VALIDATION

KEYVAN AGHABARARPOURTABAKHI
DÉPARTEMENT DE GÉNIE CHIMIQUE
ÉCOLE POLYTECHNIQUE DE MONTRÉAL

MÉMOIRE PRÉSENTÉ EN VUE DE L'OBTENTION
DU DIPLÔME DE MAÎTRISE ÈS SCIENCES APPLIQUÉES
(GÉNIE CHIMIQUE)

MARS 2008



Library and
Archives Canada

Bibliothèque et
Archives Canada

Published Heritage
Branch

Direction du
Patrimoine de l'édition

395 Wellington Street
Ottawa ON K1A 0N4
Canada

395, rue Wellington
Ottawa ON K1A 0N4
Canada

Your file Votre référence

ISBN: 978-0-494-46026-9

Our file Notre référence

ISBN: 978-0-494-46026-9

NOTICE:

The author has granted a non-exclusive license allowing Library and Archives Canada to reproduce, publish, archive, preserve, conserve, communicate to the public by telecommunication or on the Internet, loan, distribute and sell theses worldwide, for commercial or non-commercial purposes, in microform, paper, electronic and/or any other formats.

The author retains copyright ownership and moral rights in this thesis. Neither the thesis nor substantial extracts from it may be printed or otherwise reproduced without the author's permission.

AVIS:

L'auteur a accordé une licence non exclusive permettant à la Bibliothèque et Archives Canada de reproduire, publier, archiver, sauvegarder, conserver, transmettre au public par télécommunication ou par l'Internet, prêter, distribuer et vendre des thèses partout dans le monde, à des fins commerciales ou autres, sur support microforme, papier, électronique et/ou autres formats.

L'auteur conserve la propriété du droit d'auteur et des droits moraux qui protègent cette thèse. Ni la thèse ni des extraits substantiels de celle-ci ne doivent être imprimés ou autrement reproduits sans son autorisation.

In compliance with the Canadian Privacy Act some supporting forms may have been removed from this thesis.

Conformément à la loi canadienne sur la protection de la vie privée, quelques formulaires secondaires ont été enlevés de cette thèse.

While these forms may be included in the document page count, their removal does not represent any loss of content from the thesis.

Bien que ces formulaires aient inclus dans la pagination, il n'y aura aucun contenu manquant.

UNIVERSITÉ DE MONTRÉAL
ÉCOLE POLYTECHNIQUE DE MONTRÉAL

Ce mémoire intitulé :

ABSORPTION HEAT PUMP:
SIMULATION AND MODEL VALIDATION

présenté par : AGHABARARPOURTABAKHI Keyvan

en vue de l'obtention du diplôme de : Maîtrise ès sciences appliquées

a été dûment accepté par le jury d'examen constitué de :

M. PERRIER Michel, Ph.D., président

M. LEGROS Robert, Ph.D., membre et directeur de recherche

M. FRADETTE Louis, Ph.D., membre et codirecteur de recherche

M. PARIS Jean, Ph.D., membre et codirecteur de recherche

M. KAJL Stanislaw, D.Sc.Tech, membre

DEDICATION

To My Beloved Parents

ACKNOWLEDGMENTS

I would like to express my gratitude to Professor Jean Paris for accepting me in his research group, for his confidence in my abilities, his patience, and financial support and for his encouragements during my work during the last two years.

I am also extremely grateful to Dr. Louis Fradette for his help, kindness and his great availability.

Furthermore I would like to thank Dr. Felix Ziegler and Dr. Robert Legros for their support and supervision.

I would like to express my sincere thanks to my parents and my sister for their patience, unconditional love, encouragement and financial support. This work was not possible without their presence.

RÉSUMÉ

Une Pompe À Chaleur À Sorption (PACAS) est un dispositif qui peut transférer l'énergie à partir de basse température à une plus haute température. En raison des prix de l'énergie volatiles et des soucis environnementaux, ces systèmes ont gagné beaucoup d'intérêt pendant les deux dernières décennies. Une quantité substantielle de recherche a été faite pour améliorer la technologie d'absorption. Il y a également un nouvel intérêt à employer cette technologie dans des processus industriels. Le développement accéléré de PACAS a créé un besoin de simulations fiables et efficaces sur ordinateur.

L'objectif de ce travail était de développer un modèle mathématique du comportement thermique d'un PACAS. Cette thèse présente d'abord les principes des cycles d'absorption et de deux réfrigérateurs d'absorption de prototypes, disponibles à l'Ecole Polytechnique De Montréal et à l'université technique de Berlin qui ont été employés pour valider le modèle. Deux différents types de pompes à chaleur, pompe à chaleur à compression et de PACAS sont décrits. Le modèle mathématique plus tard décrit est une solution numérique d'une série de douze équations non-linéaires. Ces équations sont basées sur une chaleur et des bilans de matière des cinq échangeurs de chaleur constituant un PACAS : générateur, condensateur, amortisseur, vaporisateur, et échangeur de chaleur de solution.

Ce modèle calcule les paramètres de performance (températures à la sortie et concentrations de la solution) du prototype refroidisseurs d'absorption au cours d'une opération à l'état d'équilibre. En ayant la température de sortie de la charge thermique de chaque échangeur de chaleur et le coefficient de performance (COP) sont calculés. Il ya sept variables d'entrée qui sont les températures et les débits à l'entrée de chaud et froid et l'eau de refroidissement et la solution riche. Les résultats de cette simulation sont validés par comparaison avec des résultats expérimentaux obtenus à partir des prototypes dans des études précédentes. La sensibilité du modèle à certains paramètres (coefficient global de transmission thermique, la transmission de la chaleur et des températures d'entrée) a été étudié et vérifié l'encontre de matériel publié. Les différences entre les valeurs mesurées et les résultats des expériences valeurs simulées

(prise de température) de ce modèle sont généralement de moins de 2,9 °C. Les causes de ces différences sont également expliquées

La comparaison entre les expériences, la simulation et également littérature montre une bonne concordance entre les résultats et la fiabilité de ce modèle.

ABSTRACT

An Absorption Heat Pump (AHP) is a device which can transfer the energy from a lower temperature level to a higher temperature. Because of volatile energy prices and environmental concerns these systems have gained a lot of interest during the past two decades. There is also a new interest in using this technology in industrial processes. The accelerated development of absorption heat pumps has created a need for reliable and effective computer simulations.

The objective of this work was to develop a mathematical model of the thermal behaviour of an AHP. This thesis first presents the principles of absorption cycles and two prototype absorption chillers available at Ecole Polytechnique de Montréal and Technical University of Berlin which have been used to validate the model. The mathematical model subsequently described is a numerical solution of a series of nonlinear equations. These equations are based on heat and mass balances of the five heat exchangers constituting an AHP: generator, condenser, absorber, evaporator and solution heat exchanger.

This model calculates the output parameters (outlet temperatures and solution concentrations) of the prototype absorption chillers during a steady state operation. By having the output temperatures the heat load of each heat exchanger and Coefficient of Performance (COP) are calculated. There are seven input variables which are inlet temperatures and flowrates of hot, chilled and cooling water and rich solution. The results of this simulation are validated by comparison with experimental results obtained from the prototypes in previous studies. The sensitivity of the model to certain parameters (overall heat transfer coefficient, heat transfer area and inlet temperatures) has been studied and verified against published material. The differences between the measured values from experiments and simulated values (outlet temperatures) from this model are generally less than 2.9°C. The causes of these differences are also explained. The comparison between experiments, simulations and literature shows a good agreement between the results and the reliability of this model.

CONDENSÉ EN FRANÇAIS

Une Pompe À Chaleur À Sorption (PACAS) est un dispositif qui peut transférer l'énergie à partir de basse température à une plus haute température. En raison des prix de l'énergie volatiles et des soucis environnementaux, ces systèmes ont gagné beaucoup d'intérêt pendant les deux dernières décennies. Une quantité substantielle de recherche a été faite pour améliorer la technologie d'absorption. Il y a également un nouvel intérêt à employer cette technologie dans des processus industriels. Le développement accéléré de PACAS a créé un besoin de simulations fiables et efficaces sur ordinateur.

L'objectif de ce travail était de développer un modèle mathématique du comportement thermique d'un PACAS.

Cette thèse présente d'abord les principes des cycles d'absorption et de deux réfrigérateurs d'absorption de prototypes, disponibles à l'Ecole Polytechnique De Montréal et à l'université technique de Berlin qui ont été employés pour valider le modèle. Deux différents types de pompes à chaleur, pompe à chaleur à compression et de PACAS sont décrits. Le modèle mathématique plus tard décrit est une solution numérique d'une série de douze équations non-linéaires. Ces équations sont basées sur une chaleur et des bilans de matière des cinq échangeurs de chaleur constituant un PACAS : générateur, condensateur, amortisseur, vaporisateur, et échangeur de chaleur de solution.

Le fluide de fonctionnement des deux prototypes est l'eau - LiBr et a une capacité de refroidissement de 10kW. La station d'approvisionnement pour les deux unités fournit l'eau chaude (à l'aide d'un réchauffeur électrique), le refroidissement et l'eau réfrigérée en utilisant l'eau municipale.

Ce modèle calcule le rendement du PACAS à une opération régulière de statut par la méthode de Newton-Raphson qui résout une série non-linéaire simultanée d'équations pour atteindre la solution. Les propriétés physiques de la solution de LiBr (densité et enthalpie) sont calculées par les équations disponibles dans la littérature.

Les sept variables entrées pour ce modèle sont :

- Température de l'eau chaude à l'entrée du générateur

- Débit de l'eau chaude du générateur
- Température de l'eau froidissent à l'entrée de l'absorbeur
- Débit de l'eau froidissent de l'absorbeur
- Température de l'eau réfrigérée à l'entrée de l'évaporateur
- Débit de l'eau réfrigérée à l'entrée de l'évaporateur
- Débit de solution riche

Les douze paramètres de rendement sont :

- Température de l'eau chaude à la sortie du générateur
- Température de l'eau froidissent à la sortie de l'absorbeur
- Température de l'eau froidissent à la sortie du condenseur
- Température de l'eau réfrigérée à la sortie de l'évaporateur
- Température de la solution riche à l'entrée du générateur
- Température de la solution pauvre à la sortie du générateur
- Température de la solution riche à la sortie de l'absorbeur
- Température de la solution pauvre à l'entrée de l'absorbeur
- Température du frigorigène au condenseur
- Température du frigorigène à l'évaporateur
- Solution a riche concentration en LiBr
- Solution a pauvre concentration en LiBr

En ayant ces paramètres, la charge thermique de chaque échangeur de chaleur et le Coefficient de Performance (COP) ont pu être facilement calculés.

Afin de valider l'exactitude et la fiabilité de ces résultats, ils sont comparés avec des données expérimentales (pour les mêmes valeurs d'entrée). Chaque paramètre est mesuré pour une période donnée pendant l'expérience et montre des fluctuations même lorsque l'état d'équilibre est atteint. La valeur moyenne pour ces paramètres et l'écart type est calculée et comparée aux résultats calculés.

On a également produit un autre modèle qui a le même algorithme mais le nombre d'équations est plutôt différent (19 équations). En comparant les résultats de ce modèle et le modèle suggéré par ce travail et les données expérimentales, nous pouvons

constater que l'exactitude du modèle dans ce travail est supérieure et plus proche des valeurs expérimentales. Alors la sensibilité de ce modèle sur plusieurs paramètres est étudiée. Ces paramètres sont :

- Le coefficient de transfert de chaleur (over all)
- Des arrivées d'eau chaude, froide et réfrigérée

L'effet est étudié à partir de la charge thermique de chaque échangeur de chaleur et COP du système. Cette étude est également comparée à la publication relative qui confirme la validité de cette étude.

La comparaison entre les expériences, la simulation et également littérature montre une bonne concordance entre les résultats et la fiabilité de ce modèle.

TABLE OF CONTENTS

DEDICATION	IV
ACKNOWLEDGMENTS	V
RÉSUMÉ	VI
ABSTRACT	VIII
CONDENSÉ EN FRANÇAIS	IX
TABLE OF CONTENTS	XII
LIST OF TABLES	XVI
LIST OF FIGURES	XVII
LIST OF SYMBOLS AND ABBREVIATIONS	XIX
LIST OF APPENDICES	XXI
CHAPTER 1 : INTRODUCTION	1
1.1. Heat pumps	1
1.1.1. Overview	1
1.1.2. Types of heat pumps	2
1.1.3. Coefficient of Performance (COP)	2
1.2. Absorption heat pump	3
1.2.1. AHP components	3
1.2.2. Unit operation	4
1.2.3. Selection of the working fluids	6
1.2.4. Aqueous-LiBr AHP operation	8
1.2.4.1. Vacuum environment	8
1.2.4.2. Crystallization risk	9
1.2.4.3. Corrosion	10

1.2.5. Coefficient Of Performance (COP).....	10
1.3. Motivation	11
1.4. Objective	11
CHAPTER 2 : LITERATURE REVIEW	13
2.1. Available simulations:.....	13
2.1.1. ABSIM	13
2.1.2. Simulation developed at ZAE Bayern.....	13
2.1.3. Other simulations	14
2.2. Physical properties estimation.....	14
2.2.1. Enthalpy	14
2.2.2. Density	16
2.2.3. Boiling point and vapour pressure	16
2.3. Experimental work	18
2.3.1. Experimental work at TUB and ZAE Bayern.....	18
2.3.2. Experimental work at Polytechnique	19
2.3.3. Other experimental works.....	20
CHAPTER 3 : METHODOLOGY	21
3.1. Prototypes used in this work	21
3.1.1. PACAS prototype absorption heat pump.....	21
3.1.2. Phoenix prototype absorption heat pump.....	29
3.1.3. Prototypes in comparison.....	30
3.1.4. Experimental work	31
3.2. Hypotheses	33
3.3. Heat and mass balance equations	34

3.3.1.	Generator.....	34
3.3.2.	Condenser.....	35
3.3.3.	Evaporator	36
3.3.4.	Absorber	37
3.3.5.	Solution heat exchanger	38
3.3.6.	Overall Energy Balance	38
3.4.	Categorizing the parameters.....	39
3.4.1.	Input/output variables.....	39
3.4.2.	Dependent/independent variables	42
3.5.	Mathematical approach:	43
3.5.1.	Independent equations:.....	43
3.5.2.	Newton –Raphson method	44
3.6.	Algorithm	46
3.7.	Computer program	47
3.7.1.	Output of the program.....	47
3.8.	A second approach	49
3.9.	Comparison of the two models.....	50
3.10.	Comparison of two prototypes performances.....	52
3.11.	Re – calculation of U from the outputs	54
CHAPTER 4 : MODEL VALIDATION		56
4.1.	Experimental results	56
4.1.1.	École Polytechnique.....	56
4.1.2.	TUB.....	60
4.2.	Simulation results	62

4.3. Results Validation	64
4.3.1. Validation with Polytechnique data set.....	65
4.3.2. Validation with TUB data set.....	69
4.3.3. Comparison of the results of two models.....	72
4.3.4. Comparison analysis	73
CHAPTER 5 : SENSITIVITY OF THE MODEL	77
5.1. Heat transfer coefficient	77
5.1.1. Generator.....	78
5.1.2. Evaporator	78
5.1.3. Absorber	79
5.1.4. Condenser.....	79
5.1.5. Solution Heat Exchanger.....	80
5.2. External cycle inlet temperature.....	80
5.2.1. Generator.....	81
5.2.2. Absorber.....	81
5.2.3. Evaporator	82
CHAPTER 6 : CONCLUSION AND RECOMMENDATIONS	83
BIBLIOGRAPHY	86
APPENDIX.....	88

LIST OF TABLES

Table 1-1 Comparisons of water-LiBr and water-Ammonia.....	7
Table 3-1 PACAS, overall heat transfer coefficient and heat transfer area	22
Table 3-2 Calculated and estimated h -values for heat transfer coefficient U.....	24
Table 3-3 Phoenix AHP exchanger design.....	30
Table 3-4 Comparison of UA between two prototypes.....	31
Table 3-5 Recalculations of U from experimental and simulated values.....	55
Table 4-1 Set1 results from experimental studies at École Polytechnique.....	57
Table 4-2 Experimental results obtained from phoenix prototype	60
Table 4-3 First estimation used valid for most calculations.....	63
Table 4-4 Computed values for hypothetical input parameters.....	64
Table 4-5 Results from an overflowing in evaporator, PACAS.....	66
Table 4-6 Comparison between experiments and simulation, RUN AC4.....	67
Table 4-7 results from an overflowing in evaporator, PACAS.....	70
Table 4-8 Comparison of experiments and two simulations.....	72
Table 5-1 Input parameters.....	77

LIST OF FIGURES

Figure 1-1 Energy transformation in heat pumps.....	1
Figure 1-2 Single effect AHP.....	4
Figure 2-1 Dühring plot for a single effect Water – LiBr equilibrium chart.....	18
Figure 3-1 PACAS.....	22
Figure 3-2 Side view of the four main heat exchangers.....	26
Figure 3-3 Overview of the supply station.....	27
Figure 3-4 Phoenix Absorption Heat Pump.....	29
Figure 3-5 Example of the results of experimental studies at TUB.....	32
Figure 3-6 Examples from experimental results from Ecole Polytechnique.....	33
Figure 3-7 Inlet and outlet streams in the generator.....	35
Figure 3-8 Inlet and outlet streams in the condenser.....	36
Figure 3-9 Inlet and outlet streams in the evaporator.....	36
Figure 3-10 Inlet and outlet streams in the absorber.....	37
Figure 3-11 Inlet and outlet streams in the solution heat exchanger.....	38
Figure 3-12 Overall system boundary for heat balance.....	39
Figure 3-13 Input Streams.....	40
Figure 3-14 Output Streams.....	41
Figure 3-15 Additional Parameters.....	42
Figure 3-16 Flowchart of the calculation.....	47
Figure 3-17 Comparisons of heat exchangers U.A between two prototypes.....	52
Figure 3-18 Comparison of heat exchangers load between two prototypes for same input parameter values	53
Figure 4-1 External cycles temperatures (poly).....	58
Figure 4-2 Internal temperatures (poly).....	58
Figure 4-3 External cycle flowrate (poly).....	59
Figure 4-4 Rich and Poor Solution concentration (poly).....	59
Figure 4-5 External cycle temperature (TUB).....	61

Figure 4-6 Solution-refrigerant cycle temperature (TUB).....	61
Figure 4-7 Rich and poor solution concentrations (TUB).....	62
Figure 4-8 Heat load of each heat exchanger (TUB).....	62
Figure 4-9 Fluctuation of the flowrate in hot water pump.....	74
Figure 4-10 Fluctuation of the flowrate in refrigerant pump.....	74
Figure 4-11 Fluctuation of the hot water temperature.....	75
Figure 4-12 Fluctuation of the chilled water inlet temperature.....	75
Figure 4-13 Poor solution leaving the generator (set 1, TUB).....	76
Figure 5-1 Effect of generator heat transfer coefficient on load and COP.....	78
Figure 5-2 Effect of evaporator heat transfer coefficient on load and COP.....	78
Figure 5-3 Effect of absorber heat transfer coefficient on load and COP.....	79
Figure 5-4 Effect of condenser heat transfer coefficient on load and COP.....	79
Figure 5-5 Effect of SHX heat transfer coefficient on load and COP.....	80
Figure 5-6 Effect of hot water inlet temperature on load and COP.....	81
Figure 5-7 Effect of cooling water inlet temperature on load and COP.....	81
Figure 5-8 Effect of chilled water inlet temperature on load and COP.....	82

LIST OF SYMBOLS AND ABBREVIATIONS

\dot{Q}	Power	kW
\dot{m}	Mass flowrate	kg/s
T	Temperature	K
C_p	Heat capacity	$\frac{kJ}{kg \cdot K}$
$LMTD$	Logarithmic Mean Temperature Difference	—
U	Overall heat transfer coefficient	$\frac{kW}{m^2 \cdot K}$
A	Heat transfer area	m^2
X	LiBr concentration	$\frac{wt}{wt} \%$
h	Enthalpy	kJ
P	Pressure	kPa
COP	Coefficient Of Performance	
A, B	Dühring coefficients	
μ	Arithmetic average	
σ	Standard deviation	
Subscription		
G	Generator	

<i>A</i>	Absorber
<i>C</i>	Condenser
<i>E</i>	Evaporator
<i>SHX</i>	Solution Heat Exchanger
1,2, ...	Number of the stream
<i>r</i>	Rich solution
<i>p</i>	Poor solution
<i>Ref</i>	Refrigerant

LIST OF APPENDICES

Appendix A: Computer program.....	88
Appendix B: P&ID of the AHP.....	96
Appendix C: Results.....	97
Appendix D: h and U calculations.....	118
Appendix E: Input and output variables measured from PACAS Prototype.....	120
Appendix F: Calculations of U from outputs.....	121

CHAPTER 1 : INTRODUCTION

1.1. Heat pumps

1.1.1. Overview

Heat pumps are technical devices that transfer thermal energy from a low temperature level to a high temperature level. This transfer can only be accomplished with an energy input in form of either work or heat in order to satisfy the second law of thermodynamics as Clausius stated. The type of energy input used – work or heat – changes the technology needed to provide the heat pumping function.

The general heat pumping process through mechanical or thermal energy input is shown in figure 1-1 by F. Ziegler (1997). Here, in order to compare the two driving energy inputs, the work input is represented on a temperature axis as heat at infinite temperature. This representation is admissible, due to the high exergy content of mechanical energy compared to thermal energy. P is the mechanical power (work input or output), Q is thermal energy (heating or cooling), T is Temperature. (+) means energy (mechanical or thermal) input and (-) means output.

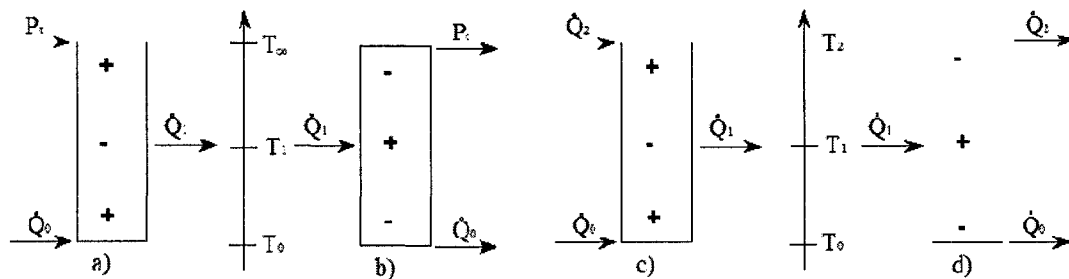


Figure 1-1: Energy transformation in heat pumps: a) mechanical compression chillers and heat pumps; b) mechanical compression heat transformer (ORC – Organic Rankine Cycle); c) sorption chillers and heat pumps; d) sorption heat transformers.

1.1.2. Types of heat pumps

As shortly seen above there are various types of heat pumps available. The most common types used in industrial or commercial applications are:

- a) Vapour Recompression Heat Pumps (VRHP)
- b) Absorption Heat Pumps (AHP)
- c) Adsorption Heat Pumps

The difference is in the type of energy used to enable this transfer. Furthermore each type has its own applications, advantages and disadvantages.

Absorption heat pumps have several advantages comparing to VRHP which could be summarized as:

- Upgrading the available and low grade heat.
- Low operating and maintenance costs.

The drawbacks of AHPs are:

- Bulky and heavy equipments
- Expensive cost of purchase and installation.

1.1.3. Coefficient of Performance (COP)

COP is an important parameter for heat pumps. Depending on the application and the driving power, COP is calculated differently. Following are few examples of calculation of COP for different heat pump types:

Vapour Recompression heat pump:

$$COP = \frac{\text{Heat output}}{\text{Mechanical power input}}$$

Chiller:

$$COP = \frac{\text{Cooling output}}{\text{energy(work or heat) input}}$$

For a typical AHP used as a chiller COP is approximately 0.7 to 1.0. The theoretical value of COP for a typical VRHP used for heating is between 2 to 5.

1.2. Absorption heat pump

Absorption Heat Pumps (AHP) are being used since late 19th century and numerous researches have been performed to improve this technology. However there has been a high interest in absorption technology during the past two decades. The recent studies mainly include methods of intensification, implementation in a process, finding new working fluids, creating the characteristic curves of AHPs and etc.

Contrary to VRHP, absorption heat pumps do not use mechanical power for operation. AHPs use what is also called thermal pumping to transfer the heat.

AHPs operate with a pair of working fluid, where one fluid is the refrigerant and the other fluid is the absorbent. A few examples of these working pairs are ammonia – water (water is the absorbent and ammonia is the refrigerant) or water – aqueous LiBr (where water is the refrigerant and aqueous LiBr is the absorbent).

By using the “thermal pump” refrigerant is transferred from low pressure to higher pressure by absorbing into the solution (absorbent) and pumping it to a higher pressure.

In order to understand the operation of this machine, the components and the unit operation is described.

1.2.1. AHP components

A single effect absorption heat pump is comprised of the following components:

- Heat exchangers:
 - Absorber
 - Generator
 - Evaporator
 - Condenser
 - Solution Heat Exchanger (SHX)
- Refrigerant expansion valves
- Pumps:
 - Refrigerant pump
 - Solution pump

1.2.2. Unit operation

The steady state operation of a single effect absorption heat pump with the binary working fluid water–LiBr is described by *Herlod et al.* (1996) as follows and is illustrated in figure 1-4:

NOTE: Rich solution is the solution which has a high concentration of refrigerant (water). Poor solution has lower concentration of absorbent (LiBr solution).

“Rich solution” (stream 10), leaves the absorber as a saturated mixture at its boiling temperature and is pumped into the generator where heat is supplied by external means (input) such as hot water, steam, combustion or any other source with a sufficiently high temperature. The required temperature is governed by the properties of the working fluid and the operation of the other components in the machine. This temperature is the highest temperature observed in the operating AHP.

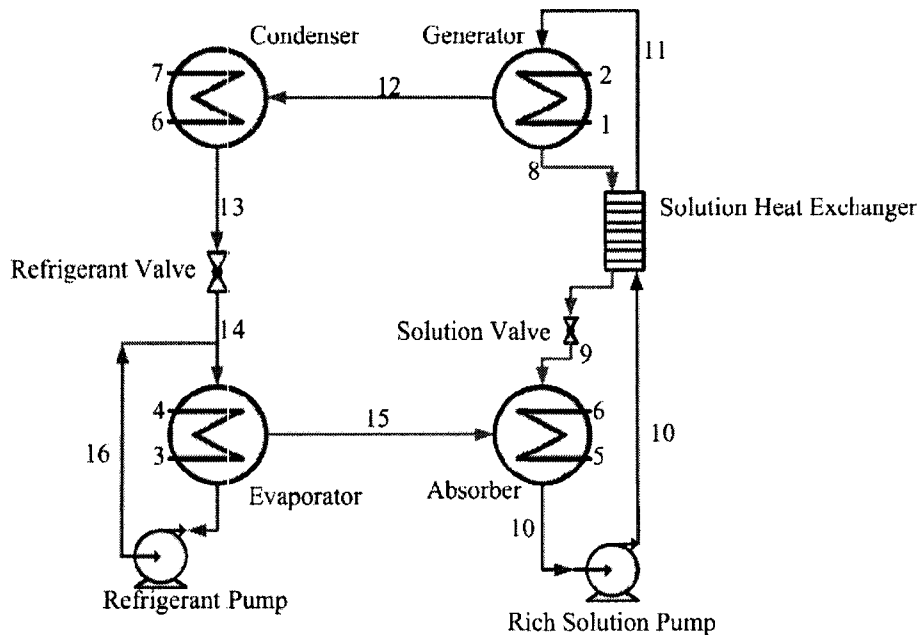


Figure 1-2: Single effect AHP

When heat is applied to the rich solution (at the boiling point), water is vaporised and flows to the condenser (stream 12). Since the solution vaporises as the *falling film* flows over the tubes, and the boiling solution is a very concentrated mixture of water and salt,

the temperature of the vapour varies from point to point. However the bulk temperature of the generated vapour in the generator is the saturated vapour temperature at the operating pressure.

It is assumed that the salt is not carried away by the droplets and the vapour consists of pure water. A demister is placed between generator and condenser to catch the droplets and only allows the vapour to pass through. Although a very small trace amount of the salt exists in the vapour which could cause corrosion in the machine, but at this point it is reasonable to assume that vapour is purely water. Due to the partial evaporation, the remaining solution has a high concentration of LiBr (poor solution, X_p wt%).

The poor solution (Stream 8) which is also at equilibrium state (boiling temperature) flows back to the absorber; on the way it passed through a Solution Heat Exchanger (SHX), often called Economizer, to pre-heat the rich solution (stream 10). No phase change occurs during the energy exchange between these two liquids. The purposes of this exchanger are to reduce the external heat input in the generator and to reduce the quantity of rejected heat in the absorber. The design of this heat exchanger has a major impact on the design of the generator.

The poor solution from the solution heat exchanger returns to the absorber (stream 9). This solution is subcooled due to energy transfer in SHX. In the absorber this stream mixes with the vapour exiting the evaporator (stream 15). By removing the excessive energy the absorption occurs. As the vapour is absorbed into the solution, it creates a more concentrated solution in the refrigerant (rich solution) which returns to the generator (stream 10, X_r wt%).

As the refrigerant vapour leaves the generator (stream 12), it enters the condenser where it is condensed by rejecting the latent heat to a cooling stream. In a typical installation, the absorber and condenser reject heat to the same stream (stream 6) at approximately same temperature. This condensate (stream 13) leaves the condenser and throttled through a choke valve. This process which is an adiabatic flashing causes the temperature to drop dramatically and produces a two-phase flow of the refrigerant (stream 14). The two-phase refrigerant flow then enters the evaporator. Evaporation

takes place, which takes the required latent heat from the evaporator environment due to the low pressure created by the absorber. Complete evaporation implies that all of the refrigerant vaporises and flows to the absorber as vapour (stream 15).

The absorption cycle is a closed cycle.

1.2.3. Selection of the working fluids

Working fluid plays an important role in the absorption systems, therefore selecting the right working pair is extremely crucial. Various conditions dictate the selection of the suitable absorbent/refrigerant pair. A proper working pair should satisfy the following criteria:

- Non-corrosive to equipment within the operating conditions
- Non-toxic
- Harmless to environment
- Non flammable and non explosive
- Cheap and easily accessible

According to Alefeld (1982), a suitable refrigerant for an absorption system should have the following characteristics:

- Mass and heat transfer properties satisfactory over the operating temperature range.
- High solubility in absorbent solution at the absorber operating temperature.
- Low solubility in absorbent at the generator operating range.
- No irreversible reaction with absorbent within operating temperature range.
- Absorbent should have a low vapour pressure compared with the refrigerant.
- Absorbent should have a low heat capacity.

Many working fluid pairs have been considered for absorption systems which satisfy most of the above mentioned criteria. A few examples are:

- Water – sodium hydroxide
- Water – sulphuric acid
- Ammonia – sodium thiocyanate

- Water – aqueous lithium bromide
- Water – ammonia
- Others...

However the most commonly used working pairs are ammonia–water and water–LiBr. Since water LiBr has a temperature constraint (water is the refrigerant and can not reach temperatures below zero) this working pair is usually used for air conditioning systems. However water ammonia can reach temperatures below zero.

Alefeld (1982) and Hainsworth (1944) have summarized a comparison between water – ammonia and water LiBr which is shown in table 1-1.

Table 1-1: comparisons of water-LiBr and ammonia-water

Property	Water – Ammonia	Water – Aqueous LiBr
Refrigerant	Ammonia	Water
High latent heat	Good	Excellent
Vapour pressure	Too high	Too low
Low freezing temperature	Excellent	Limited application
Low viscosity	Good	Good
Absorbent	Water	LiBr solution
Low vapour pressure	Poor	Excellent
Low viscosity	Good	Good
Mixture		
No solid phase	Excellent	Limited application
Low toxicity	Poor	Good
High affinity between refrigerant and absorbent	Good	Good
Temperature lift	High	Low

1.2.4. Aqueous-LiBr AHP operation

1.2.4.1. Vacuum environment

An absorption heat pump with aqueous lithium bromide operates at subatmospheric pressure. The pressure levels are determined by the vapour pressure characteristics of the working fluids. Since essentially pure water exists in the condenser and evaporator, the temperature of operation of these components defines the pressure. For example, for an evaporator temperature of 5°C, the corresponding vapour pressure of water is 0.872 kPa or approximately 0.009 atm.

The low pressures in an absorption system are initially attained by pumping out the air and any other gases from the vapour space. Dissolved gases in the liquids must also be removed. The presence of dissolved and unwanted gases is important since they negatively affect the performance of the system as they occupy the space where water could be vaporised. These gases also could affect the boiling temperature of the water. This removal occurs naturally if enough time is allowed for the gases to diffuse out of the liquid into the evacuated vapour space.

As the vacuum pump extracts gases from the vapour space, both unwanted gases and some water vapour are removed. The amount of the water vaporized due to vacuum could be easily replaced in order to maintain the required level for the operation. Removing the water vapour from the chiller environment has the following effects:

- As the water vapour evaporates from the water surface, it sweeps the vapour space, removing all unwanted gases from the system. Although the system pressure never falls below the vapour pressure of the liquids in the system, the purging effect of the evaporating vapour is highly effective in reducing the partial pressure of the gases in the system to the necessary levels.
- In an oil-lubricated vacuum pump, the water vapour tends to condense in the exhaust stages of the pump and to end up in the oil sump. This condensate reduces the lubrication of the oil and eventually causes damages to the pump. By

monitoring the discoloration of the lubrication oil or adding a cold trap (before the water gets to the pump), this negative effect could be avoided.

- To reach the required pressure level in an absorption heat pump, various vacuum pumps are available. The main requirement is the ability to remove vapour at the vapour pressure level.
- Condenser and generator are in same pressure level, the same applies for evaporator and absorber. The pressure level in condenser/generator is higher than absorber/evaporator. The pressure difference and arrangement of the vessels allow the fluids to flow without any need for extra pumps, hence extra power consumption.

1.2.4.2. Crystallization risk

Aqueous Lithium Bromide has advantages comparing to other solutions (chapter 1.3.3). However, there are few restrictions such as crystallization which could result in damages to the system and system shutdown. The nature of the salt solution is that the salt component precipitates when the mass fraction of the salt exceeds the solubility limits. The solubility limit is a strong function of the mass fraction and temperature and a weak function of the pressure. Supersaturation can occur where the salt content of the liquid is greater than the solubility limit. Once crystals begin to form it will be a favourite nucleation site for larger crystals to grow on themselves, nevertheless no other nucleation sites presence.

Various methods can be used to minimize the possibility of crossing the phase boundary. The simplest method used is to ensure a sufficiently low temperature sink for cooling the absorber. Based on the properties of aqueous lithium bromide, low temperatures in the absorber require lower absorber solution concentration and thus tend to avoid the phase boundary.

Since crystallization produces a slush-like, viscous liquid, it results in blocking the pump or drying the generator.

Water cooled absorption machines generally can operate without crystallization problems. However, crystallization occurrence requires considerable time and effort to correct. The preferred recovery method is to raise the temperature of the portion that is crystallized to a point where the viscosity is reduced sufficiently so that the pumps can circulate the solution. Once the solution is in circulation, it can be easily diluted using water from the evaporator. In a typical installation, manufacturers include controls to identify crystallization and take appropriate action to avoid the condition by reducing heat input to the generator or by diverting liquid water from the evaporator to the absorber to dilute the solution.

1.2.4.3. Corrosion

In the presence of dissolved oxygen, aqueous LiBr is highly aggressive to many metals including carbon steel and copper. Although, in the hermetic environment inside an absorption machine, very little oxygen is present and corrosion rates are much slower. For the temperature range a typical single effect application, carbon steel and copper are the preferred materials of construction. Over the extended life of a machine, significant corrosion can still occur (or in case of improper operation). In order to minimize the effect, there are primary measures available such as pH control or corrosion inhibitors.

1.2.5. Coefficient Of Performance (COP)

Absorption heat pumps are used for different purposes. For example they could be used as a chiller which is very common for residential or commercial air conditioning systems, or they could be used to transfer and upgrade heat in a process.

As previously described (chapter 1.1.3), in either case, the COP is calculated differently. By considering equations (1.X) and (1.Y):

As an AHP:

$$COP = \frac{\text{Heat output}}{\text{Heat input}} = \frac{\dot{Q}_A + \dot{Q}_C}{\dot{Q}_G}$$

As a chiller:

$$COP = \frac{\text{Cooling output}}{\text{Heat input}} = \frac{\dot{Q}_E}{\dot{Q}_G}$$

To calculate the COP presented in this work the latter is used. COP of a typical absorption chiller is in a range of 0.60 to 0.80. For heating purposes COP of a typical AHP is in a range of 1.00 to 1.30. However various operating conditions could affect this value.

1.3.Motivation

The accelerated development of absorption heat pumps in the last two decades has created a need for reliable and effective computer simulations. With recent growing trend of implementing an AHP into a process, it is crucial to be able to predict performance characteristics, analyze thermal behaviour, and perform parametric studies of AHPs.

Several system-specific computer models have been developed in recent years, using all-purpose simulations HYSYS, ASPEN, CADSIM and etc. However these simulations are restricted in their capabilities and limited to the particular system for which they were created. Their structure usually does not allow further modifications to model other systems and they generally do not contain the library for ordinary working pairs used for absorption systems, Water–LiBr in particular. Therefore these softwares are unusable for absorption systems.

The lack of accessibility to a simulation which provides the thermal behaviour of an AHP is the motivation to create a model which is easy to use, could be modified for further studies and for different applications.

A case in which this model could be very helpful is the economical assessment of AHP integration in a process.

1.4.Objective

The objective of this work is to develop a mathematical model of the prototype absorption heat pumps which are introduced in chapter 3. This model presents the

thermal behaviour of the prototypes. The simulation is based on heat and mass balances of the prototype in general and each component separately.

To reach this objective the following steps are taken:

- Develop a mathematical model to calculate the performance parameters of an AHP. The reference units are two prototype AHPs. These units are single effect absorption chillers with working fluid of aqueous LiBr and are available at Polytechnique and TUB.
- Validate the outputs of this model against the experimental results obtained by both prototypes. These experimental studies should cover a wide range of the operation to obtain comprehensive amount of data.
- Determine the sensitivity of the model to the quality of the measurements.
- Evaluate the accuracy and reliability of this model by comparing with another existing model (inspired by the model developed at ZAE Bayern).
- Evaluate the sensitivity of the model on the design parameters of the machine. These parameters are heat transfer coefficient (U) and heat transfer area (A) of each heat exchanger.
- Compare this evaluation to the sensitivity analysis in the literature.
- Compare two prototypes from a design point of view and observe the effects of these differences on the performance of each prototype.

CHAPTER 2 : LITERATURE REVIEW

2.1. Available simulations:

A few models for an AHP are available which are briefly introduced with their advantages and drawbacks:

2.1.1. ABSIM

The computer code ABSIM created by Grossman et al. (2001) has been developed for simulation of absorption systems in a flexible and modular form, making it possible to investigate various cycle configurations with different working fluids. Based on a user-supplied cycle diagram, working fluid specification and given operating conditions, the program calculates the temperature, flowrate, concentration, and pressure and vapour fraction at each state point in the system and the heat duty at each component. The modular structure of the code is based on unit subroutines links the components together according to the cycle diagram. The system of equations for the entire cycle is thus established, and a mathematical solver routine is employed to solve them simultaneously. Property subroutines contained in a separate database serve to provide thermodynamic properties of the working fluids. ABSIM has been employed over the past few years by many users worldwide to simulate a variety of absorption systems in different multi-effect configurations and working fluids.

Since the original code was MS DOS compatible, A Windows version has recently been developed. It makes it possible to create the cycle diagram on the computer screen, supply the data interactively, observe the results superimposed on the cycle diagram and plot them.

The disadvantage of this model is the high price of the software.

2.1.2. Simulation developed at ZAE Bayern

This simulation which is available for users at ZAE Bayern and TUB was developed for simulating the dynamic behaviour of the AHP and calculations regarding the heat transfer coefficient of the heat exchangers. This simulation was developed with EES

(Engineering Equation Solver, a software which provides numerical solution for complicated equations systems) to solve the heat and mass balance equations by a numerical method. Neuhann (2003) and Kohrt (2005) have used these equations and hypotheses for their work. Moreover a similar model is published in “Absorption chillers and heat pumps” written by Herold et al. (mass and energy balance equations). The details of this model are not available to public (such as the specific numerical method used) and are not published. However the hypotheses and the governing equations are available.

2.1.3. Other simulations

There are few other simulations made for specific purposes. *Xu et al.* (2007) have developed a numerical simulation of an advanced energy storage system and patented (VMETS) to predict the mass changes in two storage tanks. This model helps the system design and controlling systems of a water-LiBr single stage absorption heat pump with storage tanks.

Another numerical simulation was created by *Jeong et al.* (1998) to predict dynamic behaviour of an actual absorption heat pump built in a chemical plant which was built to recover low temperature waste heat (30 - 40°C).

In above mentioned cases the results of the simulations were verified against experimental studies to confirm the reliability of the simulations.

2.2. Physical properties estimation

There are few mathematical models available to estimate the thermodynamic properties of water – aqueous LiBr at high temperature and concentration to be used for computer programming:

2.2.1. Enthalpy

Based on measured data of vapour pressure and heat capacity there are few methods available to calculate the physical properties such as enthalpy, heat capacity, density and etc.

Kaita (2001) has developed the following equation to calculate the enthalpy of water – LiBr for the range of 50-200°C and concentration of 45-65%.

$$h_{LiBr}(T, X) = (A_0 + A_1X)T + 0.5(B_0 + B_1X)T^2 + (D_0 + D_1X + D_2X^2 + D_3X^3)$$

Where:

$$\begin{aligned} A_0 &= 3.462023 & D_0 &= 162.81 \\ A_1 &= -2.679895 \times 10^{-2} & D_1 &= -6.0418 \\ B_0 &= 1.3499 \times 10^{-3} & D_2 &= 4.5348 \times 10^{-3} \\ B_1 &= -6.55 \times 10^{-6} & D_3 &= 1.2053 \times 10^{-3} \end{aligned}$$

McNeely (1997) has suggested the following equation to calculate the enthalpy of the LiBr solution for the range of 16 to 166°C and concentration of 40 to 70 wt%.

$$h_{LiBr}(T, X) = 2.326 \{A + B(1.8T + 32) + C(1.8T + 32)^2\}$$

Where A, B and C are:

$$\begin{aligned} A &= -1.1015.07 + 79.5378 X - 2.358016 X^2 + 0.0303158 X^3 - 1.40026E \\ &\quad - 4X^4 \\ B &= 4.68108 - .3037766 X + 8.448e - 3 X^2 - 1.0477e - 4X^3 + 4.8009E \\ &\quad - 7X^4 \\ C &= -4.9107e - 3 + 3.831E - 4 X - 1.078E - 5 X^2 + 1.3152E - 7 X^3 \\ &\quad - 5.897E - 10X^4 \end{aligned}$$

Feuerecker et al. (1993) have developed the following equations for the range of 0 to 190°C and concentration of 40 to 70 wt%.

$$h_{LiBr}(T, X) = \sum_{n=0}^4 a_n X^n + T \cdot \sum_{n=0}^3 b_n X^n + T^2 \sum_{n=0}^2 c_n X^n + T^3 d_0$$

Where a_n, b_n, c_n, d_0 are:

$$\begin{aligned} a_0 &= -954.8 & b_0 &= -3.293 \times 10^{-1} & c_1 &= -1.5144 \times 10^{-4} \\ a_1 &= 47.7739 & b_1 &= 4.076 \times 10^{-2} & c_2 &= 1.3555 \times 10^{-6} \\ a_2 &= -1.59235 & b_2 &= -1.36 \times 10^{-5} & d_0 &= -2.269 \times 10^{-6} \end{aligned}$$

$$a_3 = 2.09422 \times 10^{-2}$$

$$b_3 = -7.1366 \times 10^{-6}$$

$$a_4 = -7.689 \times 10^{-5}$$

$$c_0 = 7.4285 \times 10^{-3}$$

Comparison between these three works with experimental studies by Kaita (2001) shows that the model presented by Feuerecker et al. (1993) has better accuracy for the practical range used in this work. Hence it was decided to use the Feuerecker et al. model to calculate the enthalpy in this project.

2.2.2. Density

The density of LiBr is calculated from the following empirical equation as a function of temperature and concentration.

$$\rho_{LiBr} = 1145.36 + 470.84X + 1374.79X^2 - (0.333393 + 0.571749X)T$$

X is wt% for example 45% shows a LiBr solution with 45 kg LiBr solved in 55 kg water. T is absolute temperature in degree K.

Since flow meters measure the volumetric flowrate ($\frac{L}{s}$), in order convert the flowrate to mass flowrate ($\frac{kg}{s}$), the density should be calculated at the given temperature and concentration.

2.2.3. Boiling point and vapour pressure

The empirical equations of McNeely (1979), Brunk (1982) and Feuerecker (1993) for the boiling temperature of saturated aqueous lithium bromide solution as a function of the pressure and the condensation are fits in the form of Dühring plot which was presented by Hellman et al. (1996):

$$T(p, X) = A(X) + B(X).T_s(p) \quad (2.1)$$

Where T_s is the saturation temperature of pure water at the pressure p .

The numerically generated data were fitted by Dühring coefficients according to equation 2.1 with the polynomials A and B following form:

$$A(X_i) = \sum_{i=0}^{10} a_i \times X_m^i$$

$$B(X_i) = \sum_{i=0}^{10} b_i \times X_m^i$$

Where a_i and b_i are:

i	a_i	b_i
0	0.0	1.0
1	$+1.6634856 \times 10^{+1}$	$-6.8242821 \times 10^{-2}$
2	$-5.5338169 \times 10^{+2}$	$+5.8736190 \times 10^0$
3	$+1.1228336 \times 10^{+4}$	$-1.0278186 \times 10^{+2}$
4	$-1.1028390 \times 10^{+5}$	$+9.3032374 \times 10^{+2}$
5	$+6.2109464 \times 10^{+5}$	$-4.8223940 \times 10^{+3}$
6	$-2.1112567 \times 10^{+6}$	$+1.5189038 \times 10^{+4}$
7	$+4.3851901 \times 10^{+6}$	$-2.9412863 \times 10^{+4}$
8	$-5.4098115 \times 10^{+6}$	$+3.4100528 \times 10^{+4}$
9	$+3.6266742 \times 10^{+6}$	$-2.1671480 \times 10^{+4}$
10	$-1.0153059 \times 10^{+6}$	$+5.7995604 \times 10^{+3}$

Figure 2-1 shows an absorption heat pump in the water – LiBr chart. The horizontal axis presents the temperature (°C) and the vertical axis is the pressure in kPa. The inclined lines are different concentration of LiBr solution in wt%.

By applying the Dühring coefficients the following equations state the saturation state of the streams as a function of the refrigerant temperature and the LiBr concentration.

T_8 is the temperature of the poor solution leaving the generator and T_{10} is the temperature of the rich solution leaving the absorber. T_C is the condenser temperature and T_E is the evaporator temperature.

$$T_8 = A(X_p) + B(X_p).T_C \quad (2.2)$$

$$T_{10} = A(X_r) + B(X_r).T_E \quad (2.3)$$

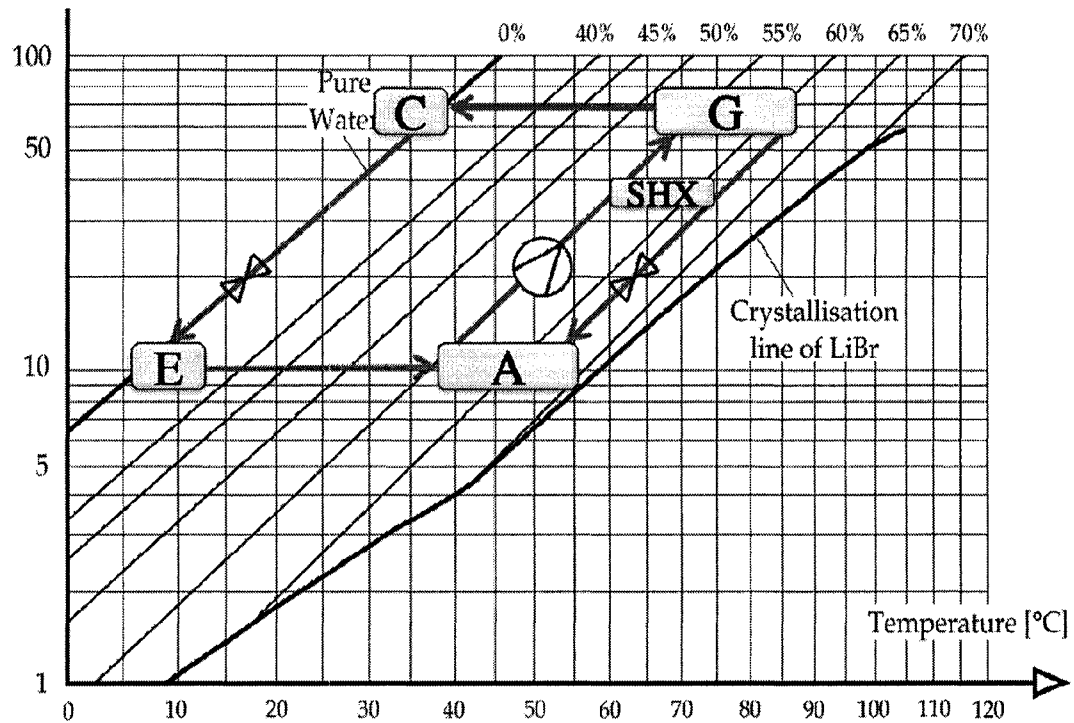


**Figure 2-1: Dühring plot for a single effect
Water – LiBr Equilibrium Chart**

2.3.Experimental work

Numerous experimental studies have been performed with AHPs. There are various objectives for these experiments such as the behaviour of a commercial air conditioning or improving the performance of an existing AHP.

2.3.1. Experimental work at TUB and ZAE Bayern

The department of Energy at Technical University of Berlin dedicates an extensive amount of research on AHPs. These studies could be categorized as follows:

- Creating characteristic curves of tri-generation system: Tri-Generation system is basically an engine which creates mechanical power and heating (via the engine cooling system) which is coupled to the prototype chiller. The author had the opportunity to perform a few experimental benchmarks with this system.

- Measuring the performance of an AHP with low temperature driving energy: these experimental studies are used to observe the behaviour of a commercial absorption chiller used in a building. The driving energy is provided by a solar heating system located on the roof of the building. The hot water created by this system is 40 – 60°C.

There are also several other experimental studies currently in progress which are classified with TUB and partners.

2.3.2. Experimental work at Polytechnique

The experimental studies at Ecole Polytechnique de Montréal could be summarized as follows:

- A statistical experimental design was carried out by A. Jahnke et al. (2005) in order to characterise the machine operation under extreme working conditions as permitted by the physical properties of the working solution and to rank the main effects of the operating variables on the response of the unit. The goal of this experimental plan was to maximise the knowledge about this system.

The results obtained through these publications were used for validation of the model developed in this work.

- One of the researches currently in progress at Polytechnique is to implement an absorption heat pump in a process, particularly in Pulp and Paper industry.

With the current volatile price of energy and the environmental concerns, the trend is to decrease the amount of energy used and try to upgrade the available (waste) heats in the plant so it could be used in other parts of the process.

By using Pinch Analysis and studying various cases it has been determined that using AHP could have tremendous impact on energy saving in various types of industries.

2.3.3. Other experimental works

There are numerous numbers of studies in progress in most countries on heat pumps. A few examples are as follows:

- An important part of the researches is to find an additive which increases the performance of the AHP. These additives could increase the wettability of the solution to increase the transferred heat in exchangers. Another aspect is to delay the crystallization (for example 250 – 1500ppm MDPA by *J. Dirksen et al. (2001)*). These additives should not negatively affect the AHP. These impacts could be creating foams or increasing the viscosity of the solution.
- AHP intensification is also an interesting topic. Intensification could be briefly described as:
 - Bulk and weight reduction while satisfying the same performance.
 - Reducing the cost and improving the efficiency.

The main focus is on Absorber and Generator. Various approaches have been tested and published. However not all methods are practical. A few examples of the most effective methods which increase the heat load and eventually the COP of an AHP are:

- Surface treatment: In macro scale, shape treatment and in micro scale by roughness treatment of the heat exchangers the amount of the heat transfer could significantly increase. This method which was studied by J.S Currie (1996) also revised the effect of compact heat exchangers to use in AHPs.
- Introducing wave producing surfaces such as mechanical vibration or ultrasonic vibration. This method was suggested by Pribaturin (2003).

CHAPTER 3 : METHODOLOGY

In order to create a mathematical model of the prototype AHPs, first the prototypes are explained. Then to create the mathematical model a few hypotheses are employed and based on these assumptions and heat and mass balances the governing equations are extracted.

3.1.Prototypes used in this work

There are two prototype absorption heat pumps available. These two prototypes have similar designs but there are differences in their construction details. The objectives of creating these prototypes were to perform experimental work and observing the behaviour of an AHP under various operating conditions, improving the performance and etc.

The operation of an absorption heat pump has been described in chapter 2. This chapter focuses on the technical characteristics of the prototypes.

3.1.1. PACAS prototype absorption heat pump

This prototype absorption heat pump is a single effect water – LiBr AHP (chiller) with a cooling capacity of 15kW (35 kW heating capacity is provided by an electrical heater).

This prototype was designed, developed and constructed in École Polytechnique de Montréal which is part of the project “Pompes A Chaleur A Sorption” (PACAS). It is the first machine of a new experimental facility at École Polytechnique. Figure 3-1 shows PACAS prototype.

A fractional-factorial design with two modalities for seven independent variables was chosen by A. Costa et al. (2003); these variables are temperature and mass flowrate at the generator (hot water), absorber (cooling water). Evaporator (chilled water) as well as the internal solution mass flowrate.

A more detailed plan of the whole machine including the power station and the measurement devices with tags of the different parts is shown in Appendix B.

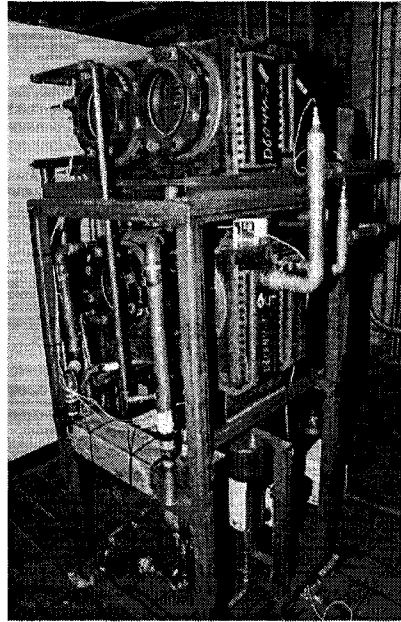


Figure 3-1: PACAS

The overall heat transfer coefficient and heat transfer area for each heat exchanger is presented in table 3-1. These values are calculated by Jahnke et al. (2005)

Table 3-1: PACAS, overall heat transfer coefficient and heat transfer area

Heat Exchanger	Overall Heat Transfer coefficient: $U \left[\frac{kW}{m^2 \cdot ^\circ C} \right]$	Heat Transfer Area: $A [m^2]$
Generator	0.95	2.24
Condenser	2.50	1.25
Evaporator	1.50	2.09
Absorber	0.70	2.51
Solution Heat Exchanger	1.00	2.19

Over all heat transfer value (U) strongly depends on the shape and function of the heat exchanger and also the wettability and behaviour of the fluids in the exchanger.

The heat transfer coefficient is calculated based on the following hypotheses:

- Solution pours over the tube bundle and behaves as falling film. The wetting behaviour ($wet_{A or G or E}$) was taken from publication by L. Hofmann et al. (1996).
- The values were calculated for 3 different tube sizes: 8mm, 12mm and 12.7mm (1/2 in). Then values were chosen based on a 1/2 in copper tube due to practical reasons.
- The chiller provides a cooling capacity of 15 kW. The other heat exchangers, absorber, generator, condenser and solution heat exchanger, have capacities of 19 kW, 20 kW, 16 kW and 14 kW, respectively.
- While the absorber takes up the largest part of the total heat exchanger area (24.4%), evaporator (20.4%), generator (21.8%) and solution heat exchanger (21.8%) are of similar size. The condenser is with only 12.2% of the total surface area by far the smallest of the heat exchangers.
- The exchangers are designed with 9 passes (meaning the number of times one and the same fluid flow passes through the heat exchanger vessel) in evaporator and absorber, 8 in the generator and 6 in the condenser.
- The efficiency of SHX is assumed to be 88%.
- All flow regimes are turbulent.
- COP of the AHP is 0.75.

The values in table 3-2 are calculated by V. Neumann (2003) from the following equation:

$$U = \frac{1}{\frac{r_2}{r_1 \cdot h_i} + \frac{r_2 \cdot \ln\left(\frac{r_2}{r_1}\right)}{K_a} + \frac{1}{h_o}}$$

The details of the calculations (Re, Nu and Pr) are presented in Appendix D.

Table 3-2: Calculated and estimated h -values for heat transfer coefficient U

	$h_i \left(\frac{kW}{m^2K} \right)$	$h_o \left(\frac{kW}{m^2K} \right)$	U calculated $\left(\frac{kW}{m^2K} \right)$	U design value $\left(\frac{kW}{m^2K} \right)$
Generator	1.2	4.185	0.933	1.5
Condenser	10.9	7.195	4.334	0.70
Evaporator	3.5	2.749	1.540	0.95
Absorber	2.2	5.508	1.572	2.50
SHX				1.00

Other characteristics are as follows:

The size is about 1.9 m high, and 0.4 m \times 0.66 m, with a metal frame of 0.8 m \times 0.9 m.

The weight is estimated of 350 kg.

From the sump of the condenser to the distribution device of the evaporator the refrigerant passes a U-tube which has the function of an expansion valve.

A throttle in the connection pipe between generator and absorber is not necessary, since the pressure loss can be achieved through the solution heat exchanger (which is a normal plate heat exchanger).

In Figure 3-2 the four main heat exchangers are shown. In fact the pairs condenser–generator and absorber–evaporator are not separate vessels, but one single component.

This is allowed since the heat exchangers of a pair work at same operational pressures.

This design is advantageous since it ensures an unhindered vapour flow from one heat exchanger of the pair to the other one, achieving an almost pressure loss-free functioning. This is important since the refrigerant (water) shows at the required operational temperatures a very low vapour pressure (around 10 mbar and 100 mbar).

On the left side of figure 3-2 the pair condenser/generator can be seen. The picture is a cut through the component. The circles represent horizontal heat exchanger tube bundles, the external water circuits (cooling and hot water) flow inside the tubes. On the right top the solution is sprinkled on the tubes of the generator. It will drop from the higher tubes to the lower tubes. As in the tubes is hot water, the water in the solution

will evaporate and the water vapour expands to the left, to the condenser. It has to pass metal plates (the demister) which can be seen as rectangular lines in the middle. They are used to hold back liquid drops.

On the bottom in the middle a double-wall structure can be seen. It separates the sumps of the components from each other.

The right-hand side of Figure 3-2 shows the evaporator/absorber pair. The arrangement of the tubes in the vessel is also has a similar design as the generator/condenser. However the number of the tubes is different.

The solution distribution simply consists of copper tubes of the same size as the bundle tubes. In the top part is a line of holes, which permits the solution to exit at equal distances. Above the tube is a V-shaped rod which forces the solution to change direction and flow down. The solution then drops on the first row of the bundle. As the holes are on the top of the tube, it is less likely for dirt particles to block the flow.

Refrigerant in the evaporator is recirculated in a recirculation circuit. Water from the evaporator sump is pumped back to the distribution device and applied on the heat exchanger surface area again. That way the wetting is much better and more water can be evaporated. The drawback is, that in order to run the pump electricity is consumed, and that with an increasing recirculation flow rate, the heat losses are higher.

The flow rate of the recirculated water and the flow rate of the solution circuit can be controlled by diaphragm valves bypassing the pumps.

A purging system allows purging air out of the machine. Purging tubes are going to the condenser, evaporator and absorber.

Purging from the evaporator and condenser is only possible, when the machine is not running. Tubes go to an area close above the sump.

In addition purging tubes go to the condenser and absorber between the heat exchanger tube bundles a little higher. This system allows purging while the machine is in function. Between the evaporator recirculation circuit and the solution circuit a shortcut is built. Normally it is closed by a valve. It can be opened to flush the evaporator from solution

or to dilute the solution circuit in case that the solution becomes too concentrated and close to crystallization.

Between the machine and the vacuum pump a condensate trap with liquid nitrogen cooling is placed to protect the vacuum pump from vapour.

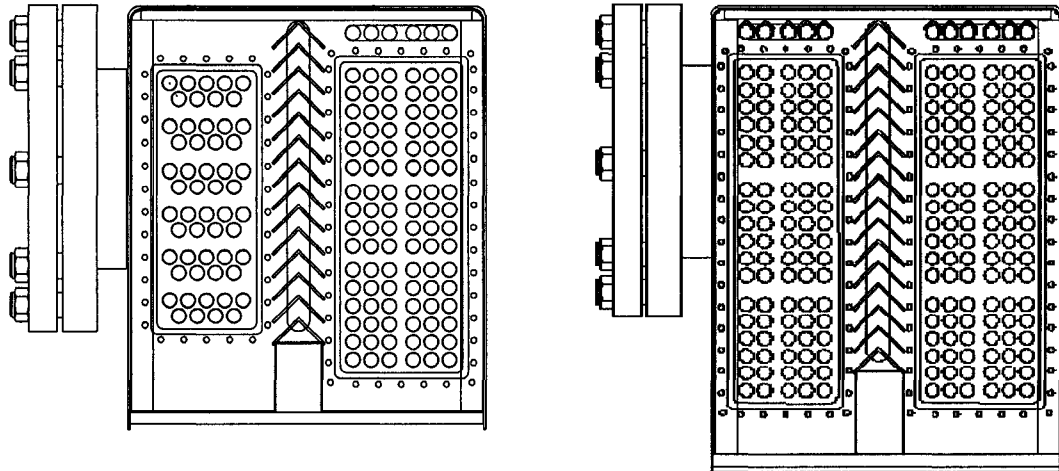


Figure 3-2: Side view of the four main heat exchangers: left: condenser/generator; right: evaporator/absorber

Power station

In order to provide the driving energy, cooling water and chilled water, a power station is designed and built for this heat pump.

The power station is connected to the absorption cooling machine with three different water circuits. Figure 3-3 illustrates the external circuits which provide the power required for the prototype.

The hot water circuit is connected to the generator and supplies the driving heat. Three heaters of 10 kW heating capacity each heats up water to a set-point temperature. It enters the generator, gives its heat to the solution, is pumped back to the heaters, and there is reheated again. The power of the heaters is controlled by the generator inlet temperature (in the picture it has 95 °C).

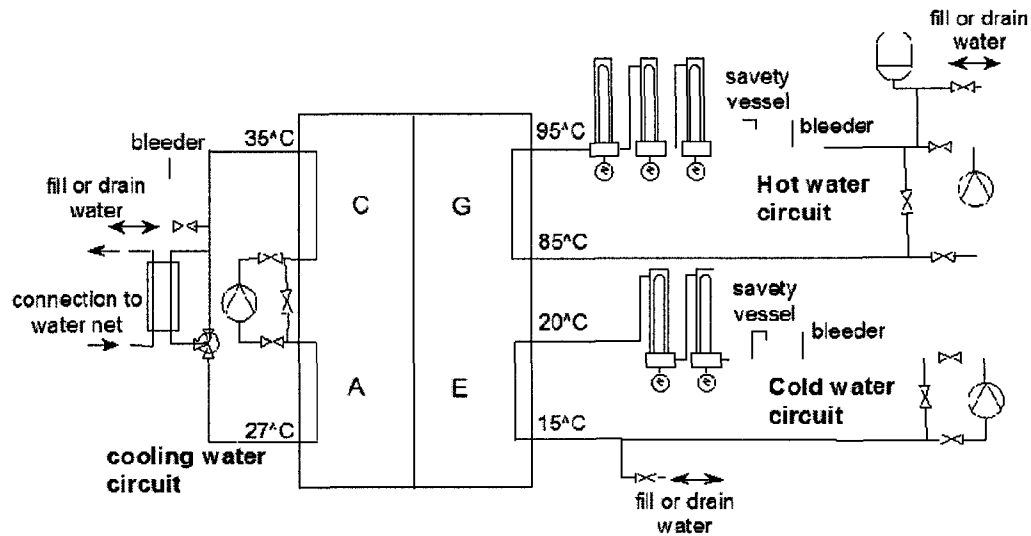


Figure 3-3: Overview of the supply station

As the density substantially changes with the temperature an expansion container is necessary.

A safety valve opens in case the pressure in the circuit rises above the safe level. This could happen under certain conditions, for example if by accident the heaters are heating, but the pump is not running. Water starts to boil in matter of seconds. This is quite dangerous as the water coming out of the hot water circuit is very hot and can burn a person standing next to the machine. In worse cases it could cause explosion in the heater or the pipes connected to it.

The circuit has been equipped with a drain. A bleeder allows removing air from the circuit.

The cold water circuit simulates the user. It could be for example a house that needs cooling and receives loads due to people living in the building and from solar radiation. These loads are simulated by two heaters of 10 kW heating capacity each. The working principle is the same as for the hot water circuit.

The cooling water circuit cools the absorber and condenser. It is connected in series: First the absorber is cooled and then the condenser. Normally the loop is connected to an external cooling tower. As no cooling tower was available it has been simulated. The

cooling circuit is connected over a plate heat exchanger to the water net of École Polytechnique. Water from the net is constantly running through the heat exchanger. The amount of this water is controlled by a manual valve. A three way valve on the side of the cooling water circuit is used to control the absorber inlet temperature.

The flow rates of each water circuit can be changed by slider valves and also by different settings of the pumps. Before and after the pumps ball valves were installed to allow easy removal of the pumps.

Three water recirculation pumps are used in the power station. These pumps are centrifuge pumps. The flow is controlled by a control gate valve placed at the discharge of the pump.

The solution pump is a gear pump which operates with a magnetic drive. The advantage of this pump is a seal free drive which provides a hermetically enclosed environment emission free and ideal for handling dangerous or valuable liquids.

To avoid cavitation these pumps are positioned at lowest possible point to ensure sufficient NPSH (Net Positive Suction Head).

Overflow problem

First measurements with PACAS prototype showed in certain conditions system is not responding (steady state could not be reached) and it fails to operate. Furthermore under several other conditions the output (heat load of the exchangers and COP) of the machine is lower than expected values.

Further studies which were performed during an internship by Martin Kohrt (2005) showed there is an anomaly in liquid hold up in lower vessel (Evaporator/Absorber). Depending on these conditions refrigerant overflows from the evaporator into the absorber. Hence the evaporation does not take place and this will result in significant decrease of the heat load of the evaporator (and therefore COP).

PACAS was tested under 20 different settings and the machine failed only four times. The other 16 measurements were flawless and machine was running as expected. The setting under which the machine was tested is presented in appendix E.

3.1.2. Phoenix prototype absorption heat pump

The other prototype was designed, developed and built in ZAE Bayern – Germany (Bavarian Center for Applied energy research) and now is available in Technical University of Berlin (TUB).

This prototype, which is called Phoenix AHP, is also a single effect AHP with Water – LiBr as the working pair. The following information is published by Kühn et al. (2005). Figure 3-4 is a display of the phoenix AHP. This absorption chiller has a nominal cooling power of 10KW at inlet conditions of 75°C hot water, 27°C cooling water and Absorber inlet and 18°C chilled water at evaporator inlet. The COP at these nominal conditions is 0.78.

The objective of this prototype was to couple with low grade heat systems such as a solar water heater or cogeneration system (couple with an engine to produce heat, power and cooling).

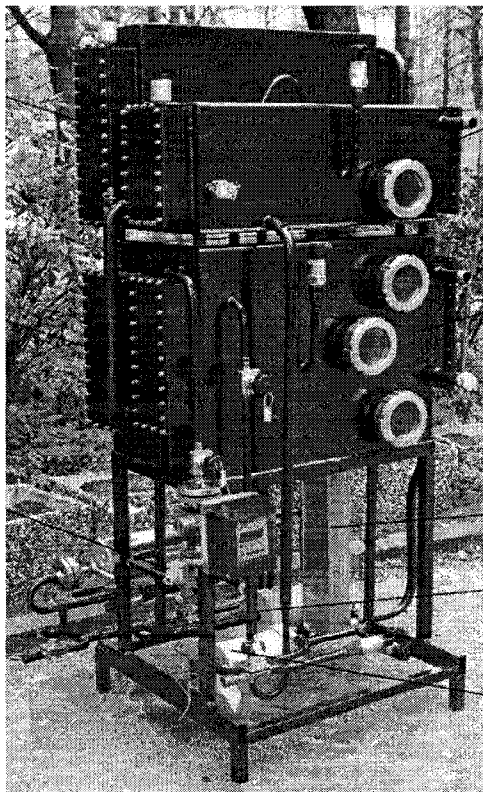


Figure 3-4: Phoenix Absorption Heat Pump

The general operating conditions of this chiller are as follows:

- Low driving hot water between 55 and 95°C, allowing solar and tri-generation operation
- High cooling water temperature between 27 and 40°C allowing wet and dry cooling.
- Compact design matching standard door size.
- Using falling film tube bundle heat exchanger in rectangular vessels.
- Vertical arrangement of the two vessels allows the backflow of the weak solution from generator to the absorber without the need for the second solution pump

The overall heat transfer coefficient and heat transfer area for each heat exchanger is presented in table 3-3.

Table 3-3: Phoenix AHP exchanger design

Heat Exchanger	Overall Heat Transfer coefficient: $U \left[\frac{kW}{m^2 \cdot ^\circ C} \right]$	Heat Transfer Area: $A [m^2]$
Generator	0.78	2.5
Condenser	2.88	1.3
Evaporator	1.6	1.6
Absorber	0.76	2.3
Solution Heat Exchanger	0.74	1.13

Since the details of the design of this prototype are classified with TUB, only the published data is described.

However since the design and the flow sheet diagram is similar to PACAS, the unit operation is also similar.

3.1.3. Prototypes in comparison

Since the unit operation of two prototypes are similar and the differences are in size and material used in the exchangers, the only difference between these two are in the heat

transfer area and overall heat transfer coefficient. Table 3-4 presents both prototypes heat transfer area and overall heat transfer coefficient to compare the values.

Table 3-4: Comparison of $U \times A$ [$\frac{kW}{^{\circ}C}$] between two prototypes

Parameter	PACAS	Phoenix
$U \times A$ Generator	2.13	1.95
$U \times A$ Condenser	3.13	3.74
$U \times A$ Evaporator	3.14	2.56
$U \times A$ Absorber	1.76	1.75
$U \times A$ Solution Heat exchanger	2.19	0.84

Since PACAS was designed at École Polytechnique, the materials and construction were different from the prototype built in ZAE Bayern. For examples the diameters of the hot water, cooling water and chilled water tubes inside the exchangers are different. These differences cause the $U.A$ differences between two prototypes.

Since the diameter of the tubes in the prototype in TUB is $\frac{3}{4}$ inch and in Ecole Polytechnique is $\frac{1}{2}$ inch the Us are different.

It should be mentioned that, to enhance the performance of the prototype, the solution heat exchanger was improved in a way so the $U.A$ is 2.6 times more than the SHX in phoenix prototype. Later on the effects of these differences are discussed.

3.1.4. Experimental work

Both prototypes were subjected to numerous tests and data from all the stream was gathered through data acquisition system.

The experimental results from the prototype at Polytechnique is gathered and processed by Jahnke et al. (2005). The experimental results from the prototype at TUB is gathered and processed by the author during an internship in spring 2007 in Technical University of Berlin.

The data acquisition system which is used for both machines is LABVIEW. This software collects the data from all transmitters such as temperature, pressure, flowrate and density every 12 seconds and generates a text file in which each set of data makes a line. Hence, for an operation of 30 minutes, a file comprised of 150 lines is created.

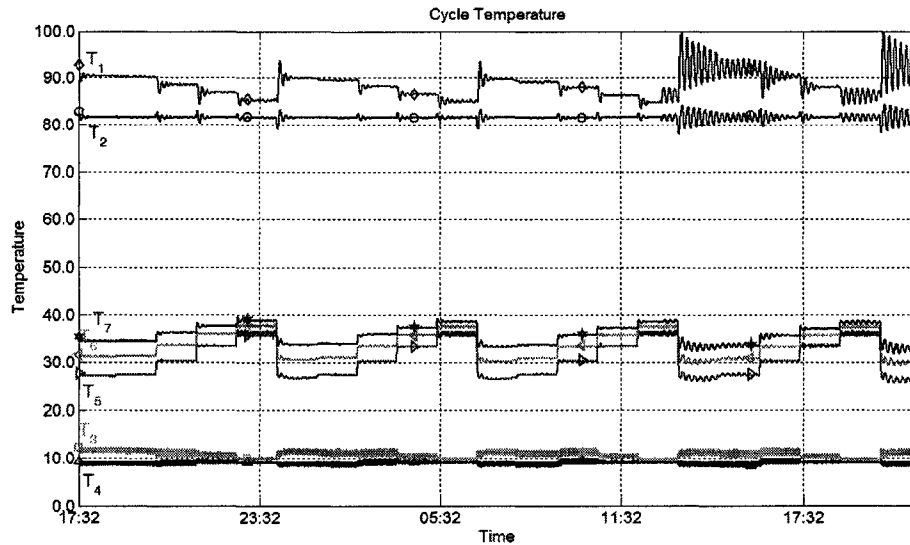


Figure 3-5: Example of the results of experimental studies at TUB

A MATLAB code is created at TUB to analyze the obtained data from each experiment.

This code reads the file and creates graphs which illustrate required parameters.

Figure 3-5 is an example of a set of experiments which was performed at Technical University of Berlin.

The results from experimental studies performed at École Polytechnique were also stored in several files. However they are processed and analyzed in EXCEL. Figure 3-6 is an example of the experimental data from Polytechnique.

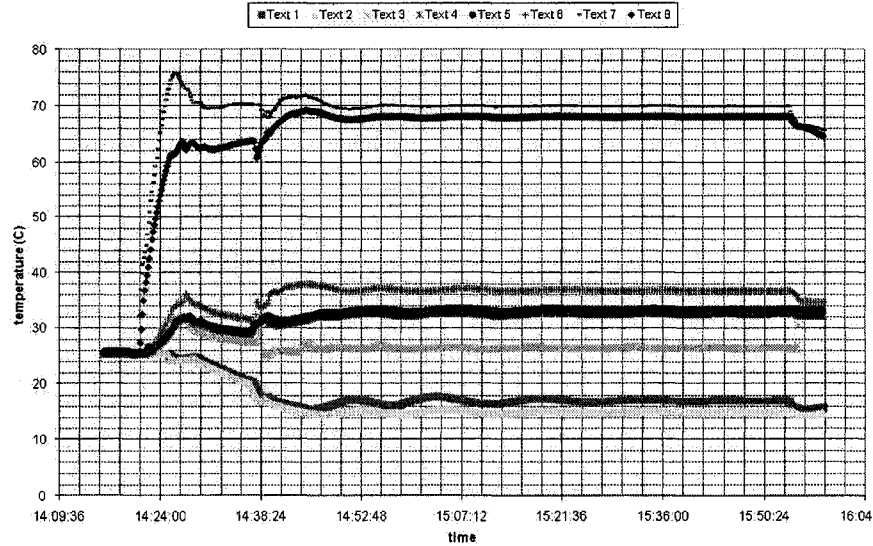


Figure 3-6: Example from experimental results from Ecole Polytechnique.

3.2.Hypotheses

The following assumptions are made to facilitate and explain the parameters involved in calculations. The hypotheses are as follows:

- i. The pressure drop in the refrigerant valve results in temperature drop in the refrigerant. The pressure drop in refrigerant line is *isenthalpic* and therefore
- ii. The solution sumps and streams leaving the vessels in the exchangers are at equilibrium. Hence the equations 2.1 and 2.2 are used for saturated state at the given temperature for the refrigerant and given temperature and concentration for the solution.
- iii. All the lines and exchangers are insulated and there is no significant heat loss from the machine to the environment.
- iv. The effect of the pumps on the temperature of the fluid is negligible. (solution and refrigerant pump)
- v. Refrigerant vapour is condensed isothermally in the condenser and subcooling does not take place, therefore:

$$T_{13} = T_{12} = T_c$$

- vi. The refrigerant condensate in the evaporator evaporates isothermally and there is no super heating, hence

$$T_{14} = T_{15} = T_E$$

- vii. The poor solution valve is fully open during the process; hence the pressure drop (and consequently temperature drop) is zero.
- viii. The refrigerant loop contains water only. (streams 12, 13, 14 and 15)
- ix. The process is established and at steady state, hence there's no accumulation in sumps.
- x. Water heat capacity C_p is assumed to be constant and the value is $4.20 \frac{kJ}{kg^\circ C}$. The heat capacity is varying from a minimum value of $4.178 \frac{kJ}{kg^\circ C}$ (at 307.5 K) to $4.217 \frac{kJ}{kgK}$ (at 373 K). These values are available in Perry's Handbook.

This change is very insignificant (less than 1%) hence this assumption hardly affects the final results.

Considering the assumptions the governing equations of the prototype AHP can be extracted.

3.3.Heat and mass balance equations

The prototype absorption heat pump is comprised of five major elements which brings five sets of energy and mass balances. Since the external cycles enter and exit the system respectively the overall balance only consists of the general energy balance. The repeated equations for LiBr mass balance are only showed in the generator equation series.

Heat and mass balances are as follows:

3.3.1. Generator

Figure 3-7 shows the inlet and outlet streams for the generator.

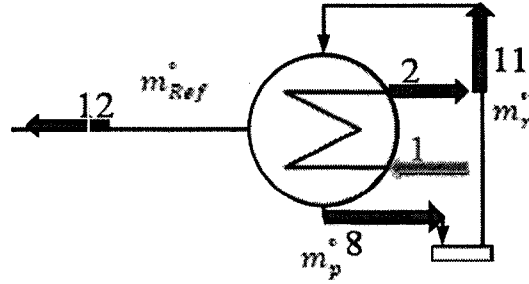


Figure 3-7: inlet and outlet streams in the generator

The general mass balance over the generator is as follows:

$$m_r^\circ = m_p^\circ + m_{Ref}^\circ \quad (3.1)$$

The mass balance over the generator for LiBr is as follows:

$$m_p^\circ \cdot X_p = m_r^\circ \cdot X_r \quad (3.2)$$

The heat given to the generator by external cycle is calculated from the following equation:

$$\dot{Q}_G = m_1^\circ \cdot C_{p1} \cdot (T_1 - T_2) \quad (3.3)$$

The energy balance over the generator is:

$$\dot{Q}_G = m_{Ref}^\circ h_{12} + m_p^\circ h_8 - m_r^\circ h_{11} \quad (3.4)$$

Generator is a heat exchanger and the heat transfer equation will be expressed as:

$$\dot{Q}_G = U_G \cdot A_G \cdot LMTD_G \quad (3.5)$$

Where $LMTD_G$ is:

$$LMTD_G = \frac{(T_1 - T_8) - (T_2 - T_{11})}{\ln \left(\frac{T_1 - T_8}{T_2 - T_{11}} \right)} \quad (3.5A)$$

3.3.2. Condenser

Figure 3-8 shows the inlet and outlet streams for the condenser.

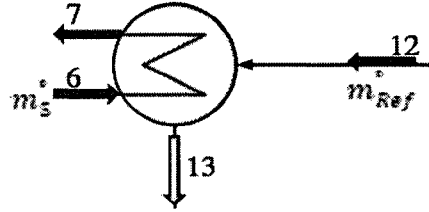


Figure 3-8: inlet and outlet streams in the condenser

The heat taken from the condenser by external cycle is calculated from the following equation:

$$\dot{Q}_C = m_5^* \cdot C_{p5} \cdot (T_7 - T_6) \quad (3.6)$$

The energy balance over the condenser is:

$$\dot{Q}_C = m_{Ref}^* \cdot (h_{12} - h_{13}) \quad (3.7)$$

As a heat exchanger the heat transfer equation for condenser will be expressed as:

$$\dot{Q}_C = U_C \cdot A_C \cdot LMTD_C \quad (3.8)$$

Where $LMTD_C$ is:

$$LMTD_C = \frac{(T_6 - T_7)}{\ln \left(\frac{T_C - T_7}{T_C - T_6} \right)} \quad (3.8A)$$

3.3.3. Evaporator

Figure 3-9 shows the inlet and outlet streams for the evaporator.

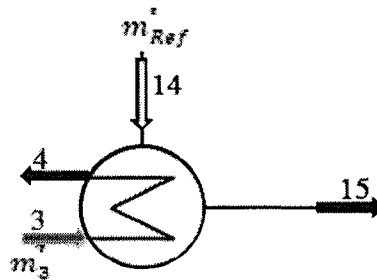


Figure 3-9: inlet and outlet streams in the evaporator

The heat given to the evaporator by external cycle is calculated from the following equation:

$$\dot{Q}_E = \dot{m}_3 \cdot C_{p3} \cdot (T_3 - T_4) \quad (3.9)$$

The energy balance over the evaporator is:

$$\dot{Q}_E = \dot{m}_{Ref} \cdot (h_{15} - h_{14}) \quad (3.10)$$

As a heat exchanger the heat transfer equation for the evaporator will be expressed as:

$$\dot{Q}_E = U_E \cdot A_E \cdot LMTD_E \quad (3.11)$$

Where $LMTD_E$ is:

$$LMTD_E = \frac{(T_3 - T_4)}{\ln\left(\frac{T_3 - T_E}{T_4 - T_E}\right)} \quad (3.11A)$$

3.3.4. Absorber

Figure 3-10 shows the inlet and outlet streams for the absorber.

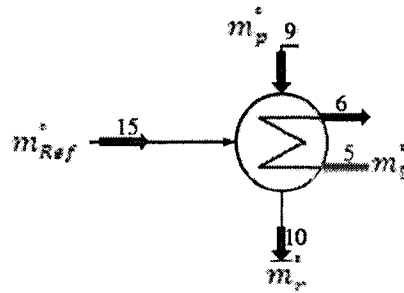


Figure 3-10: inlet and outlet streams in the absorber

The heat taken from the absorber by external cycle is calculated from the following equation:

$$\dot{Q}_A = \dot{m}_5 \cdot C_{p5} \cdot (T_6 - T_5) \quad (3.12)$$

The energy balance over the absorber is:

$$\dot{Q}_A = \dot{m}_{Ref} \cdot h_{15} + \dot{m}_p \cdot h_9 - \dot{m}_r \cdot h_{10} \quad (3.13)$$

As a heat exchanger the heat transfer equation for the absorber will be expressed as:

$$\dot{Q}_A = U_A \cdot A_A \cdot LMTD_A \quad (3.14)$$

Where $LMTD_A$ is:

$$LMTD_A = \frac{(T_9 - T_6) - (T_{10} - T_5)}{\ln \left(\frac{T_9 - T_6}{T_{10} - T_5} \right)} \quad (3.14A)$$

3.3.5. Solution heat exchanger

Figure 3-11 shows the inlet and outlet streams for the absorber.

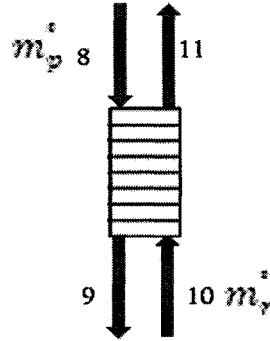


Figure 3-11: inlet and outlet streams in the solution heat exchanger

The heat given by the hot stream is:

$$\dot{Q}_{SHX} = \dot{m}_p^\circ \cdot (h_8 - h_9) \quad (3.15)$$

The heat taken by the cold stream is:

$$\dot{Q}_{SHX} = \dot{m}_r^\circ \cdot (h_{11} - h_{10}) \quad (3.16)$$

The heat transfer equation for the SHX is expressed as:

$$\dot{Q}_{SHX} = U_{SHX} \cdot A_{SHX} \cdot LMTD_{SHX} \quad (3.17)$$

Where $LMTD_{SHX}$ is calculated as follows

$$LMTD_{SHX} = \frac{(T_8 - T_{11}) - (T_9 - T_{10})}{\ln \left(\frac{T_8 - T_{11}}{T_9 - T_{10}} \right)} \quad (3.17A)$$

3.3.6. Overall Energy Balance

The overall system boundary for the energy balance is shown in figure 3-12.

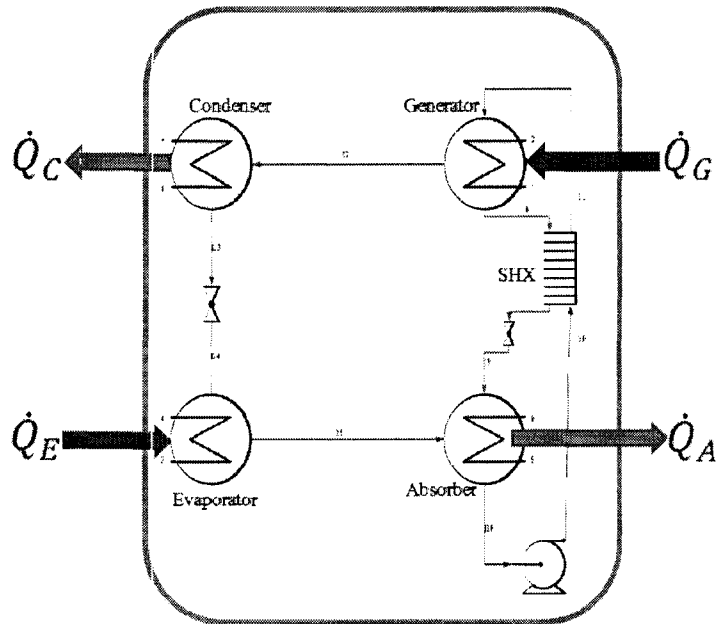


Figure 3-12: overall system boundary for heat balance

The energy balance for this system is:

$$\dot{Q}_A + \dot{Q}_C = \dot{Q}_G + \dot{Q}_E \quad (3.18)$$

3.4. Categorizing the parameters

3.4.1. Input/output variables

This model calculates the *outputs* of the machine for the given *inputs* under steady state operation. The inputs are the parameters which are adjusted by the operator while running the prototypes.

The input variables are:

- 1) Generator hot water *inlet* temperature, stream 1, T_1
- 2) Generator hot water *flowrate*, stream 1, \dot{m}_1
- 3) Evaporator Chilled water *inlet* temperature, stream 3, T_3
- 4) Evaporator chilled water *flowrate*, stream 3, \dot{m}_3
- 5) Absorber cooling water *inlet* temperature, stream 5, T_5
- 6) Absorber cooling water *flowrate*, stream 5, \dot{m}_5
- 7) Rich solution *flowrate*, stream 10, \dot{m}_r

These streams are illustrated in figure 3-13 with green arrows.

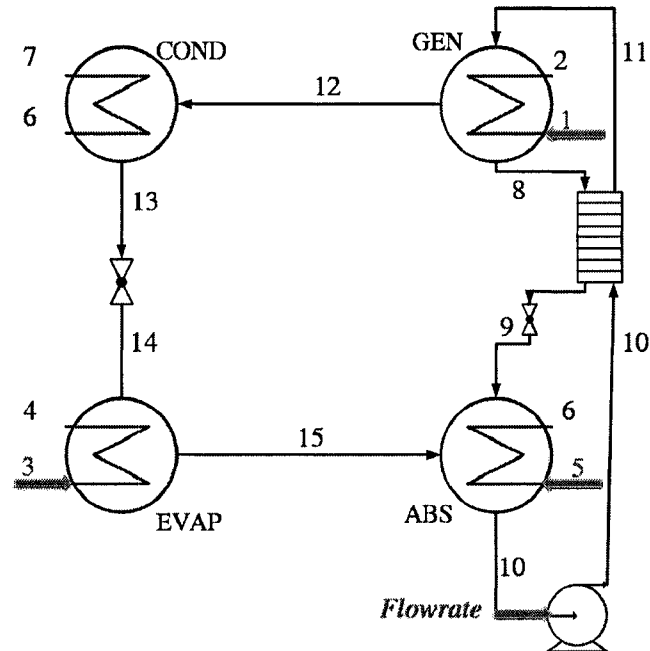


Figure 3-13: Input Streams

The output parameters which will be calculated by this model are as follows:

- 1) Generator hot water *outlet* temperature, stream 2, T_2
- 2) Absorber cooling water *outlet* temperature, stream 6, T_6
- 3) Condenser cooling water *outlet* temperature, stream 7, T_7
- 4) Evaporator Chilled water *outlet* temperature, stream 3, T_4

These streams are illustrated in figure 3-14 with red arrows.

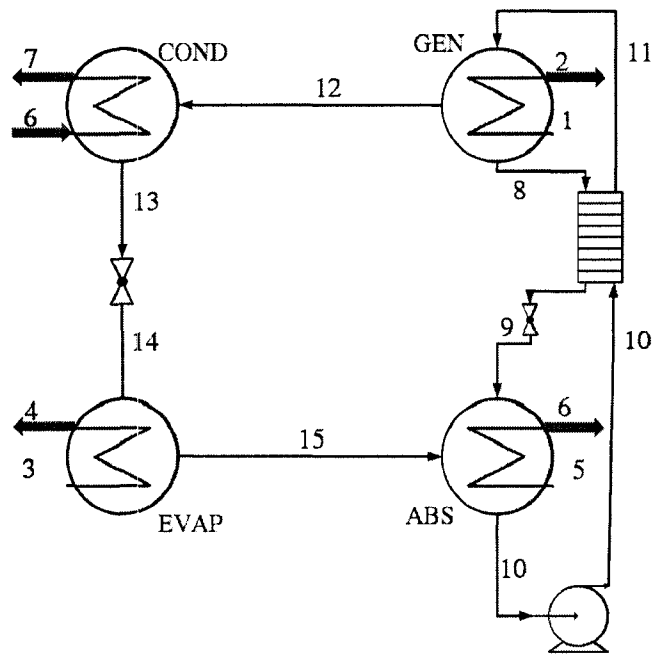


Figure 3-14: Output Streams

In order to be able to solve this problem and calculate all the output parameters, the parameters in all other streams should also be calculated. These parameters are:

- 1) Generator rich solution *inlet* temperature, stream 11, T_{11}
- 2) Generator poor solution *outlet* temperature, stream 8, T_8
- 3) Absorber poor solution *inlet* temperature, stream 9, T_9
- 4) Absorber rich solution *outlet* temperature, stream 10, T_{10}
- 5) Condenser refrigerant temperature, stream 12 and 13, T_C
- 6) Evaporator refrigerant temperature, stream 14 and 15, T_E
- 7) Rich solution LiBr concentration, stream 10 and 11, X_r
- 8) Poor solution LiBr concentration, stream 8 and 9, X_p

These streams are shown in figure 3-15

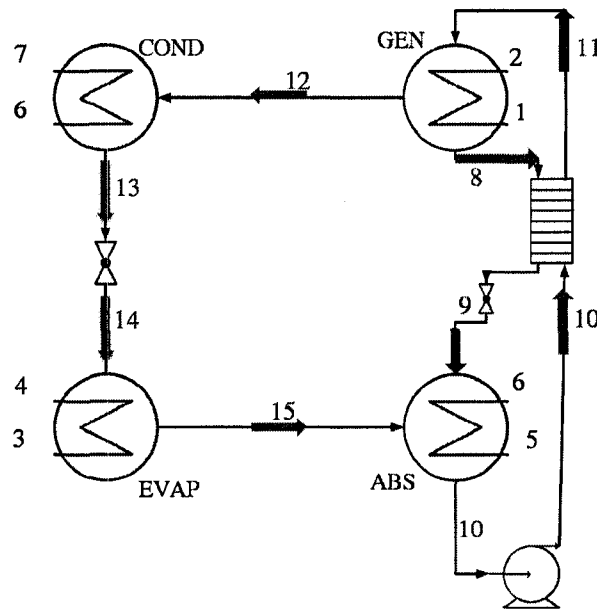


Figure 3-15: Additional Parameters

By computing the outputs of the machine, the following parameters could also be calculated:

- 1) Load of each exchanger : $\dot{Q}_G, \dot{Q}_C, \dot{Q}_A, \dot{Q}_E$
- 2) Coefficient of performance : COP

The latter parameters show the thermal characteristics of the prototype AHPs.

3.4.2. Dependent/independent variables

Based on the nature of the variables they are categorized into three categories:

- I. Constant values: These parameters are the characteristics of each prototype and depend on the design of the machine. These values are:

1) U_G, A_G	4) U_A, A_A
2) U_C, A_C	5) U_E, A_E
3) U_{SHX}, A_{SHX}	6) C_{p1}, C_{p3}, C_{p5}
- II. Input variables: These are the parameters that should be adjusted to operate the prototype and in this model are the input variables of the simulation. These variables are:

- | | |
|----------------|----------------|
| 1) T_1 | 5) \dot{m}_3 |
| 2) T_3 | 6) \dot{m}_5 |
| 3) T_5 | 7) \dot{m}_r |
| 4) \dot{m}_1 | |

III. Output variables: These variables are mathematically independent variables which are obtained through an algorithm and are the results of this model. These variables are:

- | | |
|----------|-------------|
| 1) T_2 | 7) T_{10} |
| 2) T_4 | 8) T_{11} |
| 3) T_6 | 9) T_C |
| 4) T_7 | 10) T_E |
| 5) T_8 | 11) X_r |
| 6) T_9 | 12) X_p |

IV. Dependent variables: These variables are mathematically dependent which are calculated from the output variables. These variables are:

- | | |
|----------------|--------------------|
| 1) \dot{Q}_A | 5) \dot{Q}_{SHX} |
| 2) \dot{Q}_C | 6) COP |
| 3) \dot{Q}_G | 7) \dot{m}_{Ref} |
| 4) \dot{Q}_E | 8) \dot{m}_p |

3.5.Mathematical approach:

To reach the solution for the output values (independent variables) the independent equations must be extracted from equation 3.1 to 3.18. In order to do so, the dependent variables are eliminated from the equation.

3.5.1. Independent equations:

By eliminating the dependent variables from equation 3.1 to 3.18 and using the two equations of state by Dühring the independent equations are extracted which are as the

same number of independent variables. The twelve equations – twelve variable sets of equations are to be solved by a numerical method.

The equations are as follows:

- i.* $T_8 = A(X_p) + B(X_p).T_C$
- ii.* $T_{10} = A(X_r) + B(X_r).T_E$
- iii.* $m_5^\circ.C_{p5}.(T_6 - T_5) - U_A.A_A.LMTD_A = 0$
- iv.* $m_1^\circ.C_{p1}.(T_1 - T_2) - U_G.A_G.LMTD_G = 0$
- v.* $m_3^\circ.C_{p3}.(T_3 - T_4) - U_E.A_E.LMTD_E = 0$
- vi.* $m_5^\circ.C_{p5}.(T_7 - T_6) - U_C.A_C.LMTD_C = 0$
- vii.* $m_r^\circ.(h_{11} - h_{10}) - U_{SHX}.A_{SHX}.LMTD_{SHX} = 0$
- viii.* $m_r^\circ.(h_{11} - h_{10}) - \left(\frac{x_r}{x_p}\right)m_r^\circ.(h_8 - h_9) = 0$
- ix.* $m_5^\circ.C_{p5}.(T_7 - T_6) - \left(1 - \frac{x_r}{x_p}\right).m_r^\circ.(h_{12} - h_{13}) = 0$
- x.* $m_3^\circ.C_{p3}.(T_3 - T_4) - \left(1 - \frac{x_r}{x_p}\right).m_r^\circ.(h_{15} - h_{14}) = 0$
- xi.* $m_1^\circ.C_{p1}.(T_1 - T_2) - m_r^\circ \times \left(\left(1 - \frac{x_r}{x_p}\right)h_{12} + \left(\frac{x_r}{x_p}\right).h_8 \right) - h_{11} = 0$
- xii.* $m_3^\circ.C_{p3}.(T_3 - T_4) + m_1^\circ.C_{p1}.(T_1 - T_2) - m_5^\circ.C_{p5}.(T_7 - T_5) = 0$

3.5.2. Newton –Raphson method

The suitable method to solve the simultaneous nonlinear equations is a numerical solution which is the expanded Newton – Raphson method.

This method (is explained in Appendix D) is easily expandable for a series of k simultaneous nonlinear equations:

$$f_1(x_1, \dots, x_k) = 0$$

$$\vdots$$

$$f_k(x_1, \dots, x_k) = 0$$

The linearization of this set by the application of the Taylor series expansion produces the following equation:

$$\begin{bmatrix} \frac{\partial f_1}{\partial x_1} & \dots & \frac{\partial f_1}{\partial x_k} \\ \vdots & \ddots & \vdots \\ \frac{\partial f_k}{\partial x_1} & \dots & \frac{\partial f_k}{\partial x_k} \end{bmatrix} \begin{bmatrix} \delta_1^{(1)} \\ \vdots \\ \delta_k^{(1)} \end{bmatrix} = - \begin{bmatrix} f_1^{(1)} \\ \vdots \\ f_k^{(1)} \end{bmatrix}$$

In matrix/vector notation this condenses to

$$\mathbf{J}\boldsymbol{\delta} = -\mathbf{f}$$

Where \mathbf{J} is the Jacobian matrix containing the partial derivatives, $\boldsymbol{\delta}$ is the correction vector, and \mathbf{f} is the vector of functions.

Strongly nonlinear equations are likely to diverge rapidly, which in this project is actually the case. To prevent this situation, relaxation is used to stabilize the iterative process. If $\boldsymbol{\delta}$ is the correction vector without relaxation, then relaxed change is $\rho\boldsymbol{\delta}$ where ρ is the relaxation factor:

$$\mathbf{x}^{(n+1)} = \mathbf{x}^{(n)} + \rho\boldsymbol{\delta}^{(n)}$$

The typical value for the equations in this project for ρ is 0.5 to 0.6. The choice of the relaxation factor does not affect the results and it will only change the number of iterations. Lower number of iterations means less time for computation. However the wrong relaxation factor would result into the divergence of the solution or exceeding the maximum number of iterations. Since this model allows a maximum number of iterations of 1000, after reaching this number the program stops and displays a warning “the maximum number of iteration of 1000”.

The convergence criterion is

$$|x^{(n+1)} - x^{(n)}| \leq \epsilon$$

Where in this project

$$\epsilon = 10^{-6}$$

This value was chosen in a way that the number of iterations is reasonable and the convergence occurs when the final solution is changing in the 0.00001 decimal which is accurate enough for this purpose. For values smaller than 10^{-6} (for example 10^{-7}) the number of iterations will be too much. Consequently the duration of the calculation will take too long without effecting the accuracy of the final solution (result will vary in 0.0000001 decimal).

For values larger than 10^{-6} (for example 10^{-4}) the calculations end too soon and the output of the calculations are not accurate enough (0.001).

When the convergence is reached, the last iteration values are the solution to the series of the equations.

3.6. Algorithm

The flowchart to reach the solution to this problem is illustrated in figure 3-16.

The procedure to calculate the outputs are as follows:

- 1) Define the constant parameters which are the characteristics of the prototype.
- 2) Define the input parameters and the relaxation factor.
- 3) Estimate the first values for the output parameters.
- 4) Calculate the enthalpies based on the current values of the parameters.
- 5) Perform the Newton – Raphson method for the set of the equations 6-19 to 6-30.
- 6) Check whether convergence is reached. If no, replace the old values with new values. Repeat step 5. If yes, proceed to the next step.
- 7) State the last results as the values of the output parameters.
- 8) Calculate the heating and cooling capacities and COP of the machine based on the output values.

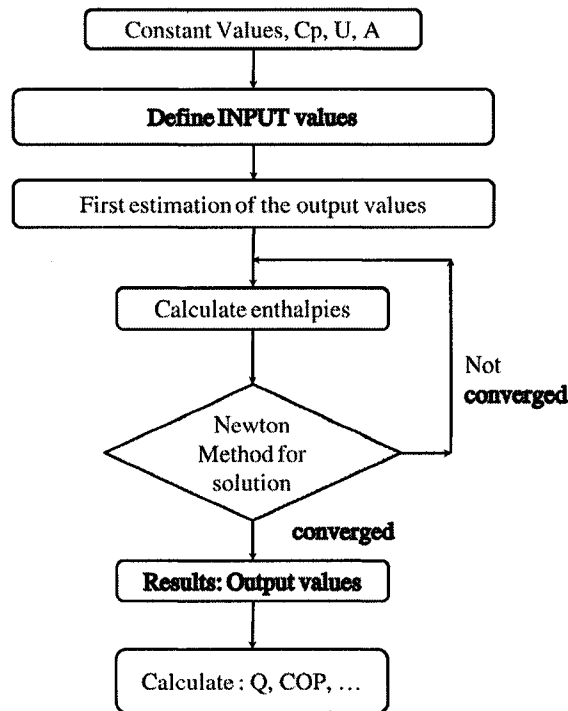


Figure 3-16: Flowchart of the calculation

- 9) It should be noticed, if at anytime, the equations diverged, the relaxation factor, or the first estimates should be changed till convergence reached. Normally the relaxation factor is around 0.5 to 0.6 and maximum number of iterations should be less than 30.

3.7. Computer program

A MATLAB program is written to solve the 12 sets of equations and calculate the output results. The program among all sub routines is presented in appendix A. this program follows the algorithm which is described in the previous chapter.

Each code has its own role in the computation:

3.7.1. Output of the program

As an example, the results are displayed in MATLAB environment as it is illustrated below:

results

T₈ = 79.945

$T_9 = 41.200$

$T_{10} = 35.474$

$T_{11} = 73.679$

$T_7 = 36.574$

$T_4 = 7.888$

$X_r = 0.552$

$T_6 = 32.211$

$T_2 = 79.496$

$T_E = 4.817$

$T_C = 38.350$

$X_p = 0.581$

solution reached after 27 iterations.

This program has been tested for most cases under which the prototypes were expected to operate which are:

- Hot water inlet temperature 50 to 110°C
- Cooling water temperature 18 to 40°C
- Chilled water temperature 6 to 20 °C
- Flowrate of external cycles .01 to 1 kg/sec

For the cases above the suitable relaxation factor is 0.4 to 0.6 and the maximum number of iteration is maximum 55 times.

If the correct relaxation factor is selected the convergence is reached and results will be displayed. Otherwise the solution diverges and “NaN” is displayed. Or in case of exceeding the maximum number of iteration, the user is warned and the program stops.

To ensure that the results on display are reliable, the user could try the iteration by entering two different but close relaxation factors (for example, 0.3 and 0.4 the results would not change for variation of relaxation factor and the first estimated values.

3.8. A second approach

A second model is also created which is based on hypotheses and equations used in the model described in chapter 2.1.2. The purpose of this model is to compare the outputs of both simulations with experimental results. This comparison shows how the hypotheses and using different equations affects the outputs and which one is more accurate.

The governing equations for this model are as follows:

$$i. \quad \dot{Q}_G = m_1^\circ \cdot C_{p1} \cdot (T_1 - T_2)$$

$$ii. \quad \dot{Q}_G = m_{Ref}^\circ h_{12} + m_p^\circ h_8 - m_r^\circ h_{11}$$

$$iii. \quad \dot{Q}_G = U_G \cdot A_G \cdot LMTD_G$$

$$iv. \quad \dot{Q}_C = m_5^\circ \cdot C_{p5} \cdot (T_7 - T_6)$$

$$v. \quad \dot{Q}_C = m_{Ref}^\circ \cdot (h_{12} - h_{13})$$

$$vi. \quad \dot{Q}_C = U_C \cdot A_C \cdot LMTD_C$$

$$vii. \quad \dot{Q}_E = m_3^\circ \cdot C_{p3} \cdot (T_3 - T_4)$$

$$viii. \quad \dot{Q}_E = m_{Ref}^\circ \cdot (h_{15} - h_{14})$$

$$ix. \quad \dot{Q}_E = U_E \cdot A_E \cdot LMTD_E$$

$$x. \quad \dot{Q}_A = m_5^\circ \cdot C_{p5} \cdot (T_6 - T_5)$$

$$xi. \quad \dot{Q}_A = m_{Ref}^\circ \cdot h_{15} + m_p^\circ \cdot h_9 - m_r^\circ \cdot h_{10}$$

$$\text{xii. } \dot{Q}_A = U_A \cdot A_A \cdot LMTD_A$$

$$\text{xiii. } \dot{Q}_{SHX} = m_p^\circ \cdot (h_8 - h_9)$$

$$\text{xiv. } \dot{Q}_{SHX} = m_r^\circ \cdot (h_{11} - h_{10})$$

$$\text{xv. } \dot{Q}_{SHX} = U_{SHX} \cdot A_{SHX} \cdot LMTD_{SHX}$$

$$\text{xvi. } T_8 = A(X_p) + B(X_p) \cdot T_C$$

$$\text{xvii. } T_9 = A(X_p) + B(X_p) \cdot T_E$$

$$\text{xviii. } T_{10} = A(X_r) + B(X_r) \cdot T_E$$

$$\text{xix. } T_{11} = A(X_r) + B(X_r) \cdot T_C$$

3.9. Comparison of the two models

In order to recreate this simulation, a similar algorithm (chapter 3.6) was followed and the only differences are the equations.

1. In the hypothesis the temperature of the refrigerant leaving the generator is equal to the temperature of the poor solution leaving the generator

$$T_8 = T_C$$

According to the experimental studies, it is obvious that there's a temperature difference and the refrigerant vapour produced in the generator has much lower temperature than the poor solution.

The reason this hypothesis was taken in this model is assumed that the rich solution behaves as a pure substance and the vapour temperature is equal to the liquid at equilibrium. However the rich solution is a solution with a high concentration of lithium bromide (55-70 wt%).

In this work, the temperature of the vapour leaving the generator (T_C) is less than the liquid in equilibrium. The explanation is that the vapour is generated by a falling film which passes several passes and each pass has a different temperature which increases as the falling film descends on the tubes containing hot water. All the vapour generated moves to the condenser which has a bulk temperature lower than the poor solution leaving the generator.

2. In this model the streams 9 and 11 are considered to be at saturated state and the boiling temperature is calculated from Dühring equations.

$$T_{11} = A(X_r) + B(X_r).T_C$$

$$T_9 = A(X_p) + B(X_p).T_E$$

But since the streams 8 and 10 are at saturated conditions and their temperatures change significantly in the solution heat exchanger, streams 9 and 11 are no longer saturated.

Introducing these equations to the model shows approximately up to 10% errors in the results.

3. This model uses the average temperature in each vessel, such as:

$$4. \quad T_G = \frac{T_8 + T_{11}}{2}$$

And then the enthalpies are calculated based on these average temperatures. Experimental studies show that the calculated enthalpy values with this method are different than measured values.

5. In this work, the enthalpies are calculated as a function of the temperature of the stream and the concentration (for the absorbent). The models used for these calculations are selected among the most recent and accurate published models to have better results.
6. This model solves the heat and mass balance equations (as stated in chapter 6). The system of the equations consists of 19 unknowns and 19 equations. This model considers the dependent and independent variables the same and solves the simultaneous nonlinear equations by an unknown numerical method (which is the only unknown section of this model). In this model the dependent variables are

eliminated so the system of equations consists of only independent variables and equations.

7. Since this simulation was produced with EES and the details of programming are not published, the numerical method used for this model is unknown. Furthermore the models which the enthalpies are calculated with are not acknowledged. It should be reminded that the selection of the software has no effect on the results.
8. In addition using various numerical methods to reach the solution has resulted in divergence of the solution. Hence the author decided to use MATLAB which facilitates the explanation and adaptability of this model.

3.10. Comparison of two prototypes performances

In this section, a comparison between two prototypes is presented. As it was described in chapter 3.1.3 there are some differences in the design of the two prototypes.

(Please refer to Table 3-1 and Table 3-2)

Due to different designs in construction of the heat exchangers, the heat transfer area is also different in each prototype. The differences in product of $U.A$ are important parameters which should be taken into account for calculations. Figure 3-17 illustrates the differences in the product $U.A$ (values are presented in table 3-3)

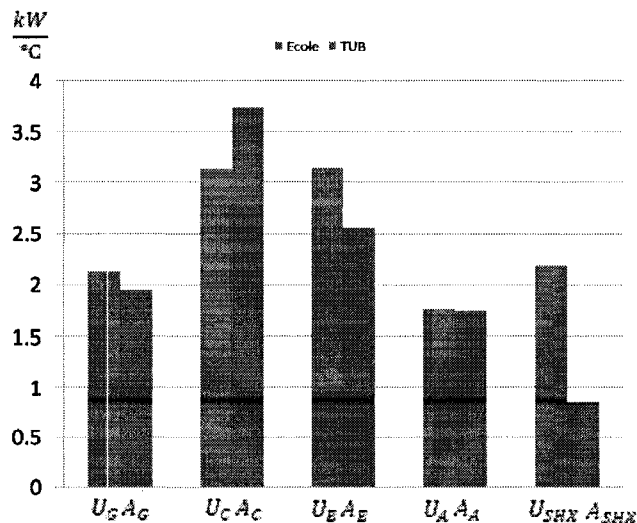


Figure 3-17: Comparisons of heat exchangers $U.A$ between two prototypes

Figure 3-18 presents the comparison of the results for the heat load for each heat exchanger in two prototypes under identical conditions.

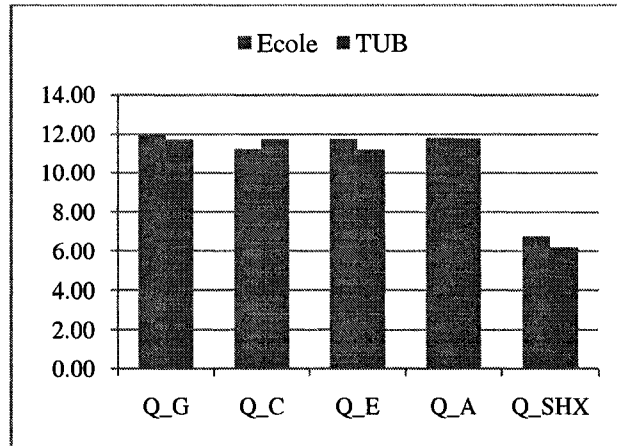


Figure 3-18: Comparison of heat exchangers load between two prototypes for same input parameter values

According to sensitivity study (please see chapter 5) for each heat exchanger, by increasing the heat transfer coefficient (or even the product $U \times A$), the heat loads are increased. By comparing the heat loads and $U \times A$ the effect of this parameter on the heat loads from both prototypes is observed.

However the expected difference in heat load for solution heat exchanger is not as the same order of magnitude as the differences of $U \times A$ and this could be due to the effectiveness of the SHX used in PACAS is lower which also results in lower COP.

Another explanation is that the differences in $U \times A$ is not biased for both prototype. As it is seen $U \times A$ of the generator, evaporator and SHX in the prototype at Polytechnique is larger than the one at TUB while $U \times A$ of condenser of the prototype at TUB is larger than the one at Polytechnique. Absorber in both cases has almost the same values for both prototypes. These differences could affect and dampen other exchanger heat loads.

However as expected COP has close values for both prototypes. As explained in chapter 5, variations in $U \times A$ does not influence the COP. These values are in agreement by both experiment and the model presented in this work.

This comparison shows that by increasing the size or improving the heat transfer coefficient of heat exchangers the heat loads of each exchanger is increased. However these changes do not mean that the COP of the AHP is also increased. In order to improve the performance of the AHP other approaches should be considered and with the current design, these COPs are the best values to be reached.

3.11. Re – calculation of U from the outputs

Another approach to verify the results of the model is to calculate the overall heat transfer coefficient (U) for each heat exchanger based on the temperatures obtained from both model and experiments. By comparing these values to the primary values given to the model and studying the differences it could be summarized whether the results obtained from model and experiments are reliable and the initial values were presenting the real heat transfer coefficient of the exchangers.

To do so the heat load for each heat exchanger is calculated from the following equation:

$$\dot{Q}_i = \dot{m}_i \times C_p \times \Delta T$$

Also the values could be calculated from the following equation:

$$\dot{Q}_i = \dot{m}_i \times \Delta H$$

And the heat transfer coefficient is calculated from the following equation:

$$U_i = \frac{\dot{Q}_i}{A_i \times LMTD_i}$$

These calculations are made for each heat exchanger as well as each set of data. As an example one set of data is presented in table 3-5 and U s are calculated based on both experimental and simulated values.

Table 3-5: Recalculation of U from the experimental and simulated values

Heat Transfer Coefficient	Set 1 – TUB		
	Experiment	Simulation	Difference
U_G	0.82	0.78	- 4.9%
U_C	2.51	2.90	13.3%
U_E	1.22	1.69	28.0%
U_A	0.64	0.76	16.3%

These calculations are performed for all the available experimental data from both prototypes (please see appendix F). The left column shows the values recalculated from the experimental values. The middle column shows the recalculated U values from the simulation which basically must be the same value introduced to the model. (if not it means the convergence was not reached properly)

As expected the values calculated from the simulation are the same values which were introduced to the simulation. However the calculated values from the experiments are rather different from the values introduced to the simulation.

These differences could be explained as follows:

The values for the heat transfer coefficient are calculated under design parameter conditions (design values, page 25 and App. D). In other words, heat transfer coefficient is calculated for a given flowrate and temperature of the fluids involved. By deviating from these values during the experiment, for example by increasing (or decreasing) the flowrate of hot water in the generator (or hot water inlet temperature), U_G will be different from the initial value. These deviations will result in changes in the output results of the simulation.

Unfortunately by reviewing the results of these calculations a solid pattern which could result in a reasonable conclusion did not achieved.

In 50% of the cases (10 out of 20 cases) all the calculated values from experiment are smaller than the design values. In rest of the cases 1 or 2 of the U values are smaller than the design values.

CHAPTER 4 : MODEL VALIDATION

In this section the results from both experimental studies and simulations are presented. The first section the experimental studies by which the results were obtained are explained.

4.1. Experimental results

4.1.1. École Polytechnique

20 sets of data are available from experiments performed by A. Jahnke et al.(2005) from experiments performed at École Polytechnique. However under four specific conditions the steady state couldn't be reached and for three of other conditions the machine had overflowing problem, therefore **13** sets are presented. The complete set of the results are available in appendix E. The data presented has been obtained with following conditions:

- The system operates for 90 minutes since the last adjustment. The system reaches the steady state conditions after approximately 60 – 65 minutes. Then the remaining time is chosen so the data stored by the acquisition system presents the reliable performance conditions.
- This last 20 minutes provides 100 values for each parameter (1 line of data per 12 second). The average and standard deviation of these values are calculated and presented.

As an example one of the results is presented in table 4-1.

Table 4-1: set1 results from experimental studies at École Polytechnique

Input parameters	Run AC4
T_1 (°C)	95.0 ± 0.5
T_3 (°C)	20.0 ± 0.7
T_5 (°C)	30.0 ± 0.7
\dot{m}_1 (kg/sec)	0.612 ± 0.010
\dot{m}_3 (kg/sec)	0.671 ± 0.030
\dot{m}_5 (kg/sec)	0.743 ± 0.030
\dot{m}_r (kg/sec)	0.184 ± 0.011
output	
T_2 (°C)	86.5 ± 0.9
T_4 (°C)	15 ± 1.1
T_6 (°C)	37.1 ± 1.0
T_7 (°C)	43.1 ± 1.2
T_8 (°C)	85.2 ± 1.7
T_9 (°C)	36.0 ± 1.6
T_{10} (°C)	43.1 ± 1.9
T_{11} (°C)	88.0 ± 2.1
T_C (°C)	42.5 ± 1.9
T_E (°C)	8.4 ± 1.2
X_r ($\frac{wt}{wt}$ %)	55 ± 2
X_p ($\frac{wt}{wt}$ %)	58 ± 1
\dot{Q}_G (kW)	21.9 ± 1.7
\dot{Q}_C (kW)	16.9 ± 2.4
\dot{Q}_E (kW)	15.6 ± 2.9
\dot{Q}_A (kW)	20.0 ± 2.3
COP	0.71 ± 0.31

These data was extracted from the experimental results which is displayed in figure 4-1 to figure 4-4

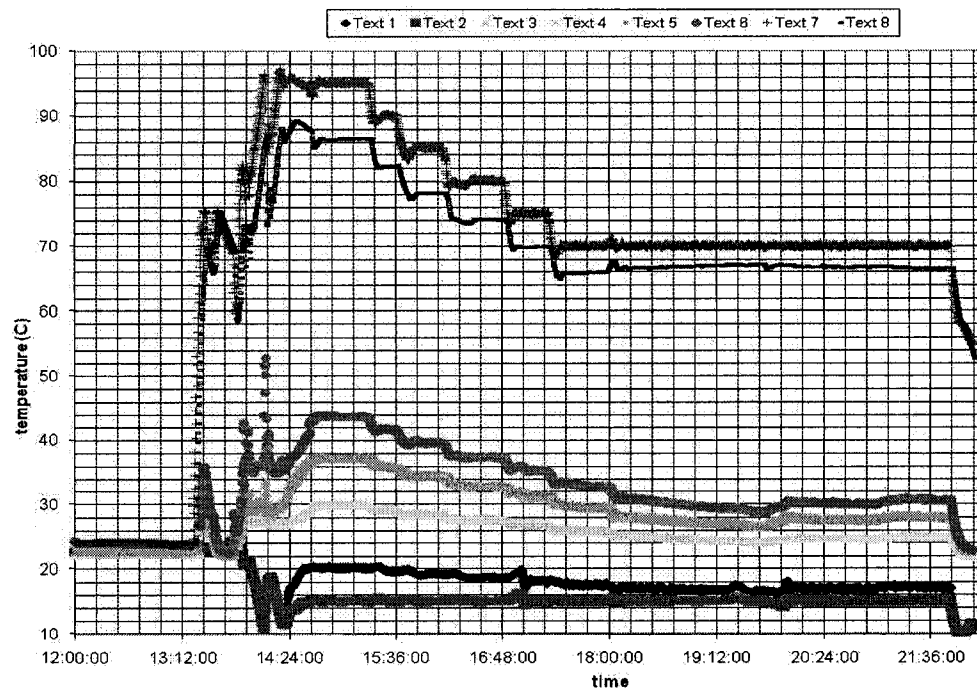


Figure 4-1: External cycles temperatures (poly)

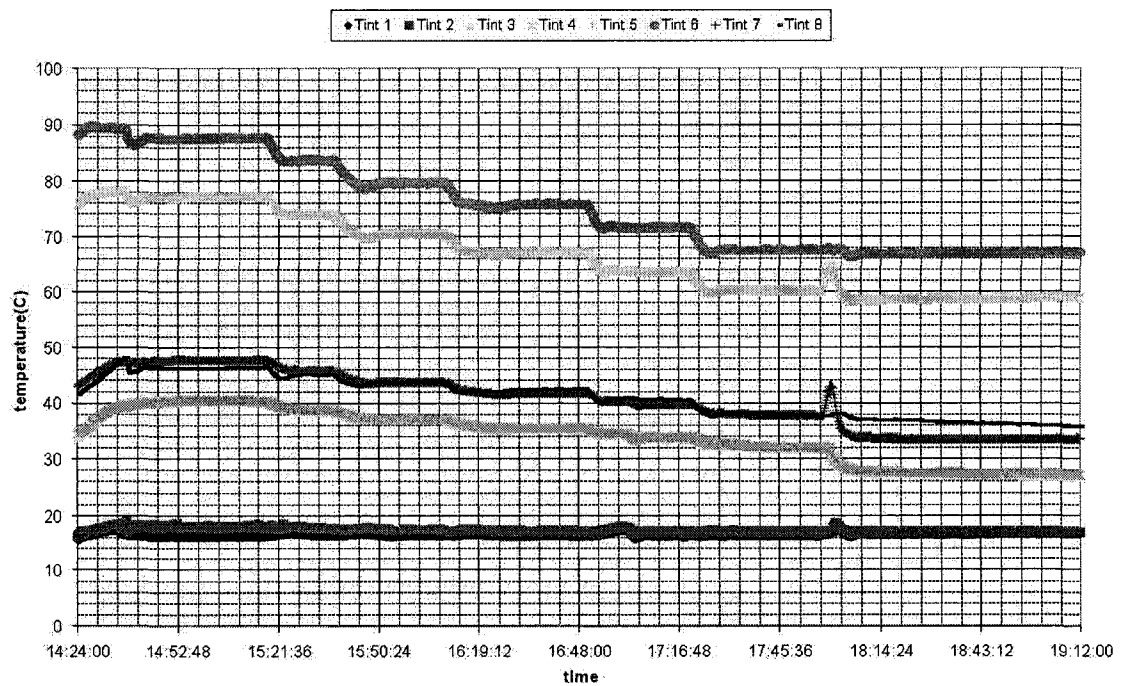


Figure 4-2: Internal temperatures (poly)

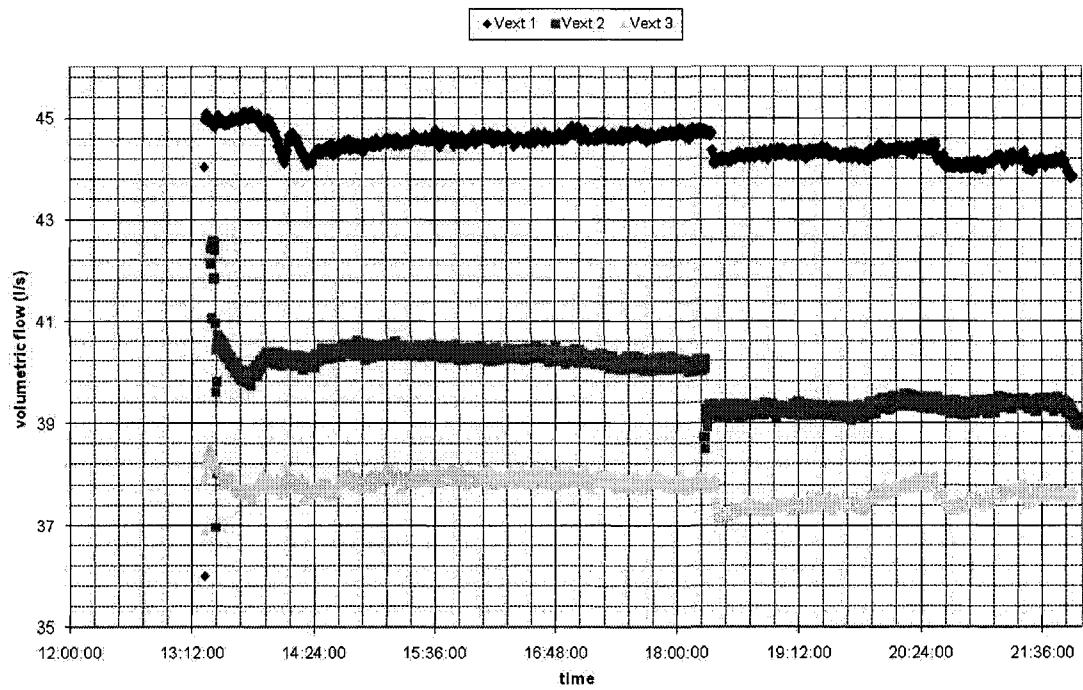


Figure 4-3: External cycle flowrate (poly)

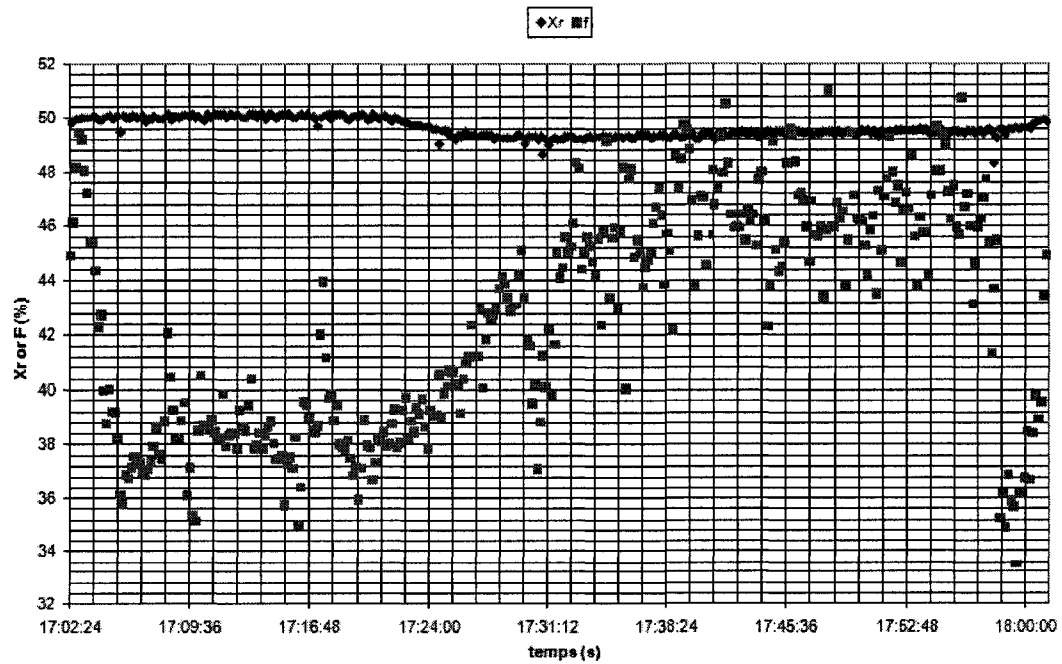


Figure 4-4: Rich and Poor Solution concentration (poly)

4.1.2. TUB

Seven sets of results are also available from experiments performed at TUB. One arbitrary set of results is presented in table 4-2. These sets of results were obtained from the experiments that the shown if figure 4-5 to 4-8.

The conditions under which the results were obtained are described in chapter 4.1.1.

Table 4-2: Experimental results obtained from phoenix prototype

Input parameters	Set 1
T_1 (°C)	90.4 ± 1.1
T_3 (°C)	11.7 ± 0.8
T_5 (°C)	27.2 ± 1.3
\dot{m}_1 (kg/sec)	0.339 ± 0.01
\dot{m}_3 (kg/sec)	0.877 ± 0.01
\dot{m}_5 (kg/sec)	0.722 ± 0.01
\dot{m}_r (kg/sec)	0.110 ± 0.003
output	
T_2 (°C)	81.6 ± 1.3
T_4 (°C)	8.8 ± 1.0
T_6 (°C)	31.2 ± 1.6
T_7 (°C)	34.5 ± 1.8
T_8 (°C)	80.6 ± 2.5
T_9 (°C)	41.5 ± 2.0
T_{10} (°C)	33.8 ± 2.9
T_{11} (°C)	78.1 ± 1.8
T_C (°C)	36.2 ± 0.6
T_E (°C)	5.2 ± 1.2
X_r ($\frac{wt}{wt}$ %)	60 ± 3
X_p ($\frac{wt}{wt}$ %)	58 ± 5
\dot{Q}_G (kW)	12.5 ± 1.5
\dot{Q}_C (kW)	10.0 ± 3.8
\dot{Q}_E (kW)	9.7 ± 2.7
\dot{Q}_A (kW)	12.2 ± 1.5
COP	$0.74 \pm .35$

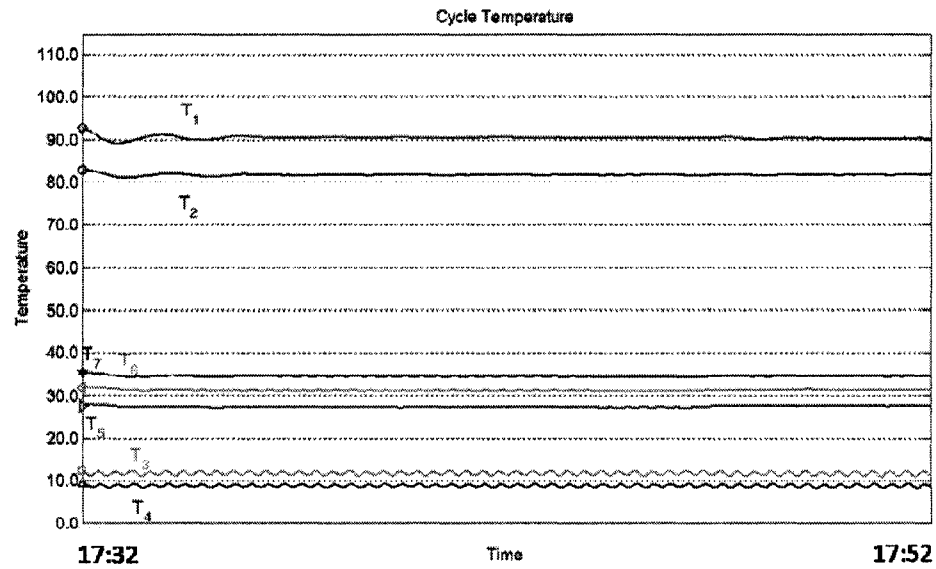


Figure 4-5: External cycle temperature (TUB)

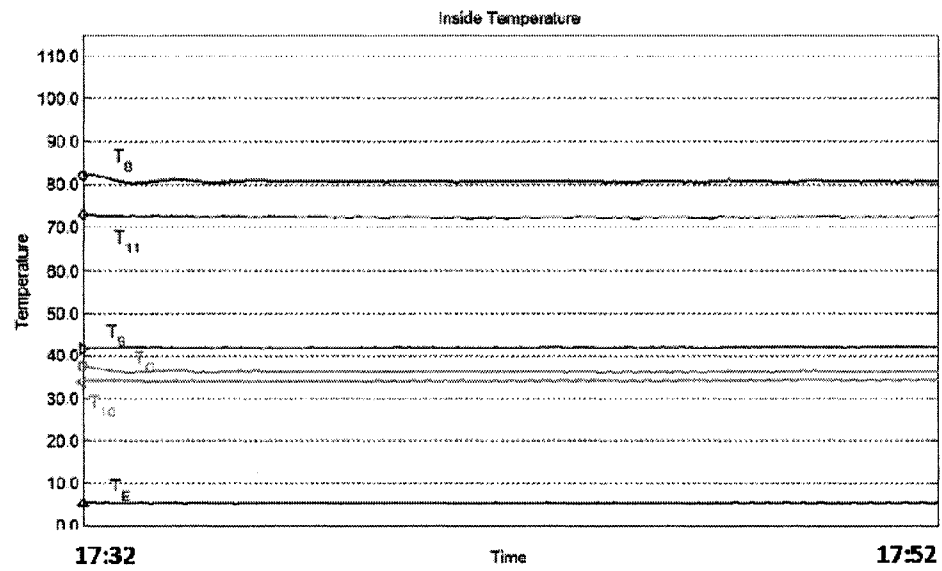


Figure 4-6: Solution-refrigerant cycle temperature (TUB)

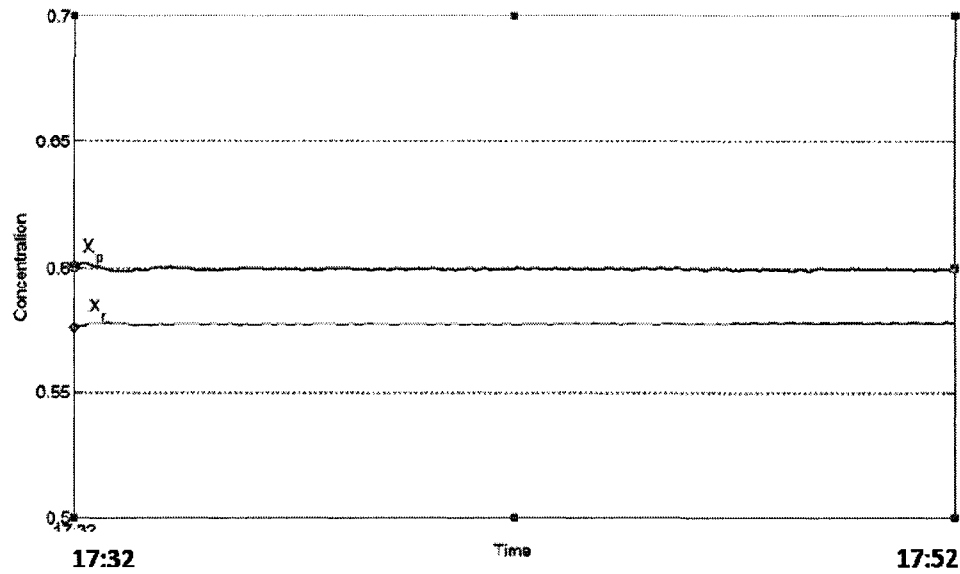


Figure 4-7: Rich and poor solution concentrations (TUB)

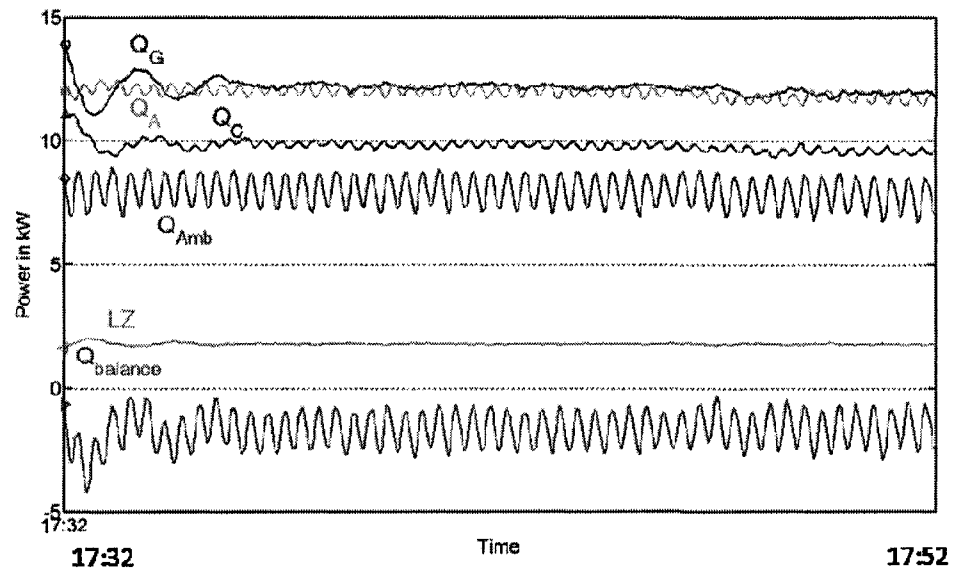


Figure 4-8: Heat load of each heat exchanger (TUB)

4.2. Simulation results

First estimation

The numerical method used in this model requires a first estimation for all the output parameters which user should introduce to the system. This first estimation is critical to

the convergence of the solution. However the value of the first estimation (within the appropriate range) does not have any effect on the output results.

The first estimation used for the following results is the same and has not been changed for each set. The values of the first estimation is presented in table 4-3

Table 4-3: First estimation used for most calculations

T_2 (°C)	70	T_{10} (°C)	61
T_4 (°C)	59	T_{11} (°C)	30
T_6 (°C)	20	T_c (°C)	25
T_7 (°C)	32	T_E (°C)	2
T_8 (°C)	3	X_r ($\frac{wt}{wt}$ %)	0.30
T_9 (°C)	30	X_p ($\frac{wt}{wt}$ %)	0.30

In order to validate the dependency of the output results on the first estimation, each value has been changed within the appropriate range which is:

- Temperature: the first value should be higher than zero. Each value which is presented in table 4-3 could be changed $\pm 15^\circ\text{C}$ and the output will not be effected. However if the values is out of range it will result in divergence and no results will be displayed.
- Concentration: the concentration could be varied from 0.2 to 0.6 and the value does not change the output of the model

Relaxation factor

The relaxation factor which is used for all the results (and is also recommended for further calculations) is 0.5 or 0.6.

With the right number of relaxation factor, the number of iterations would be between 21 and 37 times. This means a very short time of calculations of 0.5 seconds to display the results.

Table 4-4 presents the data for a hypothetical situation with the characteristics of the prototype in Ecole Polytechnique, which is the result of this model:

Table 4-4: Computed values for hypothetical input parameters

Input parameters	T_1 (°C)	100
	T_3 (°C)	18
	T_5 (°C)	25
	\dot{m}_1 (kg/sec)	0.450
	\dot{m}_3 (kg/sec)	0.900
	\dot{m}_5 (kg/sec)	0.550
	\dot{m}_r (kg/sec)	0.110
output		simulation
	T_2 (°C)	91.70
	T_4 (°C)	14.09
	T_6 (°C)	31.70
	T_7 (°C)	38.30
	T_8 (°C)	85.97
	T_9 (°C)	35.06
	T_{10} (°C)	42.98
	T_{11} (°C)	88.39
	T_c (°C)	40.58
	T_E (°C)	9.62
	X_r ($\frac{wt}{wt}$ %)	56.2
	X_p ($\frac{wt}{wt}$ %)	59.6
Calculated	\dot{Q}_G (kW)	15.7
	\dot{Q}_C (kW)	15.2
	\dot{Q}_E (kW)	13.7
	\dot{Q}_A (kW)	15.4
	COP	0.87

4.3. Results Validation

In previous chapter, the results gathered from experimental studies and the procedure to simulate the thermal behaviour for a given input parameters were given.

Overall 23 sets of data are available. Each set was simulated for the given input parameters and the result is compared to their respective experimental value in order to verify the validity and observe for the possible inaccuracies.

23 tables are prepared in appendix C. These tables present the value of both experimental and the comparison between the experimental data and the simulated values shows a good agreement between the values. There are certain differences which are insignificant and could be explained by statistical analysis. The statistical analysis is performed on the experimental values. This analysis confirms the reliability of the values.

As an example one comparison is presented below. This set is selected from the data gathered. The statistical analysis is done for the largest difference found in the comparisons done for 20 sets of data. This shows that the computed values, in spite of the differences, are still in a very good agreement.

As an example among the 20 sets of data gathered, two sets are compared in this chapter which is a comparison of the experimental results presented in previous chapter (7.1.1 and 7.1.2). For the complete set please see appendix C.

4.3.1. Validation with Polytechnique data set

Table 4-6 presents the comparison between the experimental values and computed output for same input values. This comparison has been performed for the prototype at École Polytechnique. The input values are the values measured during the experiment.

Table 4-6 and 4-7 contain four main columns:

- Experimental results: This column presents the average value of each parameter (μ). Standard deviation (σ) of each parameter is also presented.
- Simulation output: The output is calculated for the given inputs for each set. Then the simulation is done for the average value, the maximum ($\mu + \sigma$) and minimum ($\mu - \sigma$).
- Differences: this column presents the differences between respective experiment and simulation.
- Ratio of the difference and standard deviation: this ratio shows the sensitivity of the simulation to the changes of the measurements. Values larger than 1.00 shows high sensitivity of the model to variation of the measurement.

- The complete comparison for 13 sets of data is available in appendix C.

As it is described in chapter 3.1.1, PACAS had a liquid hold up anomaly under certain conditions. Under these conditions, the machine operates with steady state conditions; however the outputs are lower than expected values. Table 4-5 presents an example of the results obtained while overflowing was occurred. The simulation of the same situation is also presented. Large differences between the experiment and simulation are observed.

Table 4-5: results from an overflowing in evaporator, PACAS

Input parameters	RUN 5 - Polytechnique		
T_1 (°C)	75.4		
T_3 (°C)	25.0		
T_5 (°C)	34.0		
\dot{m}_1 (kg/sec)	0.113		
\dot{m}_3 (kg/sec)	0.743		
\dot{m}_5 (kg/sec)	0.219		
\dot{m}_r (kg/sec)	0.193		
output	Experiment	Simulation	Exp – Sim
\dot{Q}_G (kW)	3.60	5.64	-2.04
\dot{Q}_C (kW)	0.90	3.98	-3.08
\dot{Q}_E (kW)	0.30	5.52	-5.22
\dot{Q}_A (kW)	2.70	5.52	-2.82
COP	0.09	0.68	-0.59

Table 4-6: Comparison between experiments and simulation, RUN AC4, Polytechnique

	Experiment				Simulation			Differences (Δ)			Δ/σ		
	μ	σ	$\mu - \sigma$	$\mu + \sigma$	μ	$\mu - \sigma$	$\mu + \sigma$	μ	$\mu - \sigma$	$\mu + \sigma$	$\mu - \sigma$	$\mu - \sigma$	$\mu + \sigma$
T_1 (°C)	95.0	0.5	94.5	95.5	95.0	94.5	95.5				N/A		
T_3 (°C)	20.0	0.7	19.3	20.7	20.0	19.3	20.7	0			N/A		
T_5 (°C)	30.0	0.7	29.3	30.7	30.0	29.3	30.7	0			N/A		
m_1^o (kg/sec)	0.612	0.010	0.602	0.622	0.612	0.602	0.622	0			N/A		
m_3^o (kg/sec)	0.743	0.024	0.719	0.767	0.743	0.719	0.767	0			N/A		
m_5^o (kg/sec)	0.671	0.030	0.641	0.701	0.671	0.641	0.701	0			N/A		
m_r^o (kg/sec)	0.184	0.011	0.173	0.195	0.184	0.173	0.195	0			N/A		
T_2 (°C)	86.5	0.9	85.6	87.4	87.4	86.9	86.5	-0.9	-1.3	0.9	1.00	-1.44	1.00
T_4 (°C)	15	1.1	13.9	16.1	14.2	13.5	15.3	0.8	0.4	0.8	0.73	0.36	0.73
T_6 (°C)	37.1	1.0	36.1	38.1	36.8	36.2	37.8	0.3	-0.1	0.3	0.30	-0.10	0.30
T_7 (°C)	43.1	1.2	41.9	44.3	43.4	42.6	43.8	-0.3	-0.7	0.5	-0.25	-0.58	0.42
T_8 (°C)	85.2	1.7	83.5	86.9	86.6	86.3	84.4	-1.4	-2.8	2.5	-0.82	-1.65	1.47
T_9 (°C)	36.0	1.6	34.4	37.6	37.3	36.7	36.0	-1.3	-2.3	1.6	-0.81	-1.44	1.00
T_{10} (°C)	43.1	1.9	41.2	45.0	41.6	41.0	42.8	1.5	0.2	2.2	0.79	0.11	1.16
T_{11} (°C)	88.0	2.1	85.9	90.1	87.1	86.7	88.0	0.9	-0.8	2.1	0.43	-0.38	1.00
T_c (°C)	42.5	1.9	40.6	44.4	43.8	43.3	42.5	-1.3	-2.7	1.9	-0.68	-1.42	1.00
T_E (°C)	8.4	1.2	7.2	9.6	9.2	8.7	10.0	-0.8	-1.5	-0.4	-0.67	-1.25	-0.33
X_r ($\frac{wt}{wt}\%$)	55	3	52	58	56	56	56	-1	-4	2	-0.3	-1.3	0.7
X_p ($\frac{wt}{wt}\%$)	58	3	55	61	58	58	58	0	-3	3	0	-1.0	1.0

$\dot{Q}_G(kW)$	21.86	1.70	22.51	21.17	19.54	19.23	23.52	2.3	3.3	-2.4	1.36	1.93	-1.38
$\dot{Q}_C(kW)$	16.92	2.40	15.62	18.26	18.61	17.24	17.68	-1.7	-1.6	0.6	-0.70	-0.67	0.25
$\dot{Q}_E(kW)$	15.61	2.90	16.31	14.82	18.10	17.52	17.40	-2.5	-1.2	-2.6	-0.86	-0.42	-0.89
$\dot{Q}_A(kW)$	20.02	2.30	18.32	21.80	19.18	18.59	20.92	0.8	-0.3	0.9	0.37	-0.12	0.38
COP	0.71	0.31	0.72	0.70	0.93	0.91	0.74	-0.2	-0.2	0.0	-0.68	-0.60	-0.13

This comparison shows a large difference between experiment and simulation. And as it was expected this problem was due to overflowing in the evaporator. However for the 13 sets of data which the system is operating with no irregularity the results are matching and these results are available in appendix C

4.3.2. Validation with TUB data set

Table 4-7 presents the comparison of the experimental values against the computed values for same input parameters. These values were obtained by the prototype at TUB. This table includes the same columns which are explained in chapter 4.3.1.

Table 4-7: Comparison between experiments and simulation, set 1 TUB

	experiment				simulation			Differences (Δ)			Δ/σ		
	μ	σ	$\mu - \sigma$	$\mu + \sigma$	μ	$\mu - \sigma$	$\mu + \sigma$	μ	$\mu - \sigma$	$\mu + \sigma$	$\mu - \sigma$	$\mu + \sigma$	
T_1 (°C)	90.36	1.10	89.26	91.46	89.26	90.36	91.46		0		N/A		
T_3 (°C)	11.69	0.80	10.89	12.49	10.89	11.69	12.49		0		N/A		
T_5 (°C)	27.22	1.30	25.92	28.52	25.92	27.22	28.52		0		N/A		
m_1^o (kg/sec)	0.339	0.010	0.329	0.349	0.329	0.339	0.349		0		N/A		
m_3^o (kg/sec)	0.877	0.010	0.867	0.887	0.867	0.877	0.887		0		N/A		
m_5^o (kg/sec)	0.722	0.010	0.712	0.732	0.712	0.722	0.732		0		N/A		
m_7^o (kg/sec)	0.110	0.003	0.107	0.113	0.107	0.110	0.113		0		N/A		
T_2 (°C)	81.60	1.30	80.30	82.90	80.79	82.22	83.64	-0.49	-0.62	-0.74	-0.38	-0.48	
T_4 (°C)	8.83	1.00	7.83	9.83	7.61	8.48	9.34	0.22	0.35	0.49	0.22	0.35	
T_6 (°C)	31.22	1.60	29.62	32.82	29.75	30.96	32.17	-0.13	0.26	0.65	-0.08	0.16	
T_7 (°C)	34.50	1.80	32.70	36.30	33.49	34.62	35.75	-0.79	-0.12	0.55	-0.44	-0.06	
T_8 (°C)	80.65	2.50	78.15	83.15	77.33	78.65	79.97	0.82	2.00	3.18	0.33	0.80	
T_9 (°C)	35.80	2.00	33.80	37.80	32.98	34.16	35.33	0.82	1.64	2.47	0.41	0.82	
T_{10} (°C)	36.08	2.90	33.18	38.98	37.53	38.71	39.88	-4.35	-2.63	-0.90	-1.50	-0.91	
T_{11} (°C)	78.10	1.80	76.30	79.90	78.33	79.74	81.16	-2.03	-1.64	-1.26	-1.13	-0.91	
T_c (°C)	36.20	0.60	35.60	36.80	34.99	36.12	37.25	0.61	0.08	-0.45	1.02	0.13	
T_E (°C)	5.17	1.20	3.97	6.37	5.01	5.88	6.76	-1.04	-0.71	-0.39	-0.87	-0.59	
X_r ($\frac{wt}{wt}\%$)	58	3	55	61	56	56	56	-1	2	5	-0.41	0.59	
X_p ($\frac{wt}{wt}\%$)	60	4	56	64	59	59	59	-3	1	5	-0.76	0.24	

$\dot{Q}_c(kW)$	12.49	1.50	10.99	13.99	11.72	11.60	11.47	-0.73	0.88	2.51	-0.49	0.59	1.67
$\dot{Q}_c(kW)$	9.96	3.80	6.16	13.76	11.19	11.10	11.01	-5.04	-1.15	2.74	-1.33	-0.30	0.72
$\dot{Q}_E(kW)$	9.65	2.70	6.95	12.35	10.94	10.83	10.75	-4.00	-1.18	1.60	-1.48	-0.44	0.59
$\dot{Q}_A(kW)$	12.15	1.50	10.65	13.65	11.46	11.35	11.23	-0.81	0.80	2.42	-0.54	0.53	1.61
COP	0.77	0.28	0.49	1.05	0.93	0.93	0.94	-0.44	-0.16	0.12	1.58	-0.57	0.41

4.3.3. Comparison of the results of two models

As it was explained in chapter 3.8, another model was created with different sets equations (although they are all heat and mass balance equations). In this chapter, the results from each model are compared against experimental results and each other.

As an example set 2 from experimental results at TUB was chosen. Table 4-8 shows the results. Simulation A is the main model presented in this work and simulation B is the model inspired the model described in chapter 3.8.

Table 4-8: Comparison of experiments and two simulations

Input parameters	Set 1 – TUB		
T_1 (°C)	90.36		
T_3 (°C)	11.69		
T_5 (°C)	27.22		
\dot{m}_1 (kg/sec)	0.339		
\dot{m}_3 (kg/sec)	0.877		
\dot{m}_5 (kg/sec)	0.722		
\dot{m}_r (kg/sec)	0.110		
output	Experiment	Model presented in this work	Model based on ZAE
T_2 (°C)	81.6	82.2	85.9
T_4 (°C)	8.8	8.5	9.4
T_6 (°C)	31.2	31.0	29.3
T_7 (°C)	34.5	34.6	31.9
T_8 (°C)	80.7	78.7	75.7
T_9 (°C)	35.8	34.2	29.5
T_{10} (°C)	36.1	38.7	42.5
T_{11} (°C)	78.1	79.7	85.7
T_C (°C)	36.2	36.1	33.0
T_E (°C)	5.2	5.9	7.5
X_r ($\frac{wt}{wt}$ %)	58	56	57
X_p ($\frac{wt}{wt}$ %)	60	59	59
\dot{Q}_G (kW)	12.49	11.60	6.40
\dot{Q}_C (kW)	9.96	11.10	8.05

$\dot{Q}_E(kW)$	9.65	10.83	7.89
$\dot{Q}_A(kW)$	12.15	11.35	6.25
COP	0.77	0.93	1.23

4.3.4. Comparison analysis

Results are compared and as it is seen there are certain differences between the computed values and measured ones. These differences could be explained as follows:

As an example figures 4-9 to 4-12 show that the measured values are fluctuating even though the steady state operation has been reached. These oscillations could be caused by several reasons. The most important cause is the controlling program of the system. This flaw causes the following results which eventually cause fluctuation in the measured values:

- 1) The flowrate of the streams (hot, chilled and cooling water and rich solution) are not constant. The variations of these flowrates cause variations in the process. Figure 4-9 is an example of the variation of flowrate of service fluids versus time. However for both prototypes a similar trend is observed and in spite of all the efforts to improve the PID (controlling software) the problem still remains. Another issue is the flowrate of the refrigerant between condenser and evaporator (stream13 and 14). The flowrate is a result of the pressure difference between two heat exchangers and not a pump. Hence the flowrate is a function of the pressure difference which is also varying during the process. As it is observed in the experiments this flowrate is changing dramatically by time. Figure 4-10 shows the fluctuation of the refrigerant flowrate versus time. The same situation also exist for the poor solution (stream 8 and 9)

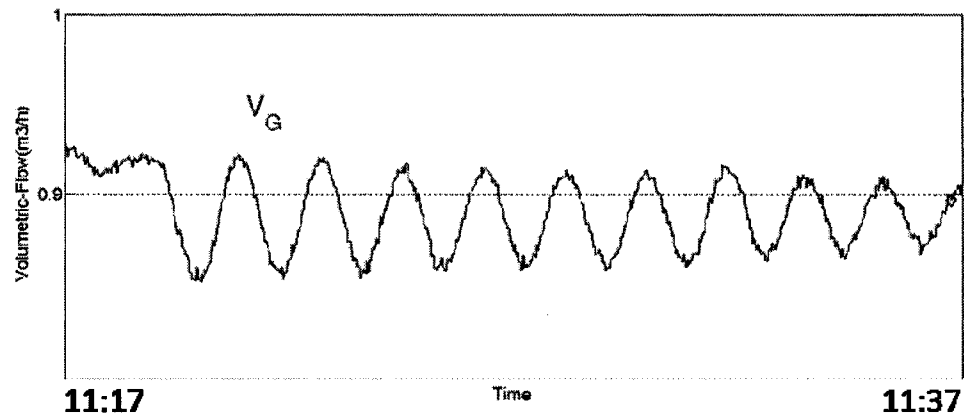


Figure 4-9: Fluctuation of the flowrate in hot water pump

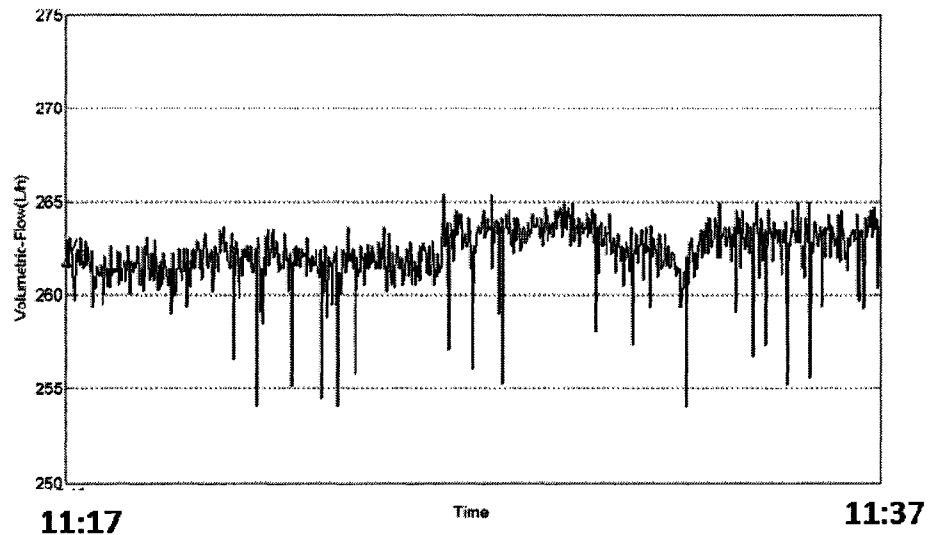


Figure 4-10: Fluctuation of the flowrate in refrigerant pump

- 2) The hot source is provided by an electrical heater which heats up the water by heating elements. The elements are heat up by on/off electrical currents. Since there is no buffer zone between the electrical heater and the generator, the hot water inlet temperature (T_1) oscillates around the fixed value. Figure 4-11 illustrates the variation of the temperature.

As it is observed during the experiments, this value could vary for 2 to 5 °C once the steady state is reached. Since the chilled water is warmed up by similar electrical heater, similar pattern is also seen for the chilled water inlet temperature (T_3). Figure 4-12 illustrates the fluctuation of this parameter by time.

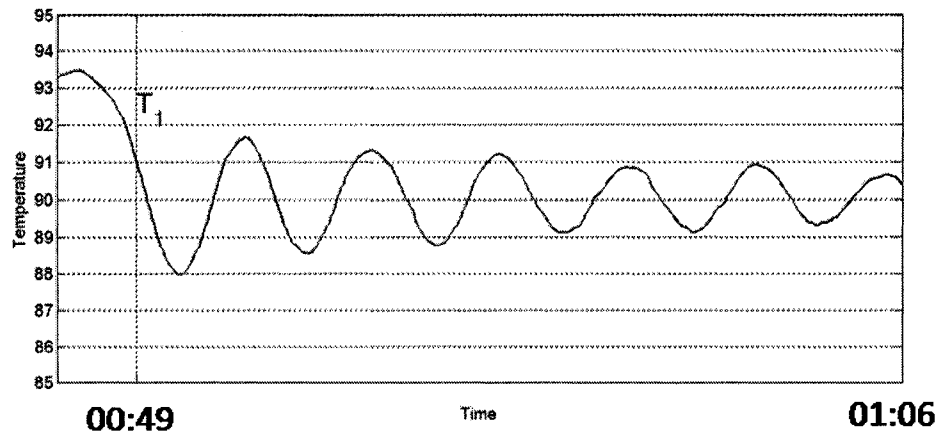


Figure 4-11: fluctuation of the hot water temperature

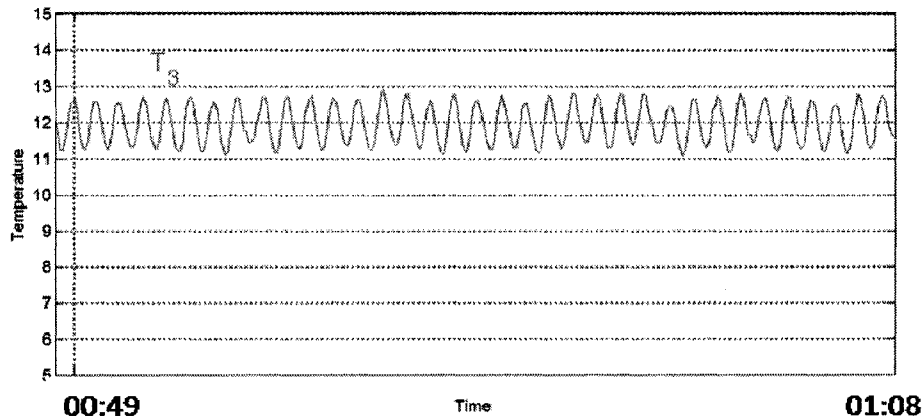


Figure 4-12: fluctuation of the chilled water inlet temperature

- 3) There are also several human errors which cause certain inaccuracies in the results obtained such as:
 - a. Incorrect calibration of the PT (temperature) sensors.
 - b. Tip of PT sensors are not exactly in the center of the pipe, therefore the temperature measured does not represent the actual temperature of the stream.

The biggest difference observed between the computed and measured parameter is (T_8) which is 2.6°C .

The experimental data for this particular measurement is shown in figure 4-13 (set 1 at TUB)

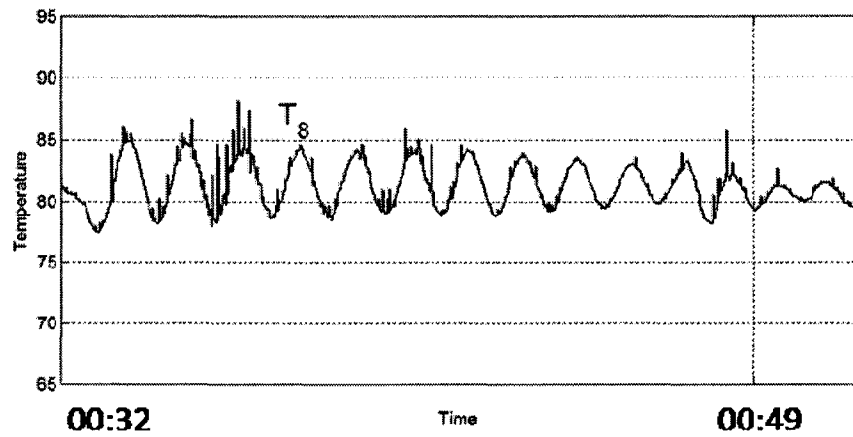


Figure 4-13: Poor solution leaving the generator (set 1, TUB)

As it is seen in figure 4-13, T_8 is varying in the range of 77 to 88°C.

The arithmetic average value for a period of 20 minutes (100 values) is

$$\mu = 82.7^{\circ}\text{C}$$

The standard deviation of the population for this parameter is:

$$\sigma = 2.9^{\circ}\text{C}$$

The value calculated by the model is

$$T_8 = 82.1^{\circ}\text{C}$$

This shows the value obtained from the model is within the range of experiment. The comparison was performed for the largest difference observed between the experiments and computed values. This shows that other differences which are smaller are also reliable and there are good agreements between these values.

Hence the model can correctly predict the operating parameters.

CHAPTER 5 : SENSITIVITY OF THE MODEL

In operating an absorption heat pump, a variation in any input variable (or any other variable related to characteristic of the machine) changes all the other dependent variables. When an input changes, the entire cycle reacts to reach a new equilibrium operating conditions.

In the present chapter, the sensitivity of the model is presented. However, it should be reminded that this is not similar to dynamic behaviour. This model does not exhibit the complex dynamic behaviour but it represents the eventual steady state behaviour of these prototypes.

In order to do so, all the input parameters are fixed except one. By varying one parameter the consequences are monitored on power output and COP of the prototype.

5.1. Heat transfer coefficient

First the effect of changes of the heat transfer coefficient of each heat exchanger on the heat capacity and COP is presented. The validity of these charts is also verified by comparison to available sensitivity analysis performed by Herold (1996) pages 125-136. The results are presented in graphs of Q Vs. U and COP Vs. U .

In this study, the input parameters are the design values of the PACAS prototype which are shown in table 5-1:

Table 5-1: Input parameters

T_1 (°C)	95
T_3 (°C)	12
T_5 (°C)	27
m_1° (kg/sec)	0.48
m_3° (kg/sec)	0.60
m_5° (kg/sec)	1.05
m_r° (kg/sec)	0.08

In all cases, the input parameters are fixed. The varying parameter is the respective heat transfer coefficient.

Figures 5-1 to 5-5 illustrate the effect of varying each heat exchanger overall heat transfer coefficient on the heating load of all exchangers:

5.1.1. Generator

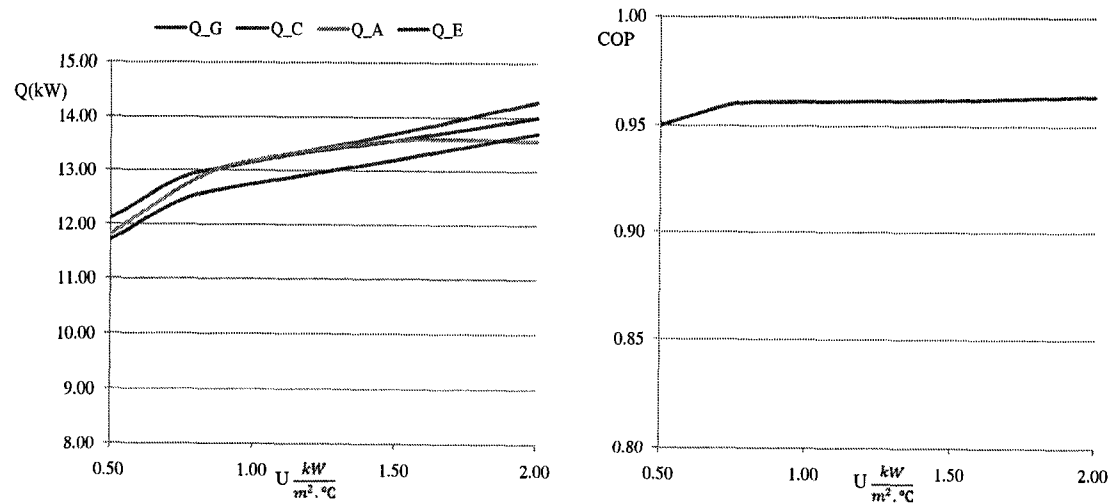


Figure 5-1: Effect of generator heat transfer coefficient on load and COP

5.1.2. Evaporator

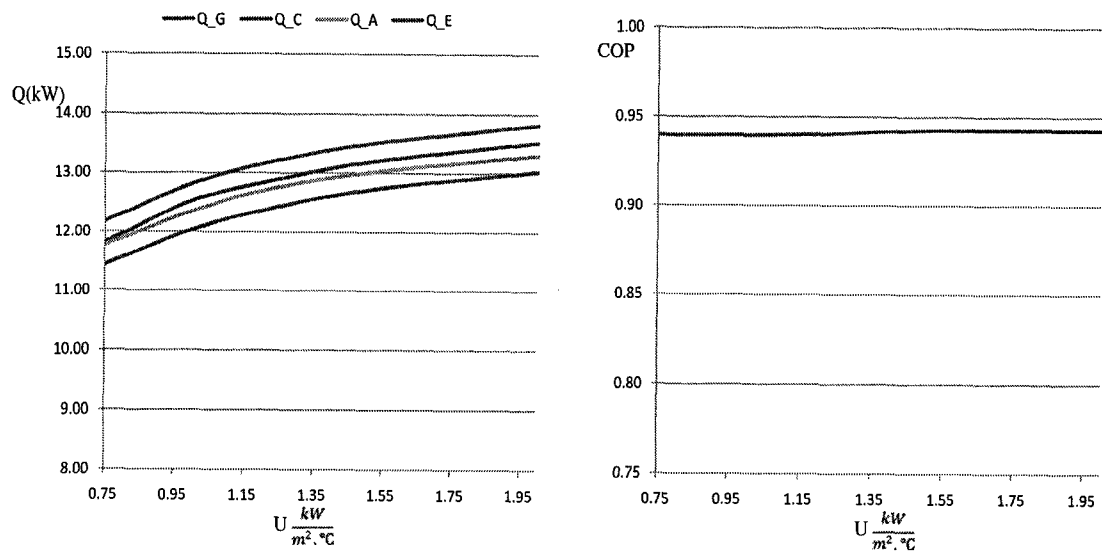


Figure 5-2: Effect of evaporator heat transfer coefficient on load and COP

5.1.3. Absorber

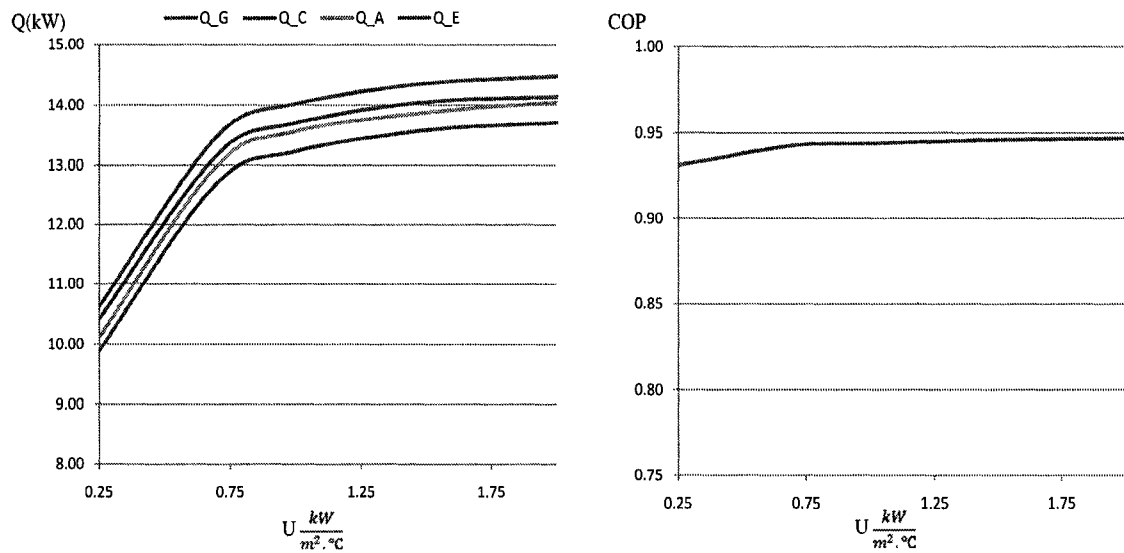


Figure 5-3: Effect of absorber heat transfer coefficient on load and COP

5.1.4. Condenser

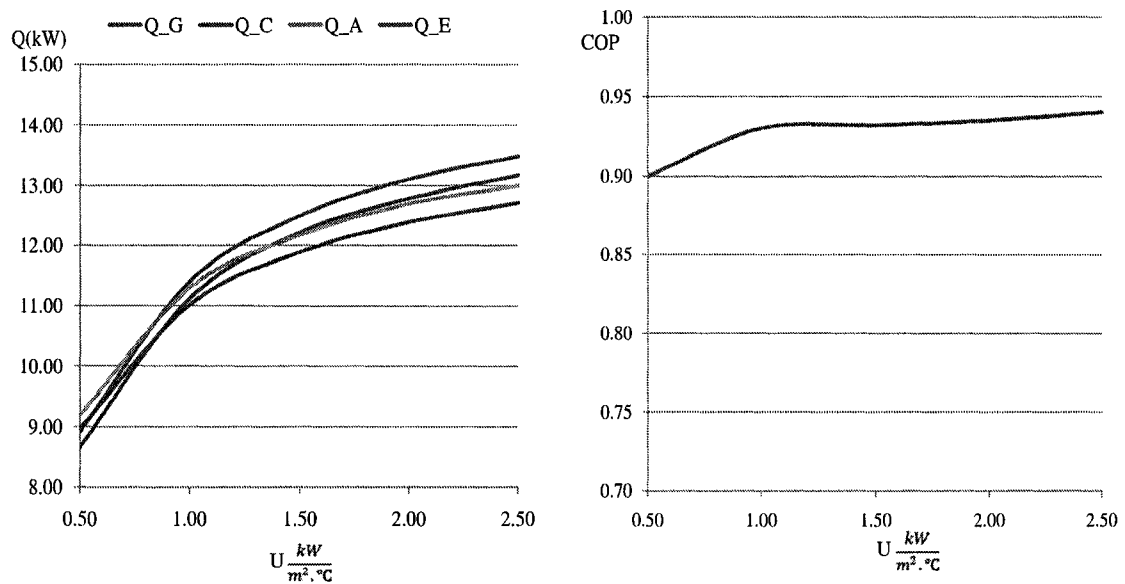


Figure 5-4: Effect of condenser heat transfer coefficient on load and COP

5.1.5. Solution Heat Exchanger

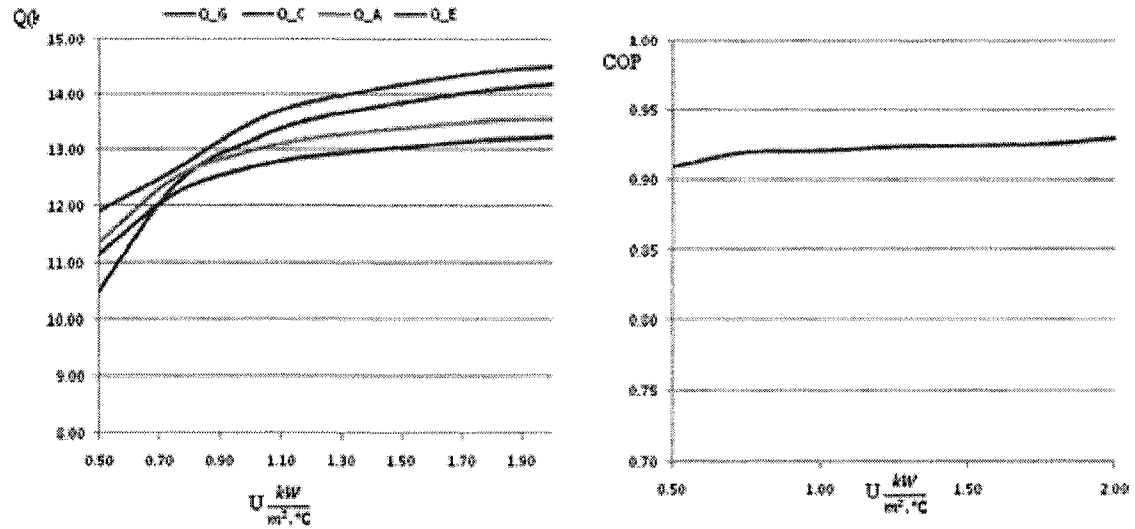


Figure 5-5: Effect of SHX heat transfer coefficient on load and COP

The influence of heat transfer coefficient on performance is summarized in figures 5-1 to 5-5. In each figure, the *COP* and capacity are plotted versus *U* of that particular heat exchanger. In all cases, the same general trend is observed. That is, the *COP* is relatively insensitive to changes in *U* except for very small values of *U* where the *COP* decreases as *U* decreases. Capacity is more sensitive to *U* with the exception of the solution heat exchanger *U* which does not have much influence on the capacity. Since *U* and *A* appears as a product (*U.A*) in all equations, any effect of variation is observed for *U* could also be predicted for the product of *U.A*. This means any effect of changes observed for *U* is also the same for *U.A*.

5.2.External cycle inlet temperature

In this section the effects of variation in the inlet temperature on heat capacities and *COP* are presented.

Figures 5-6 to 5-8 illustrate the changes in heat loads and *COP* versus temperature of hot water, cooling water and chilled water inlet. All other parameters are fixed as it is shown in table 5-1

5.2.1. Generator

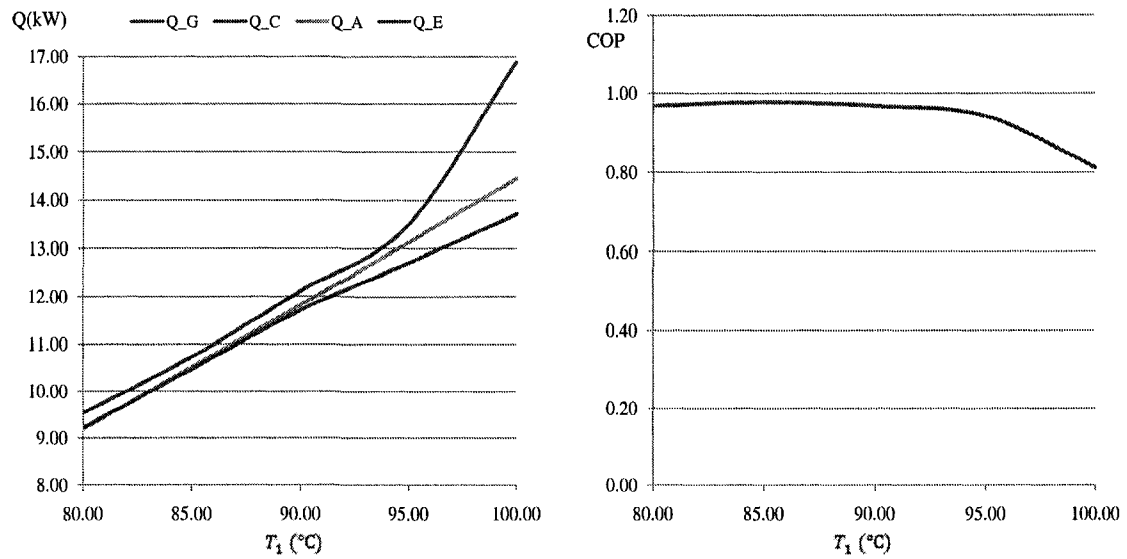


Figure 5-6: Effect of hot water inlet temperature on load and COP

5.2.2. Absorber

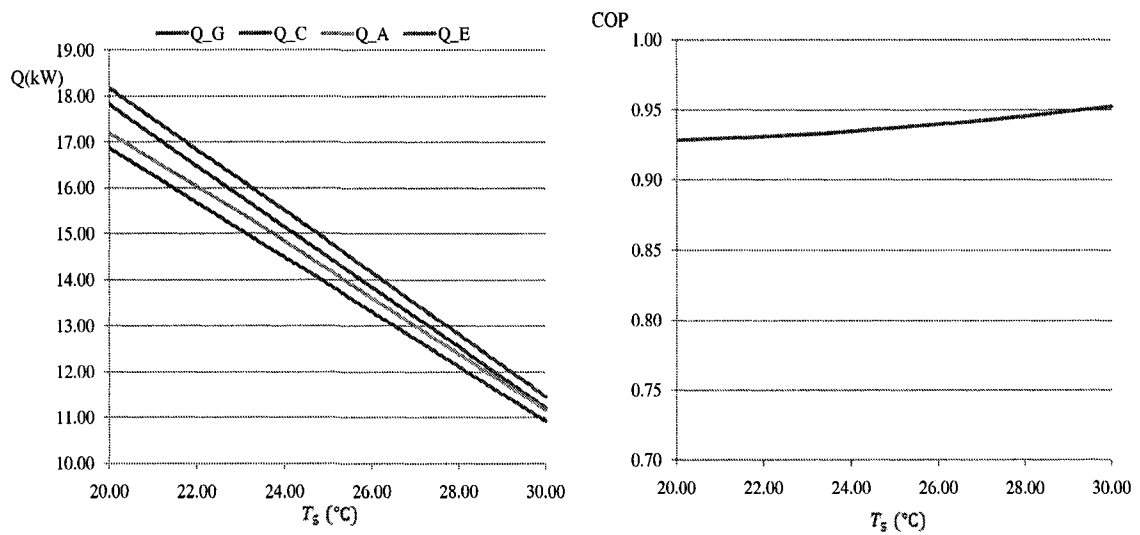


Figure 5-7: Effect of cooling water inlet temperature on load and COP

5.2.3. Evaporator

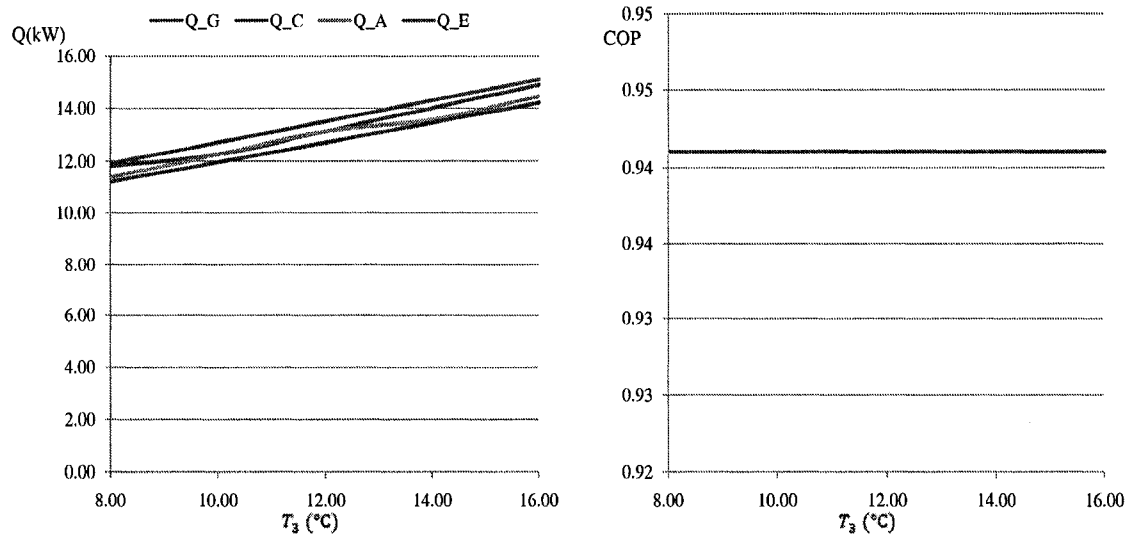


Figure 5-8: Effect of chilled water inlet temperature on load and COP

A simple example of the interdependence of the heat loads has been obtained by varying the inlet temperature while holding other input parameters constant. The summarized influence of the inlet temperature of hot, cooling and chilled water is illustrated in figures 5-6 to 5-8. The temperature is chosen so it stays in the practical range. These figures show:

- In all cases the heat loads of the exchangers are influenced by inlet temperatures. This variation is approximately linear within the practical range chosen for these calculations.
- In none of the cases COP is not influenced by the inlet temperature variations.
- Increasing the hot water inlet in the generator or chilled water in evaporator results in increasing the heat loads of all exchangers. However COP remains rather unchanged.
- Increasing the absorber cooling water inlet results in less rejection heat removed from the system, hence the decrease of the heat load of all exchangers. In this case the variation in COP is insignificant.

CHAPTER 6 : CONCLUSION AND RECOMMENDATIONS

A brief introduction of heat pumps and the process of VRHP were presented. Next the absorption heat pumps were introduced and the unit operations were explained.

A mathematical model of two prototype absorption heat pumps based on heat and mass balance equations was created.

This model calculates the performance characteristics of the machine by defining the input variables during a steady state operation.

This simulation program was created with MATLAB. A numerical iterative solution was chosen to solve the nonlinear simultaneous equations extracted from heat and mass balances. These equations are overall heat balance of the AHP and over the five heat exchangers. The iterative solution is the expanded Newton – Raphson method.

These prototype absorption chillers which are available at École Polytechnique and TUB are single effect absorption heat pumps with working fluid of aqueous LiBr. Both prototypes have similar designs. However there are differences in heat transfer coefficients and heat transfer areas.

Substantial amount of experiments were performed on both prototypes under various operational conditions. These tests were particularly helpful to understand the thermal behaviour of the machine. The experiments on the prototypes were performed by A. Costa, A. Jahnke and others and the experiments on the prototype at TUB were performed by the author.

In addition, objectives obtained at this work are summarized as follows:

- The model presented in this work is based on heat and mass balance equations and the output parameters are calculated by a code developed in MATLAB.
- This model calculates the temperature in all streams in the prototype at a steady state operation. These values are used to calculate the heat load of each heat exchanger and eventually the COP of the chiller.
- To validate the results of the simulation, they were compared to the experimental studies. Since the values obtained during the experimental measurements, the average of the values was calculated. Standard deviation of each measurement

was also calculated. The comparison between the calculated value, average and standard deviation of each parameter confirms that outputs of this simulation are reliable and accurate results.

- Comparison between the simulation in this work and the model inspired by the equations developed at ZAE Bayern shows higher accuracy in the results obtained in this work (By comparison with experimental data gathered from both prototypes). The equations used in the simulation developed at ZAE Bayern was published, however the code itself, is classified. Hence the results were reproduced under same conditions (same numerical method, same first estimations and etc). It was possible to obtain better results from the model presented in this work. This is due to less number of equations used (12 equations in this work compared to 19 equations used at ZAE model). In addition a few hypotheses were modified.

- The sensitivity of the model on heat transfer coefficient was evaluated. The sensitivity studied the effect of heat transfer coefficient of each heat exchanger on power output of all four exchangers (generator, condenser, evaporator and absorber) and COP of the machine.

This study shows that increasing the heat transfer coefficient (U) or heat transfer area (A), increases the heat load of the AHP and in all cases (all exchangers) same trend was observed. Furthermore this study shows that COP is relatively insensitive to changes in UA except for very small values of UA where the COP decreases as UA decreases.

- The effect of the inlet temperature of each external cycle (hot water inlet, cooling water inlet, chilled water inlet) on power output and COP of the prototypes was studied. This study shows that increasing the hot water and chilled water inlet result in increasing of heat loads and this variation is rather linear. COP however remains unchanged. Decreasing the cooling water inlet temperature results in increasing of the heat loads of all exchangers and COP also stays rather unchanged.

There are several steps which could be taken in order to improve the model presented in this work:

- This code measures the output for a single effect absorption chiller with working fluid of aqueous LiBr. The physical and thermodynamic properties of LiBr solution are calculated through models taken from the literature. In order to change the working fluid to other pairs (such as Water – Ammonia), these properties should be adapted to the new solution. In addition, the equations should be adapted (if necessary) for the new components. For instance, if the absorbent exists in the refrigerant loop, it should be considered in the equations.
- The sensitivity of the outputs on the heat transfer coefficient (and area) of the SHX has been studied and has been confirmed with the literature. However the effectiveness of the SHX has not been taken into account in this model. The effectiveness of this exchanger could impact the outputs of the machine. In order to improve this model further study could be carried out so it could contain this property (SHX effectiveness).
- The equations presented are for a single effect absorption heat pump. These equations could be rearranged so it could carry out the same performance for a “thermo transformer”. In addition, the equations for a double effect, double lift or any other arrangement could be extracted and this code could be adapted for different types of heat pumps.
- This model was tested according to the experimental results available. The prototypes were tested under conditions which were recommended by the design values. In order to confirm the outputs of the model, both prototypes and the model could go through extreme conditions and by comparison, it could be confirmed whether this model is also reliable for extreme conditions.
- This model does not respond for crystallization. Further step could be developing new subroutines to show the conditions under which crystallization may occur.

BIBLIOGRAPHY

Alefeld G. and Radermacher R. (1994) *Heat Conversion Systems*, CRC Press Inc.

Constantinides A. and Mostoufi N. (1999) *Numerical methods for chemical engineers with MATLAB applications*. 1st Edition, Prentice Hall PTR

Feuerecker G., Scharfe J., Greiter I. and Frank C. (1993) Measurement of thermophysical properties of LiBr solution at high temperatures and concentrations. In *AES – vol 31 international Absorption heat pump conference ASME*, P 493-99

Grossman H. (1996) Improved Property Data Correlation of Absorption Fluids for Computer Simulation of Heat Pump Cycles *ASHRAE Transactions*, v 102, n 1, p 980-997

Grossman H. and Zaltash A. (2001) ABSIM - Modular simulation of advanced absorption systems, *International Journal of Refrigeration*, v 24, n 6, p 531-543

Hainsworth, (1944) Refrigerants and Absorbents Part II, *Refrigerating Engineering Vol.* 48, pp 201-205

Herold K., Radermacher R. and Klein S. (1996) *Absorption chillers and heat pumps* 1st Edition

Hofmann L. (1996) Experimental investigation of heat transfer in a falling film absorber with aqueous solutions of LiBr with and without surfactants, *International Journal of Refrigeration*, Vol. 19, No. 5

- Jahnke A., Costa A., Ziegler F and Paris J. (2005) Experimental plan and statistical analysis of laboratory results for an absorption chiller, *International Sorption Heat Pump Conference*
- Jeong S., Kang B. and Karng S. (1998) Dynamic simulation of an absorption heat pump for recovering low grade waste heat *Applied Thermal Engineering Vol 18*
- Kaita Y. (2001) Thermodynamic properties of lithium bromide – water solution at high temperatures. *International journal of refrigeration* 24 374-390
- Kuhn A. and Ziegler F. (2005) *Operational results of a 10kW absorption chiller and adaptation of the characteristic equations*, Internal Publication, Technical University of Berlin
- McNeely L. (1979) Thermodynamic properties of aqueous solution of LiBr. *ASHRAE transactions*, 85 (part1) 413-34
- Perry R. and Green D. (1999) *Perry's chemical engineering handbook*. McGraw Hill Book Inc.
- Xu S., Zhang L., Xu. C. and Liang J. (2007) Numerical simulation of an advanced energy storage system using H₂O – LiBr as working fluid, part1: system design and modeling *International journal of refrigeration*
- Ziegler F. (1997) Sorptionwärmepumpen, *Forschungsberichte des Deutsch kälte- und kilmatechnischen Veriens (DKV) No. 57*

APPENDIX

Appendix A: computer program

Codes

Run_me.m

This is the main code which will be executed. It clears the memory from previous parameters. Then it introduces a file “eqns_independent.m” which the series of 12 equations are located.

Then, an array is introduced which contain all the first estimates. At this point user is asked for a relaxation factor. After entering the relaxation factor (ρ) the function “newton.m” is performed on the file which is previously introduced.

User can repeat the calculation as many number as necessary till convergence is reached.

eqns_independent.m

First this file calls another m file which contains all the “input variables” and “constant parameters”. Then assign all enthalpies in all streams to their respective arrays. For LiBr, the function name is “*h_LiBr.m*” and for water the function name is “*XSteam.m*”.

Then the 12 equations are introduced which the variables are x_1 to x_{12} .

Newton.m

This function performs the Newton – Raphson method on the series of nonlinear equations. The Jacobian matrix is calculated by a simple numerical method. The convergence factor is introduced as explained in chapter 6.3. The maximum number of iterations is fixed at 1000 times. In case the maximum number of iterations is reached and convergence is not still obtained, the loop breaks and the user is warned and asked to correct the relaxation factor.

LMTD.m

This function calculates the logarithmic temperature difference as function of inlet and outlet streams temperature.

XSteam.m & h_LiBr.m

XSteam.m is a complete function of water physical properties. In this program it calculates the enthalpy of the water for certain temperature.

For the enthalpy of LiBr solution, the function calculates the enthalpy of the solution with the available model [999] and returns the value.

A_LiBr.m & B_LiBr.m

These functions calculate the Dühring coefficient as a function of the solution concentration.

Run_me.m

```
% Simulation of thermal behavior of an Absorption Heat Pump

% This program presents the solution of
% the Mass and Energy balances of an AHP
% To solve the simultaneous Non-Linear equations
% Newtonian Method is used.

% clear the screen and previous parameters
clear all; clc;

% This file contains all the nonlinear, independent equations.
fname = 'eqns_independent';

% Newtonian method for simultaneous nonlinear equations
repeat = 1;
while repeat
    % initial guess
    % x = [ T_8, T_9 , T_10 , T_11 , T_7 , T_4 , X_r , T_6 , T_2 ,
    T_E , T_C, X_p ]
    x0 = [ 2 , 25 , 30.0 , 15.0 , 11.0 , 30.0, .3 , 5 , 40 , 2
    , 25, .3 ];
    % x0 = [ 3 , 30 , 61.0 , 30.0 , 22.0 , 59.0, .3 , 20 , 70 , 2
    , 25, .3 ];

    % input the relaxation factor by the user, vary between [0.1 to 1]
    rho = input('relaxation factor: Rho= ');
```



```

f(4)= mdot_r * ( h_11 - h_10 ) - ( ( mdot_r * (x(7) / x(12) )) * ( h_8
- h_9 ) );

f(5) = mdot_5*Cp_5*(x(8)-T_5) - U_A*A_A*LMTD(x(2),x(3),T_5,x(8))      ;
f(6) = mdot_1*Cp_1*(T_1-x(9)) - U_G*A_G*LMTD(T_1,x(9),x(4),x(1))      ;
f(7) = mdot_3*Cp_3*(T_3-x(6)) - U_E*A_E*LMTD(T_3,x(6),x(10),x(10))    ;
f(8) = mdot_5*Cp_5*(x(5)-x(8))- U_C*A_C*LMTD(x(11),x(11),x(8),x(5))    ;
f(9) = mdot_5*Cp_5*(x(5)-x(8))-(1-(x(7)/x(12)))*mdot_r*(h_12-h_13)
;
f(10) = mdot_3*Cp_3*(T_3-x(6)) - (1-(x(7)/x(12)))*mdot_r*(h_15-h_14)
;
f(11) = (mdot_1*Cp_1*(T_1-x(9))) - ((mdot_r * ((1-
(x(7)/x(12)))*h_12)+((x(7)/x(12))*h_8)-(h_11)))) ;
f(12) = mdot_1*Cp_1*(T_1-x(9))+mdot_3*Cp_3*(T_3-x(6))-
mdot_5*Cp_5*(x(5)-T_5);

f = f';

```

Newton.m

```

function [xnew, iter] = Newton(fnctn , x0 , rho, tol, varargin)

    if nargin < 4 | isempty (tol)

        tol = 1e-6;

    end

    if nargin < 3 | isempty (tol)

        rho = 1;

    end

    x0 = (x0(:).')';

    nx = length(x0);

    x = x0 * 1.05;

    xnew = x0;

    iter = 0;

    maxiter = 1000;

    while max (abs(x-xnew)) > tol & iter<maxiter

        iter = iter + 1;

```

```

x = xnew;

%below written line is BS

% fprintf('\n new values \n x1 = %6.4f \n x2 = %6.4f \n x3 = %6.4f
\n x4 = %6.4f \n x5 = %6.4f \n x6 = %6.4f \n x7 = %6.4f \n x8 =
%6.4f \n x9 = %6.4f \n x10 = %6.4f \n x11 = %6.4f \n x12 = %6.4f
\n\n',x);

fnk = feval(fnctn,x,varargin{:});

for k = 1:nx
    if x(k) ~= 0
        dx(k) = x(k)/500;
    else
        dx(k) = 1/500;
    end
end

a = x;
b = x;

for k = 1 : nx
    a(k) = a(k) - dx(k); fa = feval (fnctn,a,varargin{:});
    b(k) = b(k) + dx(k); fb = feval (fnctn,b,varargin{:});
    jacob (:,k) = (fb-fa)/(b(k)-a(k));
    a(k) = a(k) + dx(k);
    b(k) = b(k) - dx(k);
end

if det(jacob) == 0
    xnew = x + max([abs(dx),1.1*tol]);
else
    xnew = x - rho * inv(jacob) * fnk;
end

end

if iter >= maxiter

```

```

    disp('Warning: Maximum iteration reached')

end

h_LiBr.m


---


% this m file is the Enthalpy of Lithium Bromide solution as a function
of X

% and T

% T degree C

% X wt % (salt/solution)

function enthalpy_LiBr = h_LiBr (T,X)

    t = T + 273.15;

    XX = X * 100;

    a0 = -954.8 ;
    a1 = 47.7739;
    a2 = -1.59235;
    a3 = 2.09422*(10^(-2));
    a4 = -7.689*(10^(-5));
    b0 = -3.293*(10^(-1));
    b1 = 4.076*(10^(-2));
    b2 = -1.36*(10^(-5));
    b3 = -7.1366*(10^(-6));
    c0 = 7.4285*(10^(-3));
    c1 = -1.5144*(10^(-4));
    c2 = 1.3555*(10^(-6));
    d0 = -2.269*(10^(-6));

    SS1 = a0 + ( a1 * XX ) + ( a2 * XX * XX ) + ( a3 * XX * XX * XX ) + (
    a4 * XX * XX * XX * XX );

    SS2 = t * ( b0 + (b1 * XX ) + ( b2 * XX * XX ) + (b3 * XX * XX *XX ) )
    ;

    SS3 = (t ^ 2) * ( c0 + c1 * XX + c2 * XX * XX );

    SS4 = ( t ^ 3 ) * d0 ;

```

```
enthalpy_LiBr = SS1 + SS2 + SS3 + SS4;
```

A_LiBr.m

```
%Duhring-Feuerecker coefficient A_LiBr
```

```
function ALIBR = A_LiBr (X);

a_0 = 0.0 ;
a_1 = +1.6634856 *10^(+1) ;
a_2 = -5.5338169 *10^(+2) ;
a_3 = +1.1228336 *10^(+4) ;
a_4 = -1.1028390 *10^(+5) ;
a_5 = +6.2109464 *10^(+5) ;
a_6 = -2.1112567 *10^(+6) ;
a_7 = +4.3851901 *10^(+6) ;
a_8 = -5.4098115 *10^(+6) ;
a_9 = +3.6266742 *10^(+6) ;
a_10 = -1.0153059*10^(+6) ;

ALIBR =
a_0*(X^0)+a_1*(X^1)+a_2*(X^2)+a_3*(X^3)+a_4*(X^4)+a_5*(X^5)+a_6*(X^6)+a_
_7*(X^7)+a_8*(X^8)+a_9*(X^9)+a_10*(X^10);
```

B_LiBr.m

```
%Duhring-Feuerecker coefficient B_LiBr
```

```
function BLIBR = B_LiBr (X);

b_0 = 1.0 ;
b_1 = -6.8242821 *10^(-2) ;
b_2 = +5.8736190 *10^(0) ;
b_3 = -1.0278186 *10^(+2) ;
b_4 = +9.3032374 *10^(+2) ;
b_5 = -4.8223940 *10^(+3) ;
b_6 = +1.5189038 *10^(+4) ;
b_7 = -2.9412863 *10^(+4) ;
```

```

b_8 = +3.4100528 *10^(+4) ;
b_9 = -2.1671480 *10^(+4) ;
b_10 = +5.7995604 *10^(+3) ;

BLIBR =
b_0*(X^0)+b_1*(X^1)+b_2*(X^2)+b_3*(X^3)+b_4*(X^4)+b_5*(X^5)+b_6*(X^6)+b
_7*(X^7)+b_8*(X^8)+b_9*(X^9)+b_10*(X^10);

```

LMTD.m

```

% Logarithmic temperature difference for heat exchangers

% Th_i = Hot Fluid Inlet
% Th_o = Hot Fluid Outlet
% Tc_i = Cold Fluid Inlet
% Tc_o = Cold Fluid Outlet

function logmtd = LMTD ( Th_i , Th_o , Tc_i , Tc_o );

    del_1 = abs(Th_i - Tc_o);
    del_2 = abs(Th_o - Tc_i);

    % if (Tc_i > Tc_o) || (Th_i < Th_o) || (del_1 * del_2 <= 0) || (del_1
    == del_2)

    %     LMTD=0;

    %     ' the temperatures are not valid, please check again'

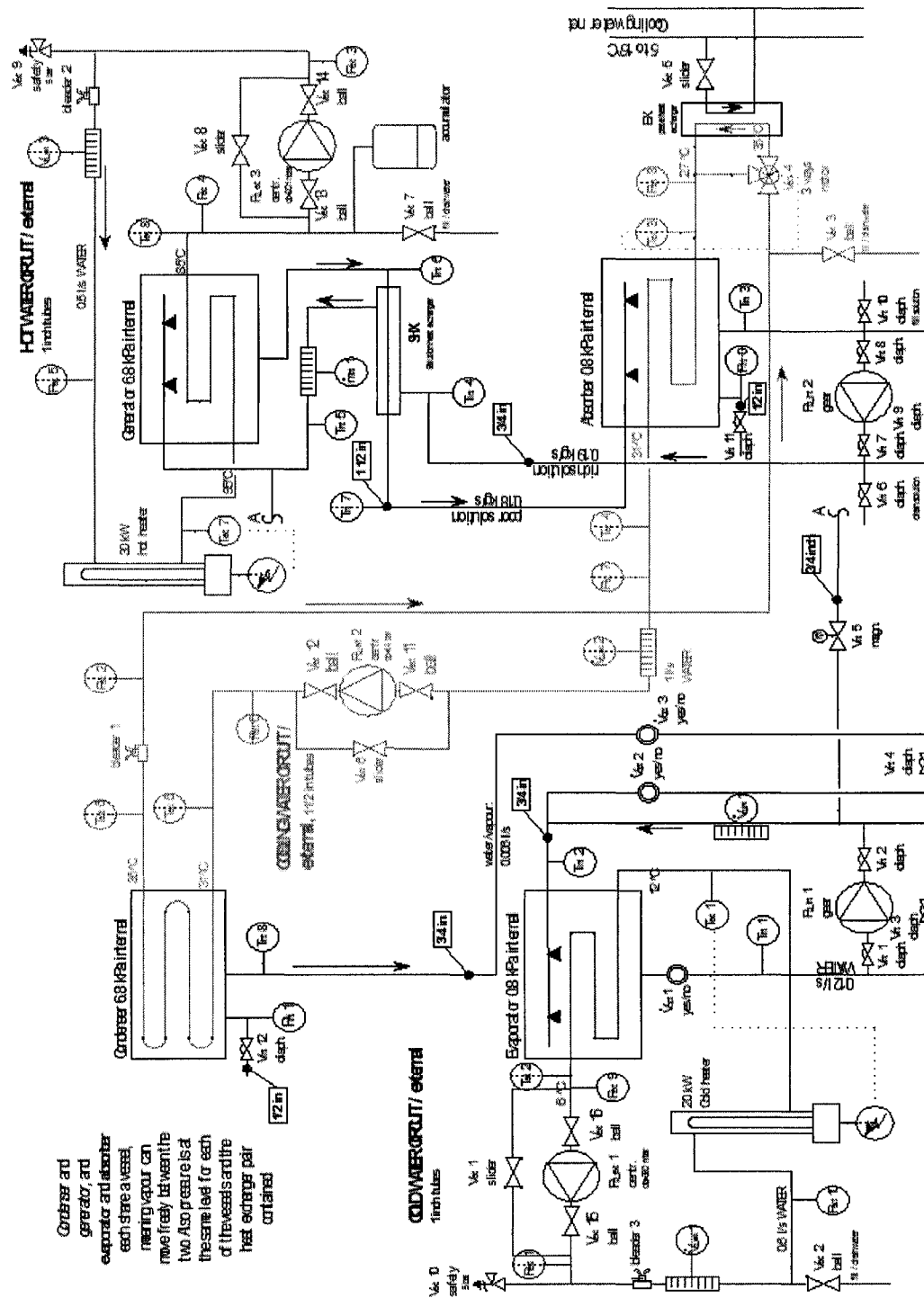
    % else

        logmtd = (del_1 - del_2) / log((del_1 / del_2));

    % end

```

Appendix B: P&ID of the AHP



Appendix C: Results

Input parameters	Set 1 – TUB		
T_1 (°C)	90.4 ± 1.1		
T_3 (°C)	11.7 ± 0.8		
T_5 (°C)	27.2 ± 1.3		
\dot{m}_1 (kg/sec)	0.339 ± 0.01		
\dot{m}_3 (kg/sec)	0.877 ± 0.01		
\dot{m}_5 (kg/sec)	0.722 ± 0.01		
\dot{m}_r (kg/sec)	0.110 ± 0.003		
output	Experiment	simulation	Exp – Sim
T_2 (°C)	81.6 ± 1.3	82.2	-0.6
T_4 (°C)	8.8 ± 1.0	8.5	0.3
T_6 (°C)	31.2 ± 1.6	30.9	0.3
T_7 (°C)	34.5 ± 1.8	34.6	-0.1
T_8 (°C)	80.6 ± 2.5	78.7	2.1
T_9 (°C)	41.5 ± 2.0	40.0	1.5
T_{10} (°C)	33.8 ± 2.9	36.7	-2.8
T_{11} (°C)	78.1 ± 1.8	79.7	-1.6
T_C (°C)	36.2 ± 0.6	36.1	0.1
T_E (°C)	5.2 ± 1.2	5.9	-0.7
X_r ($\frac{wt}{wt}$ %)	60 ± 3	59	1
X_p ($\frac{wt}{wt}$ %)	58 ± 5	56	2
\dot{Q}_G (kW)	12.5 ± 1.5	11.6	0.9
\dot{Q}_C (kW)	10.0 ± 3.8	11.1	-1.2
\dot{Q}_E (kW)	9.7 ± 2.7	10.8	-1.1
\dot{Q}_A (kW)	12.2 ± 1.5	11.3	0.9
COP	$0.74 \pm .35$	0.94	0.20

Input parameters	Set 2 – TUB		
T_1 (°C)	93.9 ± 1.0		
T_3 (°C)	12.2 ± 0.7		
T_5 (°C)	29.4 ± 1.3		
\dot{m}_1 (kg/sec)	0.238 ± 0.01		
\dot{m}_3 (kg/sec)	0.863 ± 0.01		
\dot{m}_5 (kg/sec)	0.719 ± 0.01		
\dot{m}_r (kg/sec)	0.088 ± 0.004		
output	Experiment	Simulation	Exp – Sim
T_2 (°C)	83.7 ± 1.2	83.4	0.3
T_4 (°C)	9.5 ± 1.0	9.2	0.3
T_6 (°C)	33.3 ± 1.5	32.8	0.4
T_7 (°C)	36.3 ± 1.6	36.1	0.1
T_8 (°C)	81.0 ± 0.6	81.2	-0.2
T_9 (°C)	37.0 ± 1.7	35.6	1.4
T_{10} (°C)	40.2 ± 0.5	40.2	0.0
T_{11} (°C)	73.2 ± 2.0	75.2	-2.0
T_C (°C)	37.8 ± 0.6	37.5	0.3
T_E (°C)	6.7 ± 0.8	6.9	-0.2
X_r ($\frac{wt}{wt}$ %)	59 ± 1	59	0
X_p ($\frac{wt}{wt}$ %)	58 ± 5	56	3
\dot{Q}_G (kW)	10.23 ± 1.5	10.52	-0.29
\dot{Q}_C (kW)	9.06 ± 1.8	9.96	-0.90
\dot{Q}_E (kW)	8.77 ± 1.4	9.71	-0.94
\dot{Q}_A (kW)	11.53 ± 1.9	10.28	1.25
COP	$0.86 \pm .25$	0.92	-0.07

Input parameters	Set 3 – TUB		
T_1 (°C)	92.3 ± 1.0		
T_3 (°C)	11.1 ± 0.7		
T_5 (°C)	27.3 ± 1.2		
\dot{m}_1 (kg/sec)	0.246 ± 0.01		
\dot{m}_3 (kg/sec)	0.874 ± 0.01		
\dot{m}_5 (kg/sec)	0.721 ± 0.01		
\dot{m}_r (kg/sec)	0.082 ± 0.003		
output	Experiment	Simulation	Exp – Sim
T_2 (°C)	81.67 ± 1.2	81.80	-0.13
T_4 (°C)	8.72 ± 1.0	8.12	0.60
T_6 (°C)	30.78 ± 1.6	30.85	-0.07
T_7 (°C)	33.56 ± 1.4	34.25	-0.69
T_8 (°C)	81.28 ± 2.9	79.55	1.73
T_9 (°C)	35.00 ± 2.1	33.71	1.29
T_{10} (°C)	36.63 ± 2.8	38.56	-1.93
T_{11} (°C)	77.79 ± 2.4	79.97	-2.18
T_C (°C)	34.95 ± 1.6	35.64	-0.69
T_E (°C)	5.76 ± 0.7	5.70	0.06
X_r ($\frac{wt}{wt}$ %)	59 ± 3	56	3
X_p ($\frac{wt}{wt}$ %)	61 ± 6	59	2
\dot{Q}_G (kW)	11.04 ± 1.5	10.91	0.14
\dot{Q}_C (kW)	8.43 ± 1.8	10.30	-1.87
\dot{Q}_E (kW)	8.05 ± 2.7	10.06	-2.01
\dot{Q}_A (kW)	10.48 ± 2.5	10.70	-0.22
COP	0.73 ± 0.5	0.92	-0.19

Input parameters	Set 4 – TUB		
T_1 (°C)	75.9 ± 0.4		
T_3 (°C)	18.0 ± 0.3		
T_5 (°C)	26.5 ± 0.6		
\dot{m}_1 (kg/sec)	0.319 ± 0.01		
\dot{m}_3 (kg/sec)	0.717 ± 0.01		
\dot{m}_5 (kg/sec)	0.855 ± 0.01		
\dot{m}_r (kg/sec)	0.073 ± 0.02		
output	Experiment	Simulation	Exp – Sim
T_2 (°C)	67.9 ± 0.8	68.4	-0.5
T_4 (°C)	15.6 ± 0.5	15.1	0.5
T_6 (°C)	29.8 ± 0.9	29.8	0.0
T_7 (°C)	32.8 ± 1.1	33.0	-0.2
T_8 (°C)	67.2 ± 1.6	65.9	1.3
T_9 (°C)	34.0 ± 1.3	32.8	1.2
T_{10} (°C)	33.4 ± 2.7	36.1	-2.7
T_{11} (°C)	64.1 ± 2.9	66.2	-2.1
T_C (°C)	34.4 ± 0.9	34.3	0.1
T_E (°C)	13.3 ± 0.8	12.8	0.5
X_r ($\frac{wt}{wt}$ %)	53 ± 3	51	2
X_p ($\frac{wt}{wt}$ %)	55 ± 5	54	1
\dot{Q}_G (kW)	10.65 ± 1.3	9.94	0.71
\dot{Q}_C (kW)	9.00 ± 1.2	9.60	-0.59
\dot{Q}_E (kW)	8.01 ± 2.3	9.55	-1.54
\dot{Q}_A (kW)	9.94 ± 1.2	9.87	0.07
COP	$0.75 \pm .4$	0.96	-0.21

Input parameters	Set 5 – TUB		
T_1 (°C)	65.8 ± 0.4		
T_3 (°C)	18.0 ± 0.3		
T_5 (°C)	26.4 ± 0.6		
\dot{m}_1 (kg/sec)	0.321 ± 0.01		
\dot{m}_3 (kg/sec)	0.717 ± 0.01		
\dot{m}_5 (kg/sec)	0.855 ± 0.01		
\dot{m}_r (kg/sec)	0.072 ± 0.002		
output	Experiment	Simulation	Exp – Sim
T_2 (°C)	59.9 ± 0.6	60.0	-0.1
T_4 (°C)	16.2 ± 0.7	15.7	0.5
T_6 (°C)	28.9 ± 0.9	29.0	-0.1
T_7 (°C)	31.2 ± 1.0	31.5	-0.3
T_8 (°C)	58.9 ± 1.2	58.0	0.9
T_9 (°C)	32.8 ± 1.5	31.4	1.4
T_{10} (°C)	31.9 ± 2.1	33.6	-1.7
T_{11} (°C)	57.0 ± 1.9	58.4	-1.4
T_C (°C)	32.3 ± 0.8	32.5	-0.3
T_E (°C)	14.3 ± 0.6	13.9	0.4
X_r ($\frac{wt}{wt}$ %)	50 ± 4	48	2
X_p ($\frac{wt}{wt}$ %)	51 ± 6	51	0
\dot{Q}_G (kW)	7.93 ± 0.7	7.77	0.17
\dot{Q}_C (kW)	6.77 ± 1.4	7.50	-0.73
\dot{Q}_E (kW)	5.87 ± 2.3	7.57	-1.69
\dot{Q}_A (kW)	7.39 ± 1.9	7.69	-0.30
COP	0.74 ± 0.8	0.97	-0.23

Input parameters	Set 6 – TUB		
T_1 (°C)	85.9 ± 1.2		
T_3 (°C)	18.0 ± 1.0		
T_5 (°C)	28.2 ± 1.2		
\dot{m}_1 (kg/sec)	0.316 ± 0.01		
\dot{m}_3 (kg/sec)	0.718 ± 0.01		
\dot{m}_5 (kg/sec)	0.855 ± 0.01		
\dot{m}_r (kg/sec)	0.073 ± 0.001		
output	Experiment	Simulation	Exp – Sim
T_2 (°C)	76.3 ± 1.4	77.4	-1.1
T_4 (°C)	15.3 ± 1.5	14.8	0.5
T_6 (°C)	32.0 ± 1.4	31.9	0.1
T_7 (°C)	35.5 ± 1.6	35.5	0.0
T_8 (°C)	76.0 ± 2.7	74.7	1.3
T_9 (°C)	36.7 ± 2.8	35.0	1.7
T_{10} (°C)	36.2 ± 2.9	39.0	-2.8
T_{11} (°C)	72.0 ± 2.9	74.9	-2.9
T_C (°C)	37.4 ± 1.0	37.0	0.4
T_E (°C)	13.2 ± 1.2	12.2	1.0
X_r ($\frac{wt}{wt}$ %)	54 ± 3	53	1
X_p ($\frac{wt}{wt}$ %)	57 ± 5	56	1
\dot{Q}_G (kW)	12.77 ± 2.1	11.28	1.49
\dot{Q}_C (kW)	11.41 ± 2.5	11.04	0.37
\dot{Q}_E (kW)	8.95 ± 2.1	10.54	-1.58
\dot{Q}_A (kW)	10.53 ± 2.2	10.81	-0.28
COP	0.70 ± 0.35	0.93	-0.23

Input parameters	Set 7 – TUB		
T_1 (°C)	90.9 ± 1.3		
T_3 (°C)	18.0 ± 0.9		
T_5 (°C)	28.7 ± 1.2		
\dot{m}_1 (kg/sec)	0.311 ± 0.01		
\dot{m}_3 (kg/sec)	0.719 ± 0.01		
\dot{m}_5 (kg/sec)	0.856 ± 0.01		
\dot{m}_r (kg/sec)	0.077 ± 0.001		
output	Experiment	Simulation	Exp – Sim
T_2 (°C)	80.5 ± 1.5	81.6	-1.1
T_4 (°C)	15.0 ± 1.2	14.5	0.5
T_6 (°C)	33.0 ± 1.6	32.7	0.3
T_7 (°C)	36.6 ± 1.0	36.6	0.0
T_8 (°C)	80.1 ± 1.5	78.7	1.4
T_9 (°C)	38.5 ± 2.9	36.1	2.4
T_{10} (°C)	39.6 ± 1.5	41.0	-1.4
T_{11} (°C)	77.2 ± 1.7	78.9	-1.7
T_C (°C)	38.6 ± 1.0	38.2	0.4
T_E (°C)	13.0 ± 1.9	11.8	1.2
X_r ($\frac{wt}{wt}$ %)	56 ± 3	54	2
X_p ($\frac{wt}{wt}$ %)	58 ± 5	58	1
\dot{Q}_G (kW)	13.55 ± 2.0	12.15	1.40
\dot{Q}_C (kW)	10.90 ± 2.1	11.71	-0.81
\dot{Q}_E (kW)	9.89 ± 2.4	11.53	-1.65
\dot{Q}_A (kW)	12.77 ± 2.1	11.87	0.90
COP	$0.73 \pm .5$	0.95	-0.22

Input parameters	AC4 – Polytechnique		
T_1 (°C)	95.0 ± 0.5		
T_3 (°C)	20.0 ± 0.7		
T_5 (°C)	30.0 ± 0.7		
\dot{m}_1 (kg/sec)	0.612 ± 0.01		
\dot{m}_3 (kg/sec)	0.671 ± 0.03		
\dot{m}_5 (kg/sec)	0.743 ± 0.03		
\dot{m}_r (kg/sec)	0.184 ± 0.011		
output	Experiment	Simulation	Exp – Sim
T_2 (°C)	86.5 ± 0.9	86.6	-0.1
T_4 (°C)	15 ± 1.1	14.2	0.8
T_6 (°C)	37.1 ± 1.0	36.8	0.3
T_7 (°C)	43.1 ± 1.2	43.4	-0.3
T_8 (°C)	85.2 ± 1.7	86.6	-1.4
T_9 (°C)	36.0 ± 1.6	37.3	-1.3
T_{10} (°C)	43.1 ± 1.9	41.6	1.5
T_{11} (°C)	88.0 ± 2.1	87.1	0.9
T_C (°C)	42.5 ± 1.9	43.8	-1.3
T_E (°C)	8.4 ± 1.2	9.2	-0.8
X_r ($\frac{wt}{wt}$ %)	55 ± 2	56	-1
X_p ($\frac{wt}{wt}$ %)	58 ± 1	58	0
\dot{Q}_G (kW)	21.9 ± 1.7	21.6	0.26
\dot{Q}_C (kW)	16.9 ± 2.4	18.6	-1.69
\dot{Q}_E (kW)	15.6 ± 2.9	18.1	-2.50
\dot{Q}_A (kW)	20.0 ± 2.3	19.2	0.85
COP	0.71 ± 0.31	0.84	-0.13

Input parameters	AC1 - Polytechnique		
T_1 (°C)	90.3 ± 0.3		
T_3 (°C)	15.1 ± 1.3		
T_5 (°C)	27.4 ± 0.8		
\dot{m}_1 (kg/sec)	0.436 ± 0.01		
\dot{m}_3 (kg/sec)	0.591 ± 0.01		
\dot{m}_5 (kg/sec)	0.666 ± 0.01		
\dot{m}_r (kg/sec)	0.200 ± 0.004		
output	Experiment	Simulation	Exp – Sim
T_2 (°C)	80.8 ± 0.5	80.7	0.1
T_4 (°C)	10.3 ± 1.8	8.5	1.8
T_6 (°C)	33.1 ± 1.1	33.5	-0.4
T_7 (°C)	37.7 ± 1.9	39.5	-1.8
T_8 (°C)	78.0 ± 1.5	79.4	-1.4
T_9 (°C)	35.0 ± 1.0	35.2	-0.2
T_{10} (°C)	39.2 ± 1.2	38.3	0.9
T_{11} (°C)	77.8 ± 2.1	79.7	-1.9
T_C (°C)	40.1 ± 1.0	39.7	0.4
T_E (°C)	8.1 ± 1.2	7.4	0.7
X_r ($\frac{wt}{wt}$ %)	58 ± 2	57	1
X_p ($\frac{wt}{wt}$ %)	56 ± 5	55	1
\dot{Q}_G (kW)	17.30 ± 2.0	17.56	-0.26
\dot{Q}_C (kW)	12.80 ± 2.1	14.79	-1.99
\dot{Q}_E (kW)	13.80 ± 2.5	15.38	-1.58
\dot{Q}_A (kW)	15.90 ± 2.1	17.07	-1.17
COP	0.69 ± 0.30	0.93	-0.24

Input parameters	AC2 - Polytechnique		
T_1 (°C)	87.4 ± 0.2		
T_3 (°C)	15.1 ± 1.1		
T_5 (°C)	27.4 ± 1.0		
\dot{m}_1 (kg/sec)	0.392 ± 0.01		
\dot{m}_3 (kg/sec)	0.586 ± 0.01		
\dot{m}_5 (kg/sec)	0.670 ± 0.01		
\dot{m}_r (kg/sec)	0.189 ± 0.002		
output	Experiment	Simulation	Exp – Sim
T_2 (°C)	77.6 ± 0.5	77.8	-0.2
T_4 (°C)	10.5 ± 2.0	8.9	1.6
T_6 (°C)	32.7 ± 1.3	33.0	-0.3
T_7 (°C)	37.1 ± 1.7	38.5	-1.4
T_8 (°C)	77.8 ± 1.3	76.5	1.3
T_9 (°C)	35.1 ± 1.0	34.6	0.5
T_{10} (°C)	38.1 ± 2.0	37.4	0.7
T_{11} (°C)	78.9 ± 2.3	76.8	2.1
T_C (°C)	36.5 ± 2.8	38.7	-2.2
T_E (°C)	6.4 ± 1.7	7.9	-1.5
X_r ($\frac{wt}{wt}$ %)	58 ± 4	55	3
X_p ($\frac{wt}{wt}$ %)	55 ± 6	56	-1
\dot{Q}_G (kW)	16.20 ± 1.0	15.82	0.38
\dot{Q}_C (kW)	13.20 ± 2.8	15.47	-2.27
\dot{Q}_E (kW)	11.40 ± 2.9	14.26	-2.86
\dot{Q}_A (kW)	15.00 ± 2.0	15.75	-0.75
COP	0.71 ± 0.7	0.96	-0.25

Input parameters	AC3 - Polytechnique		
T_1 (°C)	95.3 ± 0.1		
T_3 (°C)	15.0 ± 0.9		
T_5 (°C)	27.5 ± 1.1		
\dot{m}_1 (kg/sec)	$0.452 \pm .01$		
\dot{m}_3 (kg/sec)	$0.597 \pm .01$		
\dot{m}_5 (kg/sec)	$0.663 \pm .02$		
\dot{m}_r (kg/sec)	$0.181 \pm .003$		
output	Experiment	Simulation	Exp – Sim
T_2 (°C)	85.4 ± 0.5	85.2	0.2
T_4 (°C)	9.9 ± 2.1	8.0	1.9
T_6 (°C)	33.6 ± 1.1	34.2	-0.6
T_7 (°C)	38.7 ± 2.4	40.6	-1.9
T_8 (°C)	85.4 ± 0.6	85.2	0.2
T_9 (°C)	84.7 ± 1.0	83.9	0.8
T_{10} (°C)	33.7 ± 2.2	35.8	-2.1
T_{11} (°C)	40.1 ± 0.4	39.7	0.4
T_C (°C)	86.0 ± 2.6	84.1	1.9
T_E (°C)	38.5 ± 2.7	40.8	-2.3
X_r ($\frac{wt}{wt}$ %)	54 ± 3	56	-2
X_p ($\frac{wt}{wt}$ %)	59 ± 6	59	0
\dot{Q}_G (kW)	18.70 ± 1.1	19.17	-0.47
\dot{Q}_C (kW)	15.02 ± 2.8	17.82	-2.80
\dot{Q}_E (kW)	13.90 ± 2.9	16.54	-2.64
\dot{Q}_A (kW)	17.10 ± 2.0	18.66	-1.56
COP	0.69 ± 0.6	0.92	-0.23

Input parameters	RUN 2 - Polytechnique		
T_1 (°C)	70.0		
T_3 (°C)	15.0		
T_5 (°C)	26.5		
\dot{m}_1 (kg/sec)	0.618		
\dot{m}_3 (kg/sec)	0.254		
\dot{m}_5 (kg/sec)	0.185		
\dot{m}_r (kg/sec)	0.184		
output	Experiment	Simulation	Exp – Sim
T_2 (°C)	68.2	66.4	1.8
T_4 (°C)	13.1	8.2	4.9
T_6 (°C)	32.6	38.4	-5.8
T_7 (°C)	36.0	48.1	-12.1
T_8 (°C)	N/A	66.3	N/A
T_9 (°C)	N/A	32.5	N/A
T_{10} (°C)	N/A	34.0	N/A
T_{11} (°C)	N/A	67.2	N/A
T_C (°C)	N/A	38.2	N/A
T_E (°C)	N/A	10.2	N/A
X_r ($\frac{wt}{wt}$ %)	N/A	52	N/A
X_p ($\frac{wt}{wt}$ %)	N/A	51	N/A
\dot{Q}_G (kW)	4.80	9.48	-4.68
\dot{Q}_C (kW)	2.70	7.53	-4.83
\dot{Q}_E (kW)	2.00	7.27	-5.27
\dot{Q}_A (kW)	4.70	9.23	-4.53
COP	0.42	0.77	-0.35

This is an example of overflowing of refrigerant from the evaporator into the absorber. As it is observed the differences of the simulation and experimental values are high.

Input parameters	RUN 9 - Polytechnique		
T_1 (°C)	70.0 ± 0.8		
T_3 (°C)	6.0 ± 0.9		
T_5 (°C)	26.5 ± 0.6		
\dot{m}_1 (kg/sec)	0.131 ± 0.01		
\dot{m}_3 (kg/sec)	0.737 ± 0.01		
\dot{m}_5 (kg/sec)	0.611 ± 0.01		
\dot{m}_r (kg/sec)	0.153 ± 0.004		
output	Experiment	Simulation	Exp – Sim
T_2 (°C)	63.5 ± 1.3	62.6	0.9
T_4 (°C)	5.8 ± 1.6	4.7	1.1
T_6 (°C)	27.6 ± 1.0	28.1	-0.5
T_7 (°C)	28.1 ± 1.8	29.6	-1.5
T_8 (°C)	62.3 ± 0.6	61.9	0.4
T_9 (°C)	28.7 ± 1.0	29.3	-0.6
T_{10} (°C)	31.1 ± 1.1	30.4	0.7
T_{11} (°C)	63.0 ± 1.1	62.4	0.6
T_c (°C)	31.6 ± 1.3	30.4	1.2
T_E (°C)	4.3 ± 1.0	3.6	0.7
X_r ($\frac{wt}{wt}$ %)	52 ± 2	53	-1
X_p ($\frac{wt}{wt}$ %)	53 ± 4	54	-1
\dot{Q}_G (kW)	3.60 ± 1.5	4.07	-0.47
\dot{Q}_C (kW)	1.20 ± 2.6	3.85	-2.65
\dot{Q}_E (kW)	0.70 ± 3.0	3.30	-2.60
\dot{Q}_A (kW)	2.90 ± 1.5	4.11	-1.21
COP	0.35 ± 0.3	0.68	-0.33

Input parameters	RUN 10 - Polytechnique		
T_1 (°C)	75.0 ± 0.3		
T_3 (°C)	14.8 ± 0.6		
T_5 (°C)	28.8 ± 0.9		
\dot{m}_1 (kg/sec)	0.619 ± 0.01		
\dot{m}_3 (kg/sec)	0.746 ± 0.01		
\dot{m}_5 (kg/sec)	0.670 ± 0.01		
\dot{m}_r (kg/sec)	0.158 ± 0.004		
output	Experiment	Simulation	Exp – Sim
T_2 (°C)	69.9 ± 0.5	69.9	0.0
T_4 (°C)	11.6 ± 1.0	10.8	0.8
T_6 (°C)	32.7 ± 1.4	31.4	1.3
T_7 (°C)	36.5 ± 0.9	36.0	0.5
T_8 (°C)	68.0 ± 1.2	68.5	-0.5
T_9 (°C)	32.1 ± 1.7	32.7	-0.6
T_{10} (°C)	36.1 ± 1.9	35.0	1.1
T_{11} (°C)	69.4 ± 1.0	68.7	0.7
T_C (°C)	37.1 ± 1.2	36.2	0.9
T_E (°C)	10.8 ± 1.7	9.6	1.2
X_r ($\frac{wt}{wt}$ %)	53 ± 3	52	1
X_p ($\frac{wt}{wt}$ %)	57 ± 5	54	3
\dot{Q}_G (kW)	13.30 ± 1.2	13.25	0.05
\dot{Q}_C (kW)	10.70 ± 2.1	11.95	-1.25
\dot{Q}_E (kW)	10.00 ± 2.0	11.54	-1.54
\dot{Q}_A (kW)	11.00 ± 1.8	9.32	1.68
COP	$0.75 \pm .20$	0.87	-0.12

Input parameters	RUN 16 - Polytechnique		
T_1 (°C)	110.0 ± 0.7		
T_3 (°C)	15.0 ± 0.3		
T_5 (°C)	34.1 ± 0.7		
\dot{m}_1 (kg/sec)	0.590 ± 0.01		
\dot{m}_3 (kg/sec)	0.740 ± 0.01		
\dot{m}_5 (kg/sec)	0.657 ± 0.01		
\dot{m}_r (kg/sec)	0.215 ± 0.002		
output	Experiment	Simulation	Exp – Sim
T_2 (°C)	101.3 ± 1.4	101.3	0.0
T_4 (°C)	11.0 ± 0.5	10.3	0.8
T_6 (°C)	40.8 ± 1.1	41.5	-0.7
T_7 (°C)	46.1 ± 1.6	47.3	-1.1
T_8 (°C)	100.0 ± 1.2	98.8	1.2
T_9 (°C)	43.1 ± 1.9	44.0	-0.9
T_{10} (°C)	49.0 ± 1.8	47.9	1.1
T_{11} (°C)	97.8 ± 2.1	99.7	-1.9
T_C (°C)	48.0 ± 1.9	47.1	0.9
T_E (°C)	5.2 ± 1.8	6.8	-1.6
X_r ($\frac{wt}{wt}$ %)	58 ± 2	60	-2
X_p ($\frac{wt}{wt}$ %)	63 ± 3	62	1
\dot{Q}_G (kW)	21.60 ± 2.2	21.52	0.08
\dot{Q}_C (kW)	14.70 ± 1.8	15.76	-1.06
\dot{Q}_E (kW)	12.40 ± 1.6	14.74	-2.34
\dot{Q}_A (kW)	18.50 ± 1.7	20.53	-2.03
COP	0.75 ± 0.30	0.68	-0.10

Input parameters	RUN 14 - Polytechnique		
T_1 (°C)	110.0 ± 0.8		
T_3 (°C)	15.0 ± 0.7		
T_5 (°C)	26.4 ± 0.9		
\dot{m}_1 (kg/sec)	0.577 ± 0.010		
\dot{m}_3 (kg/sec)	0.550 ± 0.010		
\dot{m}_5 (kg/sec)	0.652 ± 0.010		
\dot{m}_r (kg/sec)	0.181 ± 0.005		
output	Experiment	Simulation	Exp – Sim
T_2 (°C)	104.2 ± 1.1	103.3	0.9
T_4 (°C)	10.8 ± 1.5	9.5	1.3
T_6 (°C)	31.8 ± 1.1	32.3	-0.5
T_7 (°C)	36.5 ± 1.6	37.8	-1.3
T_8 (°C)	97.0 ± 1.7	96.1	0.9
T_9 (°C)	40.3 ± 2.1	39.2	1.1
T_{10} (°C)	45.2 ± 1.8	44.3	0.9
T_{11} (°C)	97.6 ± 2.0	96.4	1.2
T_C (°C)	43.6 ± 1.7	42.9	0.7
T_E (°C)	4.7 ± 1.9	3.4	1.3
X_r ($\frac{wt}{wt}$ %)	63 ± 2	61	2
X_p ($\frac{wt}{wt}$ %)	64 ± 4	63	1
\dot{Q}_G (kW)	14.10 ± 2.9	16.25	-2.15
\dot{Q}_C (kW)	12.70 ± 2.8	15.07	-2.37
\dot{Q}_E (kW)	9.80 ± 2.9	12.71	-2.91
\dot{Q}_A (kW)	14.90 ± 2.6	16.16	-1.26
COP	0.70 ± 0.5	0.78	-0.08

Input parameters	RUN 6 - Polytechnique		
T_1 (°C)	110.0 ± 0.6		
T_3 (°C)	15.0 ± 0.9		
T_5 (°C)	26.5 ± 0.7		
\dot{m}_1 (kg/sec)	0.089 ± 0.010		
\dot{m}_3 (kg/sec)	0.743 ± 0.010		
\dot{m}_5 (kg/sec)	0.161 ± 0.010		
\dot{m}_r (kg/sec)	0.139 ± 0.005		
output	Experiment	Simulation	Exp – Sim
T_2 (°C)	88.0 ± 1.1	88.5	-0.5
T_4 (°C)	13.7 ± 1.6	12.6	1.1
T_6 (°C)	37.0 ± 1.9	38.0	-1.0
T_7 (°C)	46.7 ± 1.8	48.4	-1.7
T_8 (°C)	87.6 ± 1.6	88.1	-0.5
T_9 (°C)	39.1 ± 1.7	38.6	0.5
T_{10} (°C)	42.4 ± 1.5	41.0	1.4
T_{11} (°C)	89.7 ± 1.6	88.4	1.3
T_C (°C)	48.6 ± 1.9	49.5	-0.9
T_E (°C)	11.6 ± 1.7	10.5	1.1
X_r ($\frac{wt}{wt}$ %)	53 ± 2	55	-2
X_p ($\frac{wt}{wt}$ %)	57 ± 4	56	1
\dot{Q}_G (kW)	8.20 ± 2.6	8.00	0.20
\dot{Q}_C (kW)	4.90 ± 2.7	7.04	-2.14
\dot{Q}_E (kW)	4.10 ± 2.1	5.89	-1.79
\dot{Q}_A (kW)	7.10 ± 2.1	7.78	-0.68
COP	0.50 ± 0.3	0.74	-0.24

Input parameters	RUN 15 - Polytechnique		
T_1 (°C)	110.0 ± 0.9		
T_3 (°C)	6.1 ± 1.2		
T_5 (°C)	34.0 ± 1.0		
\dot{m}_1 (kg/sec)	0.123 ± 0.010		
\dot{m}_3 (kg/sec)	0.740 ± 0.010		
\dot{m}_5 (kg/sec)	0.616 ± 0.010		
\dot{m}_r (kg/sec)	0.157 ± 0.005		
output	Experiment	Simulation	Exp – Sim
T_2 (°C)	106.0 ± 1.0	105.9	0.1
T_4 (°C)	4.0 ± 1.3	3.5	0.5
T_6 (°C)	38.0 ± 1.5	37.7	0.3
T_7 (°C)	42.0 ± 1.7	42.1	-0.1
T_8 (°C)	102.0 ± 0.8	101.6	0.4
T_9 (°C)	41.0 ± 0.6	41.1	-0.1
T_{10} (°C)	45.0 ± 0.8	45.4	-0.4
T_{11} (°C)	102.0 ± 0.9	101.9	0.1
T_c (°C)	44.0 ± 1.1	44.0	0.0
T_E (°C)	1.0 ± 1.2	0.4	0.6
X_r ($\frac{wt}{wt}$ %)	53 ± 1	53	0
X_p ($\frac{wt}{wt}$ %)	56 ± 1	56	0
\dot{Q}_G (kW)	12.09 ± 1.5	12.53	-0.4
\dot{Q}_C (kW)	10.30 ± 1.9	11.29	-1.0
\dot{Q}_E (kW)	9.29 ± 1.7	10.92	-1.6
\dot{Q}_A (kW)	12.87 ± 1.9	12.16	0.7
COP	0.77 ± 0.2	0.87	0.10

Input parameters	RUN 1 - Polytechnique		
T_1 (°C)	69.9 ± 0.5		
T_3 (°C)	6.7 ± 1.1		
T_5 (°C)	26.5 ± 0.8		
\dot{m}_1 (kg/sec)	0.107 ± 0.015		
\dot{m}_3 (kg/sec)	0.256 ± 0.010		
\dot{m}_5 (kg/sec)	0.195 ± 0.010		
\dot{m}_r (kg/sec)	0.158 ± 0.005		
output	Experiment	Simulation	Exp – Sim
T_2 (°C)	64.3 ± 0.8	64.6	-0.3
T_4 (°C)	6.3 ± 2.1	4.4	1.9
T_6 (°C)	30.0 ± 1.8	29.4	0.6
T_7 (°C)	30.3 ± 2.3	32.5	-2.2
T_8 (°C)	64.0 ± 0.5	63.7	0.3
T_9 (°C)	28.7 ± 1.1	29.6	-0.9
T_{10} (°C)	32.2 ± 1.6	30.8	1.4
T_{11} (°C)	66.9 ± 2.3	64.5	2.4
T_C (°C)	31.1 ± 1.7	32.6	-1.5
T_E (°C)	3.5 ± 1.2	4.1	-0.6
X_r ($\frac{wt}{wt}$ %)	52 ± 2	53	-1
X_p ($\frac{wt}{wt}$ %)	55 ± 3	54	1
\dot{Q}_G (kW)	2.50 ± 1.0	2.38	0.12
\dot{Q}_C (kW)	0.30 ± 2.3	2.54	-2.24
\dot{Q}_E (kW)	0.40 ± 2.4	2.47	-2.07
\dot{Q}_A (kW)	2.90 ± 1.7	2.37	0.53
COP	0.14 ± 1.2	1.04	-0.90

Input parameters	RUN 8 - Polytechnique		
T_1 (°C)	110.0 ± 0.2		
T_3 (°C)	15.1 ± 0.9		
T_5 (°C)	34.0 ± 0.8		
\dot{m}_1 (kg/sec)	0.603 ± 0.010		
\dot{m}_3 (kg/sec)	0.266 ± 0.010		
\dot{m}_5 (kg/sec)	0.194 ± 0.010		
\dot{m}_r (kg/sec)	0.153 ± 0.010		
output	Experiment	Simulation	Exp – Sim
T_2 (°C)	105.5 ± 0.5	105.4	0.1
T_4 (°C)	12.2 ± 1.7	11.0	1.2
T_6 (°C)	43.1 ± 1.6	44.0	-0.9
T_7 (°C)	54.9 ± 1.9	56.0	-1.1
T_8 (°C)	99.8 ± 2.1	101.7	-1.9
T_9 (°C)	28.9 ± 1.8	28.5	0.4
T_{10} (°C)	33.4 ± 1.6	32.9	0.5
T_{11} (°C)	101.0 ± 1.4	102.1	-1.1
T_C (°C)	63.0 ± 1.7	61.5	1.5
T_E (°C)	5.0 ± 1.2	4.3	0.7
X_r ($\frac{wt}{wt}$ %)	57 ± 1	56	1
X_p ($\frac{wt}{wt}$ %)	53 ± 2	54	-1
\dot{Q}_G (kW)	11.40 ± 1.1	11.66	-0.26
\dot{Q}_C (kW)	7.00 ± 1.9	8.30	-1.30
\dot{Q}_E (kW)	3.20 ± 2.1	4.57	-1.37
\dot{Q}_A (kW)	7.40 ± 2.0	8.15	-0.75
COP	0.28 ± 0.50	0.39	-0.11

Input parameters	RUN 7 - Polytechnique		
T_1 (°C)	110.7 ± 0.5		
T_3 (°C)	6.0 ± 0.9		
T_5 (°C)	34.0 ± 0.2		
\dot{m}_1 (kg/sec)	0.099 ± 0.01		
\dot{m}_3 (kg/sec)	0.259 ± 0.01		
\dot{m}_5 (kg/sec)	0.199 ± 0.01		
\dot{m}_r (kg/sec)	0.200 ± 0.001		
output	Experiment	Simulation	Exp – Sim
T_2 (°C)	95.6 ± 1.6	97.1	-1.5
T_4 (°C)	3.9 ± 2.7	2.1	1.8
T_6 (°C)	40.2 ± 0.8	39.9	0.3
T_7 (°C)	44.1 ± 1.3	45.3	-1.2
T_8 (°C)	95.0 ± 2.6	96.9	-1.9
T_9 (°C)	39.1 ± 2.8	40.4	-1.3
T_{10} (°C)	40.8 ± 2.1	42.7	-1.9
T_{11} (°C)	99.2 ± 2.0	98.3	0.9
T_C (°C)	45.8 ± 1.5	46.1	-0.3
T_E (°C)	2.0 ± 1.0	1.2	0.8
X_r ($\frac{wt}{wt}$ %)	60 ± 2	61	-1
X_p ($\frac{wt}{wt}$ %)	63 ± 4	62	1
\dot{Q}_G (kW)	6.70 ± 2.5	5.63	1.07
\dot{Q}_C (kW)	2.30 ± 2.2	4.52	-2.22
\dot{Q}_E (kW)	1.30 ± 2.9	4.25	-2.95
\dot{Q}_A (kW)	5.20 ± 1.8	4.94	0.26
COP	0.19 ± 0.1	0.75	-0.56

Appendix D: h and U calculations

$A_{tot} = 8.087$	$A_{tube} = 0.00008107$	$COP = 0.7526$	$diameter = 0.0127$
$\eta_{SHX} = 0.88$	$f = 30$	$length = 0.6$	$\dot{m}_p = 0.1854$ $\dot{m}_{vap} = 0.006394$
$\dot{m}_r = 0.1918$	$SF = 4$	$thickness = 0.00127$	$wet_A = 111.8$ $wet_E = 114.5$
$wet_G = 115.6$	$x_p = 58.91$	$x_m = 57.93$	$x_r = 56.95$

where:

A_{tot} total main heat exchanger area (without SHX area) [m²]
 A_{tube} area of a single tube [m²]
diameter, length, thickness length, external diameter and thickness of a tube [m]
COP efficiency of the chiller [-]
 η_{SHX} efficiency of the solution heat exchanger [-]
f solution recirculation rate [-]
 \dot{m} mass flow; index p for poor solution, index r for rich solution, index vap for vapour [kg/s]
SF safety factor for calculation of pressure drops in the bundles
wet describes wetting behaviour of the working fluid in the heat exchanger; index A for absorber, index E for evaporator, index G for generator [l/mh]
x fluid concentration; index p for poor solution, index r for reach solution, index m for mean solution concentration [weight %]

Appendix E: Input and output variables measured from PACAS Prototype

Run	Input Variables							Outputs					Over flow
	T ₁	T ₃	T ₅	m ₁	m ₃	m ₅	m _r	Q _G	Q _C	Q _E	Q _A	COP	
10	75.0	14.8	28.8	0.6185	0.7464	0.6703	0.1582	13.30	10.70	10.00	11.00	0.75	No
16	110.0	15	34.1	0.5900	0.7496	0.6568	0.2153	21.60	14.70	12.40	18.50	0.58	No
14	110.0	15	26.4	0.5774	0.5503	0.6522	0.1811	14.10	12.70	9.80	14.90	0.70	No
6	110.0	15	26.5	0.0894	0.7431	0.1611	0.1393	8.20	4.90	4.10	7.10	0.50	No
9	70.0	6	26.5	0.1311	0.7374	0.6113	0.1533	3.60	1.20	0.70	2.90	0.35	No
2	70.0	15	26.5	0.6184	0.2538	0.1847	0.1841	4.80	2.70	2.00	4.70	0.42	Yes
5	110.0	6.1	26.5	0.5954	0.7390	0.1907	0.2076	13.60	7.90	5.40	10.90	0.40	Yes
15	110.0	6.1	34.0	0.1233	0.7404	0.6160	0.1572	8.90	4.50	3.30	7.00	0.37	No
4	75.4	25	34.0	0.1128	0.7249	0.2193	0.1931	3.60	0.90	0.30	2.70	0.09	Yes
11	70.0	6.0	34.0	0.6167	0.2500	0.6500	0.1950	No Results					No
3	70.0	6.0	34.0	0.6167	0.7333	0.1833	0.1300	No Results					No
12	70.0	15.0	34.0	0.0833	0.2500	0.6500	0.1300	No Results					Yes
AC1	90.3	15.1	27.4	0.4356	0.5910	0.6663	0.2000	17.30	12.80	13.80	15.90	0.69	No
AC2	87.4	15.1	27.4	0.3924	0.5860	0.6696	0.1893	16.20	13.20	11.40	15.00	0.71	No
AC3	95.3	15.0	27.5	0.4518	0.5976	0.6663	0.1813	18.70	15.02	13.90	17.10	0.69	No
AC4	95.0	20.0	30.0	0.6123	0.7432	0.6714	0.1835	21.19	16.93	15.60	20.42	0.71	No
1	69.9	6.7	26.5	0.1069	0.2558	0.1948	0.1584	2.50	0.30	0.40	2.90	0.14	No
8	110.0	15.1	34.0	0.6033	0.2655	0.1941	0.1530	11.40	7.00	3.20	7.40	0.28	No
13	109.8	6.0	26.5	0.5932	0.2623	0.6584	0.1526	25.50	18.80	13.00	19.00	0.51	Yes
7	110.7	6.0	34.0	0.0785	0.2592	0.1992	0.1995	6.70	2.30	1.30	5.20	0.19	No

Appendix F: Recalculation of heat transfer coefficient from the results

Set 1 – TUB			
output	Experiment	Simulation	Error %
U_G	2.51	2.90	13.3
U_C	1.22	1.69	28.0
U_E	0.64	0.76	16.3
U_A	0.82	0.78	-4.9

Set 2 – TUB			
output	Experiment	Simulation	Error %
U_G	0.50	0.78	35.82%
U_C	2.51	2.82	10.76%
U_E	1.38	1.72	19.94%
U_A	0.75	0.76	0.76%

Set 3 – TUB			
output	Experiment	Simulation	Error %
U_G	0.64	0.78	17.65%
U_C	2.56	2.88	11.22%
U_E	1.25	1.71	26.91%
U_A	0.71	0.76	6.81%

Set 4 – TUB			
output	Experiment	Simulation	Error %
U_G	0.73	0.78	6.60%
U_C	2.44	2.89	15.59%
U_E	1.51	1.70	11.07%
U_A	0.80	0.76	-5.16%

Set 5 – TUB			
output	Experiment	Simulation	Error %
U_G	0.69	0.78	11.04%
U_C	2.59	2.88	10.01%
U_E	1.38	1.70	18.77%
U_A	0.70	0.76	8.45%

Set 6 – TUB			
output	Experiment	Simulation	Error %
U_G	0.76	0.78	2.10%
U_C	2.42	2.88	16.00%
U_E	1.70	1.70	0.06%
U_A	0.74	0.76	3.02%

Set 7 – TUB			
output	Experiment	Simulation	Error %
U_G	0.85	0.78	-9.59%
U_C	2.39	2.88	16.94%
U_E	1.88	1.70	-10.58%
U_A	0.71	0.76	6.89%

Run AC1 – Polytechnique			
output	Experiment	Simulation	Error %
U_G	0.87	0.95	8.18%
U_C	2.67	2.44	-9.40%
U_E	1.39	1.50	7.38%
U_A	0.84	0.69	-20.91%

Run AC2 – Polytechnique			
output	Experiment	Simulation	Error %
U_G	1.43	0.95	-51.42%
U_C	2.58	2.46	-4.65%
U_E	1.28	1.49	14.07%
U_A	0.84	0.70	-19.70%

Run AC3 – Polytechnique			
output	Experiment	Simulation	Error %
U_G	0.86	0.95	9.34%
U_C	2.48	2.43	-1.97%
U_E	1.52	1.48	-2.30%
U_A	0.53	0.71	25.89%

Run AC4 – Polytechnique			
output	Experiment	Simulation	Error %
U_G	1.39	0.96	-44.97%
U_C	3.29	2.49	-32.08%
U_E	1.26	1.50	16.05%
U_A	0.98	0.70	-40.18%

Run 1 – Polytechnique			
output	Experiment	Simulation	Error %
U_G	0.74	0.95	22.71%
U_C	0.72	2.50	71.42%
U_E	0.99	1.53	35.23%
U_A	0.80	0.70	-14.75%

Run 6 – Polytechnique			
output	Experiment	Simulation	Error %
U_G	0.89	0.94	5.10%
U_C	1.10	2.49	55.95%
U_E	0.94	1.50	37.62%
U_A	0.46	0.79	41.23%

Run 7 – Polytechnique			
output	Experiment	Simulation	Error %
U_G	0.61	0.95	35.44%
U_C	2.22	2.48	10.35%
U_E	1.38	1.55	10.85%
U_A	0.58	0.68	15.01%

Run 8 – Polytechnique			
output	Experiment	Simulation	Error %
U_G	0.73	0.95	23.11%
U_C	1.70	2.49	31.72%
U_E	1.12	1.50	24.90%
U_A	0.82	0.70	-17.01%

Run 9 – Polytechnique			
output	Experiment	Simulation	Error %
U_G	0.81	0.93	13.34%
U_C	2.70	2.50	-7.93%
U_E	1.44	1.50	4.13%
U_A	0.53	0.69	23.25%

Run 10 – Polytechnique			
output	Experiment	Simulation	Error %
U_G	0.90	0.95	4.91%
U_C	2.26	2.50	9.80%
U_E	1.52	1.50	-1.86%
U_A	0.81	0.70	-15.77%

Run 14 – Polytechnique			
output	Experiment	Simulation	Error %
U_G	1.06	0.95	-11.60%
U_C	2.61	2.50	-4.53%
U_E	1.53	1.49	-2.20%
U_A	0.66	0.69	4.95%

Run 15 – Polytechnique			
output	Experiment	Simulation	Error %
U_G	0.94	0.95	1.03%
U_C	2.28	2.49	8.47%
U_E	1.34	1.49	10.15%
U_A	0.79	0.70	-13.41%